TRAUMATIC BRAIN INJURY: ASSESSING THE PATHOGENIC IMPACT OF CHRONIC SMOKING AND POTENTIAL COUNTERMEASURES

by

FARZANE SIVANDZADE

A dissertation submitted in partial fulfillment of the
requirements for the degree of

BIOLOGICAL AND BIOMEDICAL SCIENCES

2022

Oakland University
Rochester, Michigan

Doctoral Advisory Committee:

Luca Cucullo, Ph.D. Chair
Mohamed Al-Shabrawey, Ph.D.
Zijuan Liu, Ph.D.

ACKNOWLEDGMENTS

I would like to express my special thanks and gratitude to my advisor, Prof. Luca Cucullo, who gave me the opportunity to work and learn in his research lab under his supervision. His guidance and advice carried me through all the stages of my study and research. I would also like to thank my committee members, Dr. Mohamed Al-Shabrawey and Dr. Zijuan Liu for their helpful comments and endless support.

I would like to thank Dr. Faleh Alqahtani for his dedicated support and guidance. He was always willing and enthusiastic to assist in any way he could throughout the research project. Also, I would like to thank my former and present peers, Dr. MD Abul Kaisar, Dr. Shikha Prasad, Dr. Snehal Raut, Aditya Bhalerao, and Salvatore Mancuso, who have supported me throughout this research project.

Last but not least, I'd like to give special thanks to my family and partner as a whole for their continuous support and understanding when undertaking my research project and writing my dissertation. Their prayer for me was what sustained me this far.

Farzane Sivandzade

PREFACE

I am a Ph.D. candidate and graduate research assistant in Dr. Luca Cucullo's lab focused on cellular & molecular biology, neurotoxicology, and neuroinflammation. Before joining his lab as a Ph.D. student, I received a bachelor's degree in chemical engineering from Shiraz University and two master's degrees in biomedical engineering (from Sharif University of Technology) and Pharmaceutical Sciences (from a Texas Tech University Health Sciences Center) under the guidance of Dr. Cucullo prior his move to OUWB. After re-joining his lab at OUWB, I continued working on a funded project aimed at unraveling tobacco smoke's physiological and pathophysiological impact on blood-brain barrier function/integrity and evaluating potential countermeasures involving the repurposing of antidiabetic drugs affecting the NRF2-ARE pathway. This project was highly significant to the U.S. FDA in making science-based decisions that help safeguard public health from potential harm caused by the chronic use of tobacco and vape-based products, including electronic cigarettes. My research provided novel data to further the development of therapeutic strategies aimed at preventing/reducing cigarette-induced cerebrovascular dysfunction and resulted in numerous publications in high-impact journals in the field as well as several presentations and abstracts in high-ranked conferences. My work aimed at unraveling the physiological and pathophysiological impact of tobacco smoke and vaping on the exacerbation of TBI injuries. In addition, I evaluated the use of various antidiabetic drugs as potential therapeutic agents to reduce the burden of TBI and improve patient outcomes. My academic training and research

experience to date have provided me with an excellent background in pharmaceutical and biomedical sciences to carry on the proposed studies. I have authored 22 peer-reviewed publications (13 publications as a first author), which have appeared in some of the most notable journals in my field, including *Redox Biology*, the *Journal of Cerebral Blood Flow and Metabolism*, and the *International Journal of Molecular Sciences.*

ABSTRACT

TRAUMATIC BRAIN INJURY: ASSESSING THE PATHOGENIC IMPACT OF CHRONIC SMOKING AND POTENTIAL COUNTERMEASURES

by

Farzane Sivandzade

Adviser: Luca Cucullo, Ph.D.

Traumatic brain injury is among the most prevalent causes of cerebrovascular and neurological damage worldwide. Premorbid conditions such as smoking could exacerbate post-traumatic brain injury damage and impact recovery due to vascular endothelial dysfunction. Cigarette smoke produces reactive oxygen species (ROS) and oxidative stress (OS), driving endothelial dysfunction and damaging the blood-brain barrier (BBB) endothelium. Interestingly, these pathogenic modulators of BBB impairment are similar to those initiated by hyperglycemia. Thus, this work investigated the pathophysiological mechanisms underlying traumatic brain injury (TBI) exacerbation following chronic smoking and vaping exposure to determine key pathological parameters leading to loss of BBB function and integrity. I also assessed the effectiveness of metformin and rosiglitazone to prevent/reduce the loss of BBB function and integrity and protect the brain from the exacerbation of post-TBI likely promoted by the chronic exposure to tobacco smoke (TS) or electronic cigarette (EC) vape and unravel the corresponding mechanism (s) of action. For this purpose, I used both *in vitro* (primary brain microvascular endothelial cells) and *in vivo* mice models (male and C57BL/6J mice)

subjected to TS/EC and TBI, with/without antidiabetic treatments. The outcomes of these studies would define the complex interplay between smoking and TBI and lead to new approaches for alleviating TBI outcomes.

TABLE OF CONTENTS

TABLE OF CONTENTS-Continued

TABLE OF CONTENTS-Continued

TABLE OF CONTENTS-Continued

TABLE OF CONTENTS-Continued

TABLE OF CONTENTS-Continued

LIST OF TABLES

LIST OF FIGURES

LIST OF FIGURES-Continued

LIST OF ABBREVIATIONS

AD	Alzheimer's Disease
AIF	Apoptosis-Inducing Factor
ALS	Amyotrophic Lateral Sclerosis
AMPA	α-amino-3-hydroxy5-methyl-4-isoxazole -propionic acid
AMPK	AMP-activated protein kinase
ApoE	Apo-lipoprotein E
ARE	Antioxidative Response Element
BBB	Blood-Brain Barrier
CAT	Catalase
CDC	Center for Disease Control and Prevention
CNS	Central Nervous System
EC	Electronic Cigarette
ELISA	Enzyme-Linked Immunosorbent Assay
HD	Huntington's disease
HG	Hyperglycemia
4-HNE	4-hydroxynonenal
HO-1	Heme Oxygenase 1
ICAM-1	Intercellular Adhesion Molecule-1
IF	Immunofluorescence
IL-6	Interleukin-6
IL-10	Interleukin-10
KEAP1	Kelch Like ECH Associated Protein 1

LC3	Light Chain 3
mBMEC	Mouse Brain Microvascular Endothelial Cells
MF	Metformin
MMP-9	Matrix Metalloproteinase-9
MPO	Myeloperoxidase
NF-κB	Nuclear Factor kappa B
NMDA	N-methyl-D-aspartic acid
NQO-1	NAD(P)H: Quinone reductase I
NRF2	Nuclear Factor erythroid-2 related Factor 2
OS	Oxidative Stress
PD	Parkinson's Disease
PECAM-1	Platelet Endothelial Cell Adhesion Molecule 1
PARP-1	Poly (ADP-Ribose) Polymerase 1
PPARγ	Peroxisome Proliferator-Activated Receptor
ROS	Reactive Oxygen Species
RSG	Rosiglitazone
RT-PCR	Real-Time Polymerase Chain Reaction
SAA1	Serum Amyloid A1
SOD	Superoxide Dismutase
STAT3	Activator of Transcription-3
TBI	Traumatic Brain Injury
TD2M	Type-2 diabetes mellitus

TJ	Tight Junction
TGF-β	Transforming Growth Factor β
TNF-α	Tumor Necrosis Factor-alpha
TS	Tobacco Smoking
UCH-L1	Ubiquitin C-terminal Hydrolase L1
VCAM-1	Vascular Cell Adhesion Protein 1
VEGF	Vascular Endothelial Growth Factor
WB	Western Blotting
ZO-1	Zonulae Occludentes-1

LIST OF PUBLICATIONS

1. Sivandzade F.; Alqahtani F.; Bhalerao A.; Mancuso S.; Dhaibar H.; Cruz-Topete D.; Cucullo L. Metformin and Rosiglitazone Reduce Tobacco Smoke-Enhanced Oxidative Stress Damage of the Blood-Brain Barrier After Traumatic Brain Injury. *European Journal of Cell Biology* **2022**. (Under Review)

2. Rehman Z.; Farooq T.; Javaid S.; Ashraf W.; Rasool MF.; Samad N.; Tariq M.; Anjum SMM.; Sivandzade F.; Alotaibi F.; Alqahtani F.; Imran I. Combination of Levetiracetam with Sodium Selenite Prevents Pentylenetetrazole-Induced Kindling and Behavioral Comorbidities in Rats. *Saudi Pharmaceutical Journal* **2022**.

3. Samad N.; Imran A.; Bhatti S.; Imran I.; Alqahtani F.; Alasmari AF.; Sivandzade F. Vitamin D2 Protects Acute and Repeated Noise Stress Induced Behavioral, Biochemical, and Histopathological Alterations: Possible Antioxidant Effect. *Saudi Journal of Biological Sciences* **2022**.

4. Almutairi M.; Sivandzade F.; Albekairi T.; Alqahtani F.; Cucullo L. Neuroinflammation and its Impact on the Pathogenesis of Covid-19. *Frontiers in Medicine* **2021**.

5. Rahman HMA.; Javaid S.; Ashraf W.; Rasool MF.; Anjum SMM.; Saleem H.; Siddique F.; Chtita S.; Sivandzade F.; Alqahtani F.; Alotaibi MR.; Imran I. Neuropharmacological Investigation, Ultra-High-Performance Liquid Chromatography Analysis, and in Silico Studies of Phyla Nodiflora. *Journal of Physiology and Pharmacology: an Official Journal of the Polish Physiological Society* **2021**.

6. Sivandzade F.; Alqahtani F.; Cucullo L. Impact of Chronic Smoking on Traumatic Brain Microvascular Injury: an *in Vitro* Study. *Journal of Cellular and Molecular Medicine* **2021**.

7. Sivandzade F.; Cucullo L. Regenerative Stem Cell Therapy for Neurodegenerative Diseases: an Overview. *International Journal of Molecular Sciences* **2021**.

8. Chowdhury EA.; Noorani B.; Alqahtani F.; Bhalerao A.; Raut S.; Sivandzade F.; Cucullo L. Understanding the Brain Uptake and Permeability of Small Molecules Through the BBB: a Technical Overview. *Journal of Cerebral Blood Flow & Metabolism* **2021**.

9. Alqahtani F.; …; Sivandzade F.; et al. Coadministration of Ketamine and Perampanel Improves Behavioral Function and Reduces Inflammation in Acute Traumatic Brain Injury Mouse Model. *BioMed Research International* **2020**.

10. Sivandzade F.; Alqahtani F.; Sifat A.; Cucullo L. the Cerebrovascular and Neurological Impact of Chronic Smoking on Post Traumatic Brain Injury Outcome and Recovery: an *in Vivo* Study. *Journal of Neuroinflammation* **2020**.

11. Sivandzade F.; Alqahtani F.; Cucullo L. Traumatic Brain Injury and Blood-Brain Barrier (BBB): Underlying Pathophysiological Mechanisms and the Influence of Cigarette Smoking as a Premorbid Condition. *International Journal of Molecular Sciences* **2020**.

12. Bhalerao A.; Sivandzade F.; Archie SR.; Chowdhury EA.; Noorani B.; Cucullo L. *in Vitro*-Modeling of the Neurovascular Unit: Advances in the Field. *Fluids and Barriers of the CNS* **2020**.

13. Sivandzade F.; Cucullo L. Anti-Diabetic Countermeasures Against Tobacco Smoke-Dependent Cerebrovascular Toxicity: Use and Effect of Rosiglitazone. *International Journal of Molecular Sciences* **2019**.

14. Bhalerao A.; Sivandzade F.; Archie SR.; Cucullo L. Public Health Policies on E-Cigarettes. *Current Cardiology Reports* **2019**.

15. Sivandzade F.; Bhalerao A.; Cucullo L. Cerebrovascular and Neurological Disorders: Protective Role of NRF2. *International Journal of Molecular Sciences* **2019**.

16. Sivandzade F.; Cucullo L. Assessing the Protective Effect of Rosiglitazone Against Electronic Cigarette/Tobacco Smoke-Induced Blood-Brain Barrier Impairment". *BMC Neuroscience* **2019**.

17. Sivandzade F.; Bhalerao A.; Cucullo L. Analysis of the Mitochondrial Membrane Potential Using the Cationic JC-1 Dye as a Sensitive Fluorescent Probe. *Bio Protocol* **2019**.

18. Sivandzade F.; Prasad S.; Bhalerao A.; Cucullo L. NRF2 and NF-κB Interplay in Cerebrovascular and Neurodegenerative Disorders: Molecular Mechanisms and Possible Therapeutic Approaches. *Redox Biology* **2018**.

19. Sivandzade F.; Cucullo L. *in-Vitro* Blood–Brain Barrier Modeling: a Review of Modern and Fast-Advancing Technologies. *Journal of Cerebral Blood Flow & Metabolism* **2018**.

20. Kaisar MA.; Sivandzade, F.; Bhalerao A.; Cucullo L. Conventional and Electronic Cigarettes Dysregulate the Expression of Iron Transporters and Detoxifying Enzymes at the Brain Vascular Endothelium: *in Vivo* Evidence of a Gender Specific Cellular Response to Chronic Cigarette Smoke Exposure. *Neuroscience Letters* **2018**.

21. Sivandzade F.; Mashayekhan S. Design and Fabrication of Injectable Microcarriers Composed of Acellular Cartilage Matrix and Chitosan. *Journal of Biomaterials Sciences, Polymer Edition* **2018**.

22. Sivandzade F. an Analytical Model for the Prediction of Controlled Release from Bulk Biodegrading Polymer Microspheres. *Asian Journal of Pharmaceutical and Clinical Research* **2018**.

CHAPTER ONE

TRAUMATIC BRAIN INJURY AND BLOOD–BRAIN BARRIER: UNDERLYING PATHOPHYSIOLOGICAL MECHANISMS AND THE INFLUENCE OF CIGARETTE SMOKING AS A PREMORBID CONDITION

1.1 Introduction

Traumatic brain injury (TBI) is defined as an insult to the brain caused by a direct or indirect external mechanical force. TBI has long been among the foremost leading causes of death and disability in the United States, thus becoming a serious public health concern in modern society [1-6]. According to the Centers for Disease Control and Prevention (CDC), every year, about 2.5 million people in the U.S. seek emergency care for TBI secondary to motor vehicle accidents, falls, assaults, sports-related events, and other mechanisms. In addition, every year, more than 5.3 million Americans live with a lifelong disability caused by TBI [7-9]. In those that survive, the effects of TBI can cause emotional, physiological, cognitive, motor, and behavioral impairments ranging from mild to severe [5,10]. Mild TBI accounts for over 80% of head injuries [1]. Mild TBI typically results in transient symptoms, including sensitivity to light and sound, headache, vision impairment, difficulties with cognition and balance. The severity of TBI is classified into three degrees (depending on the length of unconsciousness following the head injuries), including mild TBI (loss of consciousness ≈ 15 s), moderate TBI (loss of consciousness of several minutes), and severe TBI (loss of consciousness ≥ 1 h) [11]. Approximately 20–40% of patients die after a severe TBI due to brain injury or secondary complications. Those that survive often have reduced life expectancies,

chronic neurological disabilities, pituitary dysfunction, and cognitive and psychological disorders, including depression and aggression [1,11-13]. In fact, after a moderate or severe TBI, most patients require hospitalization for medical management. During the post-hospital recovery phase, they often deal with reduced cognitive abilities, anxiety and depression disorder, and impaired balance and coordination. Needless to say these post-traumatic effects burden the patient with a higher risk of re-hospitalization, an additional economic burden for the individual and his/her family and reduced quality of life [13]. Researchers in the field have been focusing on several aspects of TBI, including the physical characteristics of the trauma and the lapse time between trauma and the initial onset of neuropathologies [14]. The development of TBI is divided into two general stages: primary (immediate) injury and secondary (delayed) injury [15]. The primary trauma encompasses all acute pathological changes, such as shearing injuries, contusions, and hematomas [2,16]. Secondary changes, including cerebral edema formation, oxidative stress (OS), inflammation, excitotoxicity, imbalanced calcium homeostasis, enhanced vascular permeability, and blood–brain barrier (BBB) impairment, often occur following vascular and parenchymal damage in the brain. Secondary injury events can significantly exacerbate post-TBI and worsen clinical outcomes [17-19] (see also Fig. 1.1). Concerning the BBB's involvement, substantial evidence suggests that TBI impairs the BBB, and BBB damage is implicated in the loss of neurons, altered brain function, and possibly the response to therapy. Post-traumatic dysfunction of the BBB is one of the significant factors determining the progression of injury and affecting the time course and the extent of neuronal repair [20].

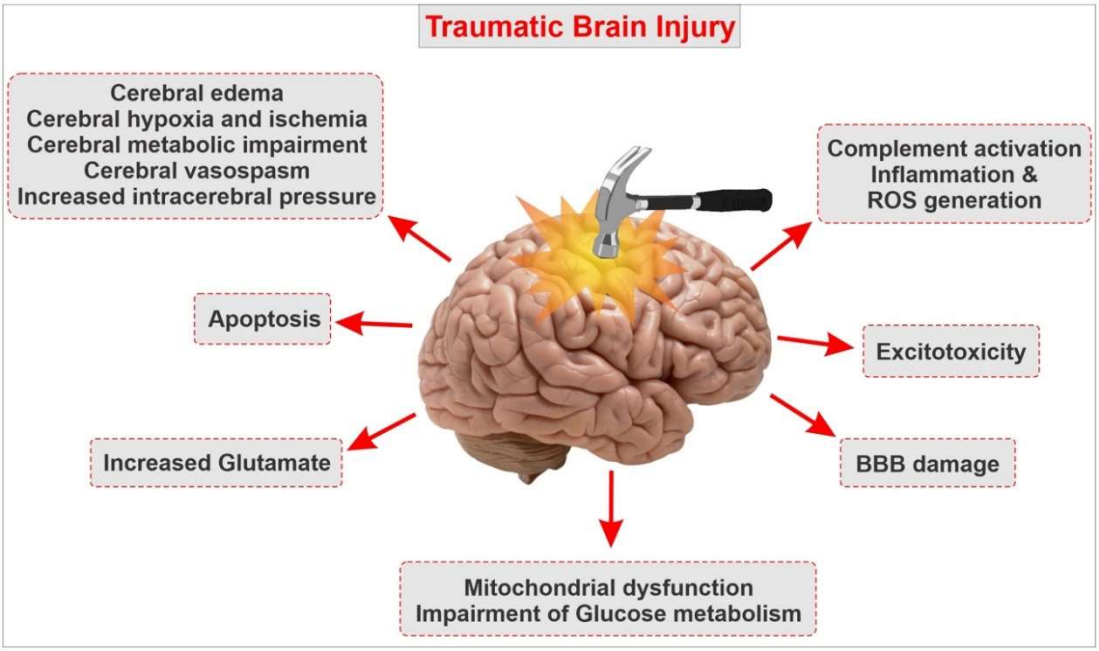

Figure 1.1 Simple schematic outlining the pathophysiological responses following TBI and the complex outburst of secondary impairments.
Note that secondary injury processes of TBI include BBB disruption, neuroinflammation, excitotoxicity, metabolic impairments, apoptosis, OS, ischemia, and others. Associated with BBB impairment, microglial and astrocyte activation, leukocyte infiltration, and upregulation of pro-inflammatory cytokines are characteristic of the neuroinflammatory response of TBI [21].

This chapter covers the pathogenesis of TBI and encompasses the major pathophysiological factors that promote post-traumatic dysfunction of the BBB and its involvement in the onset of post-TBI neuropathologies. We also provide a brief review of the current treatment used to alleviate the burden of TBI.

1.2 The Blood–Brain Barrier Interface

The BBB is a dynamic functional interface between the blood and the central nervous system (CNS), which allows nutrients, essential amino acids, ions, etc., to transport between the peripheral circulation and the brain. At the same time, it inhibits

many pathogens and toxic compounds from entering the brain [22,23]. The primary functions of the BBB are to maintain homeostasis in the brain and protect the brain from potentially endogenous and xenobiotics, leading to optimal neuronal activity [3,11]. Generally, the BBB is formed by the brain endothelial cells. The junctions between endothelial cells are tightly connected through the adherens junction (AJ) proteins, such as cadherins, and tight junctional proteins, such as Occludin and Claudins [24]. Besides, astrocytes, microglia, and pericytes are also critical for the normal function of the BBB and the phenotype of brain endothelial cells so that they contribute to the formation and maintenance, selectivity, and specificity of the BBB [14,25]. Glial and endothelial cells functionally interact with each other in a paracrine manner contributing to the integrity of the BBB. The efflux transporters present in the endothelial cells support the selective function of the BBB by actively moving various lipophilic drugs out of brain endothelial cells. Together, the physical and metabolic barrier of the BBB plays a crucial role in maintaining brain homeostasis.

1.3 Chronic Smoking: A Major Comorbid Factor for Blood-Brain Barrier Dysfunction and Significant Neurological Disorders

Tobacco smoke (TS) is a diverse mixture of over 4700 toxic compounds, including carcinogens and mutagenic chemicals, as well as stable and unstable free radicals and reactive oxygen species (ROS). Chronic smoking is one of the leading preventable causes of morbidity and mortality that affects the function of almost every organ of the body, giving rise to a range of illnesses that reduce life expectancy in smokers [26]. TS is responsible for approximately 6 million deaths per year worldwide, and more than 480,000 deaths yearly just in the United States (US). Smoking has been

strongly associated with an enhanced risk of stroke and other cerebrovascular and neurological disorders such as Alzheimer's, Disease (AD), Parkinson's Disease (PD), Amyotrophic Lateral Sclerosis (ALS), Huntington's Disease (HD), Multiple Sclerosis (MS), and vascular dementia [27]. The mechanisms through which TS promotes the onset and progression of various cerebrovascular and neurodegenerative diseases are multifaceted. They include OS, BBB dysfunction, inflammation, alteration of cellular redox metabolic activities, and the activation of immune responses [28,29]. There is considerable evidence suggesting the pivotal role of OS in endothelial dysfunction and following BBB damage in the cerebrovascular level. The exposure of TS even at non-toxic concentration induces a robust inflammatory response in cells that influences the cerebrovascular endothelium and circulating immune cells. The inflammatory response and reduced cerebral blood flow, both common in chronic smokers, result in exaggerated damage to BBB, suggesting its contribution to cerebrovascular disease and ischemic stroke [30]. It has been claimed by various studies that smoking increases the risk of neuroinflammatory disorders, i.e., Alzheimer's disease and multiple sclerosis [30]. A previous study showed that chronic prenatal exposure to nicotine could induce the unusual discharge of neurochemicals, followed by several pathological consequences in children. The study also demonstrated that nicotine causes an abnormal differentiation of neuronal cells, decreases synaptic activity, and promotes apoptosis, thus leading to abnormal brain development. TS may provoke the expression of several adhesion molecules and the release of tumor necrosis factor-alpha (TNF-α), interleukin-6 (IL-6), and matrix metalloproteinase-2 (MMP-2). Altogether, these are essential in the regulation

of leukocytes movement across the endothelium into adjacent tissue and contribute toward perivascular inflammation. Altered BBB integrity and increased atherogenesis may eventually lead to ischemic insult. The pro-inflammatory role of TS might be the result of its impact on the transcription of genes that are involved in the pathogenesis of atherosclerosis and modulate the inflammatory reaction at the BBB level. TS can cause the significant upregulation of various transcription factors, which can play an essential role in the gene expression of cytokines, chemokines, and different adhesion molecules, i.e., E-selectin and Intercellular Adhesion Molecule-1 (ICAM-1). TS can also upregulate the Signal Transducer and Activator of Transcription-3 (STAT3), an angiogenesis modulator that acts through the IL-6/STAT3 signaling pathway. STAT3 links extracellular signals to transcriptional control of proliferation and cycle progression [31]. Furthermore, TS may also contribute to the upregulation of Apo-lipoprotein E (ApoE) and Serum Amyloid A1 (SAA1) genes. ApoE plays a role in regulating lipoprotein metabolism, and it is known to associate with elevated cholesterol and risk of atherosclerosis and ischemic stroke. The transcriptional product of the SAA1 gene is serum amyloid, a potent chemoattractant that modulates tissue infiltration and the adhesion of monocytes and leukocytes [32]. In addition, amyloid in brain vessels can enhance BBB permeability. All these events result in the loss of BBB integrity during ischemic insults and contribute to the development of cerebrovascular diseases. TS can also downregulate Claudin-5 expression, an essential interendothelial tight junction protein involved in maintaining BBB integrity and function. There is considerable controversy regarding the influence of premorbid and comorbid conditions that

commonly accompany TBI, such as cigarette smoking, on the expected rate and extent of recovery from TBI [9]. Indeed, considering the influence of premorbid and comorbid conditions may lead to spurious conclusions about the mechanisms underlying the pathophysiology of the TBI [9].

1.4 Pathophysiology and Underlying Causes of Traumatic Brain Injury

The pathophysiology of TBI can be divided into primary and secondary injury mechanisms. The primary mechanical injury is due to physical trauma from a direct head impact. It may result in intracranial and extracranial hemorrhage, tissue destruction, and axonal shearing following damage to the blood vessels, brain tissue, and the BBB [11]. Secondary injury usually occurs within a variable period (days to months and sometimes even years) after the onset of the initial injury. The pathogenic events unfolding during the onset of the secondary damage ultimately compromise cell and tissue viability at the metabolic and molecular levels [18]. Cerebral edema formation and increased intracranial pressure are other critical factors that are prodromal to secondary brain injury [11]. Several neurotransmitters, biochemical mediators, cytokines, and genetic changes play a pivotal role in the molecular mechanisms of tissue injury after TBI [33]. This pro-inflammatory environment (promoting OS and the increased expression of endothelial cell adhesion molecules) facilitates the activation and the influx of immune cells into the brain parenchyma, thus determining the progression of injury, including excitotoxicity and neuronal loss [20,34,35]. Although the primary brain injury is the initial pathogenic factor, the secondary brain injury is generally more severe and complex. It promotes the expansion of the initial mechanical brain injury in surrounding healthy tissue [15,19].

Several studies reported that TBI chronically leads to the onset of various cerebrovascular and neurodegenerative disorders such as Alzheimer's disease, chronic traumatic encephalopathy, epilepsy, and other long-term problems, including the loss of executive function, inappropriate social behavior, and cognitive disabilities [36,37].

1.5 Traumatic Brain Injury and Breakdown of the Blood-Brain Barrier

BBB disruption is a major pathophysiological feature of TBI and is associated with neuroinflammatory events contributing to brain edema and cell death [2]. Due to the highly heterogeneous characteristic of the brain, in response to a direct impact or external forces applied to the head, different brain structures are subject to different acceleration rates, resulting in the generation of considerable tensile, shear, and compressive forces within the brain. Both astrocytes and microglia can rapidly respond to injury by increasing the production of multiple factors that may significantly affect BBB function. The BBB permeability is mainly modulated by the expression of tight junctional proteins on endothelial cells [2]. However, the primary injury of TBI leads to damaged endothelial cells and a loss of blood flow followed by disrupted tight junctional proteins and the basal membrane, thus leading to a loss of barrier integrity and subsequent elevated permeability [20] (see also Fig. 1.2). BBB breakdown not only triggers leukocyte recruitment and the migration of inflammatory cells activating astrocytes, but it also causes the release of pro-inflammatory cytokines, cytotoxic proteases, and ROS to activate microglia, affecting neuronal activity [11]. A physical barrier termed "glial scar" forms around the damaged area to protect the surrounding intact neural tissue from the

destructive immune response and prevent the spread of inflammation to neighboring neurons and undamaged areas.

Moreover, local inflammation occurs, expanding the injury site and exacerbating the damage [3]. The glial scar encloses an area containing inhibitory molecules that impede the regrowth of neurons and block the repair of the BBB [4,11]. Furthermore, disruption of the BBB after TBI promotes the activation of the coagulation cascade, resulting in the formation of an intravascular blood clot and ischemia [2]. In addition, the reduced integrity of the BBB enables the efflux of plasma proteins into the extravascular space. This latter efflux ultimately induces neuroinflammation by promoting transforming growth factor β (TGF-β) activation. These studies suggest a strong association between the degree of BBB disruption and the onset of neuroinflammatory processes caused by circulating immune cells and the influx of neutrophils into the damaged area of the CNS [2]. This set of events promotes the onset of a vicious cycle, which helps further damage the BBB. On the other hand, a leakier BBB may facilitate the efflux of water from the brain parenchyma, thus reducing post-TBI cerebral edema [2]. In fact, researchers have demonstrated that transient and size-selective modulation in the BBB paradoxically enhances the movement of water from the brain parenchyma to the blood vessels, leading to decreased brain swelling.

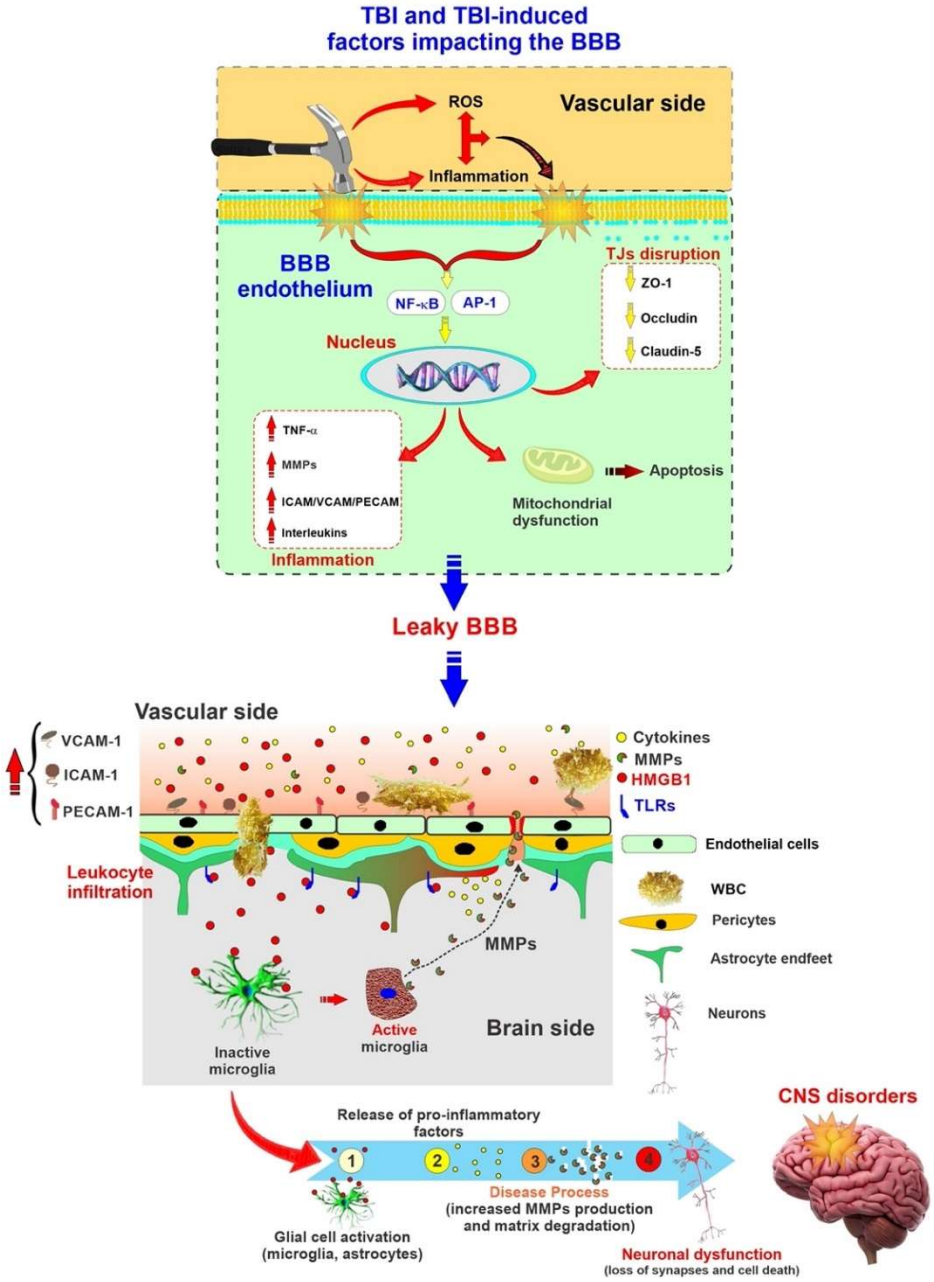

Figure 1.2 Schematic illustration depicting TBI and TBI-dependent factors impacting the BBB and the onset of secondary brain injuries.Representation of BBB as a source and target of neuroinflammation in TBI. Note that inflammation and ROS generation associated with TBI can further impact the BBB in addition to mechanical trauma. The loss of BBB integrity further promotes neuronal damage and the onset of CNS disorders [21].

1.6 Post-Traumatic Brain Injury Cell Death Mechanisms

Mechanisms of neuronal cell death post-TBI have been mainly categorized into necrosis and apoptosis. At the same time, there are at least a dozen mechanisms of neuronal death, including intrinsic and extrinsic apoptosis, oncosis, necroptosis, parthanatos, ferroptosis, sarmoptosis, autophagic cell death, autosis, autolysis, paraptosis, pyroptosis, phagoptosis, and mitochondrial permeability transition [38]. Necrosis is a passive process characterized by the loss of ionic balance and membrane integrity of the cell, leading to cell and intracellular organelle swelling [33]. On the other hand, apoptosis is an energy-consuming process characterized by condensation and fragmentation of the cytoplasm and nucleus with the maintenance of organelle structure, which occurs as programmed cell death and a controlled part of an organism's growth or development [16,33]. TBI promotes the upregulation of many cell-cycle activators, such as c-myc, cyclins, and cyclin-dependent kinases, and the downregulation of cell-cycle inhibitors. Moreover, after TBI, caspase-dependent signaling pathways (which play a significant role in cell death) are activated, resulting in an imbalance between proapoptotic and anti-apoptotic molecules enhancing cell death [39,40]. Besides, apoptosis-inducing factor (AIF) released into the cytosol, which modulates cell death, causes condensation of chromatin in the nucleus's periphery and DNA fragmentation. Studies have shown that the release of AIF is dependent on Poly (ADP-Ribose) Polymerase 1 (PARP-1), causing depletion of cytosolic NAD+ and, consequently, mitochondrial dysfunction and outer membrane permeabilization [33]. It accounts for why PARP-1 inhibition after TBI has proven to be neuroprotective. Autophagic programmed cell death (the natural, regulated

mechanism of the cell that removes unnecessary or dysfunctional components) involves the lysosomal degradation of organelles and proteins. Autophagy is often the dominant mechanism for programmed cell death in conditions of mitochondrial permeabilization and inhibition of caspases [16]. On the other hand, neuronal cell death is a much more complicated process involving autophagy and paraptosis. Paraptosis has a non-apoptotic morphology and is regulated by genes. Neuronal cell death is categorized as physiologic and excitotoxic [33]. Physiologic cell death is a developmental death due to injuries such as ethanol or TBI. It is characterized by initial mitochondrial swelling followed by vacuolization of the endoplasmic reticulum after the rupture of the nuclear membrane. Excitotoxic cell death (often seen a few hours after TBI) refers to the rapid swelling and rupture of organelles with the clumping of chromatin in the center of the nucleus [41].

Autophagy is one of the main types of neuronal death after TBI. Autophagy flux occurs with the fusion of the autophagosome with the lysosome to form autolysosomes, which degrades the cytoplasmic organoids. Three general methods to detect autophagic flux are Microtubule-associated protein 1A/1B-light chain 3 (LC3) turnover, protein p62 degradation, and tandem fluorescent-tagged LC3 assay. Autophagy has a dual role in TBI, depending on its flux [42]. In mild cases, autophagy flux is increased, which is expected to be beneficial for cell survival. Conversely, flux is decreased in moderate to severe cases, which leads to neuronal death and aggravated pathological phenotypes [42]. Increased LC3-II and autophagosomes are observed in the experimental weight drop injury model of TBI, and caloric restriction after mild TBI results in increased Beclin 1, LC3, and mTOR. TBI could inhibit the PI3K-AKT-mTOR signaling pathway, NRF2-

ARE signaling pathway, TLR4-NF-κB signaling pathway [43], and activate FoxO3a and Drp1 [44] proteins, which are the upstream of autophagy and their regulation by TBI may promote autophagosome formation and cause BBB disruption [42].

1.7 Excitotoxicity

Cellular excitotoxicity is a pathological process in which neuron cells are damaged by excessive stimulation of neurotransmitters such as glutamate and other excitatory factors. Cellular excitotoxicity, which is a crucial mediator in the pathophysiology of TBI, primarily occurs as a result of upregulated N-methyl-D-aspartic acid (NMDA) and α-amino-3-hydroxy5-methyl-4-isoxazole -propionic acid (AMPA) receptors [45]. Raised glutamate released from parenchymal brain cells activates the AMPA receptors, prompting the receptor-associated ion channels to open, thus upregulating the influx of sodium and calcium ions [2,46]. Glutamate levels are the highest immediately after TBI, and these heightened levels are sustained for 24–48 h due to the disruption of the BBB. In addition, there is some evidence that glutamate promotes ROS production [47,48]. There are some other molecules, including TGF-β, vascular endothelial growth factor (VEGF), and matrix metalloproteinases (MMPs), which become abnormally elevated in the brain following TBI, thus contributing to BBB impairment and the loss of barrier integrity [2]. The damage to the BBB will eventually facilitate the development of cerebral edema and the onset of other post-TBI secondary injuries [2]. Specifically, recent studies have revealed increased synthesis and elevated levels of MMPs and reduced expression of MMPs inhibitors and endogenous MMPs regulators in plasma and the cerebrospinal fluid of brain tissue from patients and animal

models of TBI. Moreover, the upregulation of VEGF, as a major regulator of endothelial cell proliferation, angiogenesis, and vascular permeability, and the downregulation of Claudin-5 expression was correlated to BBB dysfunction [22,26,49,50].

TGF-β, a molecule with a pivotal role in cell proliferation and differentiation, gets released in large amounts from platelets after vascular wall damage. Several studies have shown an increase in the expression of both TGF-β and TGF-β receptors on vascular endothelium post-TBI. There are conflicting studies regarding the positive or negative impact of TGF-β on BBB permeability, so some believe TGF-β plays a role in maintaining BBB integrity through stabilizing endothelial cells and pericytes' interaction via N-cadherin. Other studies instead suggest that TGF-β derived-tyrosine phosphorylation reduces Claudin-5 and VE-cadherin expression.

1.8 Neuroinflammation

Neuroinflammatory responses to injury have a significant pathophysiological role in developing post-TBI secondary brain damage (although its role in primary injury is limited). Immediately after the impact, the mechanical disruption of the BBB causes the extravasation of red blood cells, accompanied by a limited influx of leukocytes due to the rapid activation of the coagulation cascade. The process results in a significant reduction in blood flow in affected brain tissue. Neuroinflammation involves the influx of leukocytes into the injured brain parenchyma penetrating across the BBB. This is followed by the influx of neutrophils, monocytes, and lymphocytes within a relatively short period (hours to days) post-TBI [51]. During this critical time frame, the production of inflammatory mediators, including cytokines (such as IL-6, IL-10, TNF-α, and IL-1β)

increases. Following the cytokines' upregulation, cell adhesion molecules expressed on the surface of the cerebrovascular endothelium also increase. All these processes eventually lead to the influx of inflammatory cells from the blood into the brain to initiate a host of restorative processes, including neurogenesis, synaptogenesis, oligodendrogenesis, and angiogenesis in the brain as the spontaneous functional recovery after TBI [52,53]. Another factor of relevance is that the activation of microglial cells not only causes the amplification of the inflammatory response but also ROS production along with neurotoxic molecules. The result is the onset of other secondary mechanisms of cell death. As mentioned previously, cytokines are pro-inflammatory mediators that include interferons, interleukins, and chemokines secreted from immune cells. Based on recent *in vivo* studies, the synthesis of pro-inflammatory cytokines is rapidly upregulated in rodent models of TBI. Among the major cytokines, TNF-α and IL-1β play a vital role in exacerbating tissue damage; thus, there is a dose–response correlation between the cytokines expression level and mortality, including intracranial pressure and multiorgan failure [33]. While TNF-α increases as early as one hour after TBI, IL-1β upregulates gradually to peak at 6–8 h post-TBI. Pro-inflammatory cytokines also have multiple effects on the BBB, promoting loss of barrier integrity, downregulation and altered distribution of tight junctional proteins, and ROS production [20].

Moreover, further details have revealed that TNF-α enhances the formation of actin stress fibers, followed by cell retraction and the formation of intercellular gaps. In addition to the detrimental effect on BBB viability, the most critical role of these pro-inflammatory mediators is inducing the synthesis of chemokine and the expression of cell

adhesion molecules on the surface of the endothelial layer. In several studies on human brain microvascular endothelial cells, it has been demonstrated that cells exposed to TNF-α or IL-1β promoted the expression of E-selectin, Intercellular Adhesion Molecule 1 (ICAM1), and vascular cell adhesion molecule-1 (VCAM1) on the cell surface. Furthermore, the rapid induction of endothelial expression of E-selectin and an upregulated expression of ICAM1 post-TBI have been reported in both clinical, and animal studies and have been positively correlated with increasing severity of the injury and worsening neurological outcome.

Nuclear factor kappa-light chain-enhancer of activated B cells (NF-κB) is a protein complex that controls pro-inflammatory cytokine production in most cell types, including neurons, astrocytes, microglia, oligodendrocytes, and endothelial cells of neurovascular and cerebrovascular units [16]. Recent studies have demonstrated a critical physiological role in the CNS's NF-κB signaling pathway, serving crucial functions in cellular responses to neuronal injury [54]. It is well established that post-TBI leads to the activation of NF-κB in glial cells and neurons in the same brain region undergoing atrophy, which is associated with inflammatory processes. Moreover, it is reported that repression of the NF-κB inhibitor system in an experimental model of TBI promoted neuronal cell death, worsened the neurological outcome, and increased the post-TBI mortality rate [55].

1.9 Cerebral Edema Formation

Cerebral edema is among the very significant secondary injury consequences of TBI and the leading cause of death in more than half of all deaths after severe TBI [11].

Understanding the development of cerebral edema is crucial because it considerably affects the high morbidity and mortality after TBI [2]. Post-traumatic cerebral edema caused the expansion of brain volume against an enclosed skull. It raised intracranial pressure inside the unyielding cranial cavity, causing herniation and reduced cerebral perfusion pressure, promoting cerebral ischemia. According to valid studies, cerebral edema results from a combination of endothelial cell damage, tight junction disruption, and abnormal transcellular transport due to vessel damage resulting in interstitial accumulation of plasma-derived, osmotically active molecules followed by water. Cerebral edema could also be caused by changes in cell metabolism and the failure of membrane-associated pumps and ion transporters, resulting in the cellular accumulation of osmotically active molecules followed by water [2].

1.10 Oxidative Stress and Influence of Cigarette Smoking on the Pathophysiology of Traumatic Brain Injury

Excessive ROS production following cell damage, neuronal cell death, and brain dysfunction result from several secondary biochemical and metabolic changes in the cells [19]. OS, which results from the uncontrolled generation of ROS, has been known as the major pathophysiological mechanism responsible for secondary injury post-TBI. Post-traumatic OS leads to the peroxidation of membrane polyunsaturated fatty acids, protein carbonylation, and DNA oxidation through ROS, which may affect BBB permeability and fluidity, leading to membrane damage and eventual apoptosis and tissue necrosis [56-58]. Antioxidant mechanisms, including superoxide dehydrogenase, catalase, and peroxidases, are often detrimentally affected by TBI, which leads to increased oxidative injury [59]. There is evidence that the interstitial level of hydroxyl radicals increases

rapidly after TBI, and it may play a significant role in the lipid peroxidation of the membrane, eventually causing highly active aldehydes, such as 4-hydroxynonenal (4-HNE). Several *in vitro* and *in vivo* models of the BBB have shown that 4-HNE significantly increases BBB permeability. At the same time, the administration of lipid peroxidation inhibitors reduces the post-traumatic increase in BBB permeability. Normal BBB function is highly dependent on the ability of BBB to protect themselves from noxious effects of ROS through endogenous molecules such as glutathione (GSH). The pharmacological depletion of GSH significantly increases the paracellular BBB to low molecular weight substances. The exposure of the BBB to a mixture of ROS predominantly containing superoxide anion radicals (produced as a result of NADPH oxidase (Nox) upregulation), hydroxyl radicals, and hydrogen peroxide were shown to rapidly increase the BBB permeability. The loss of BBB integrity was associated with the redistribution and degradation of tight junctional proteins, DNA degradation, and lipid peroxidation [13,58]. It is well known that nitric oxide rapidly reacts with superoxide anion radicals, resulting in various free radicals and eventually OS. Although the cerebrovascular endothelium itself produces nitric oxide in small quantities, the moderate to high nitric oxide exposure significantly promotes the paracellular permeability of BBB. Moreover, OS may play a significant role in promoting post-traumatic neuroinflammation as a result of increased adhesion and migration of monocytic cells as well as the expression of intercellular adhesion molecules across the endothelial monolayers. Furthermore, bradykinin is known as a ROS production promoter, so it activates phospholipase A2, which induces Nox activity, further leading to ROS

production [20]. It has been proven that Nox inhibitors reduce inflammation, neuronal degeneration, OS, and cerebral edema post-TBI [60]. According to recent studies, NRF2 plays a significant neuroprotective role in TBI and other neurodegenerative disorders so that NRF2 activation counteracts TBI-induced OS, loss of BBB integrity, etc. [15,17]. Unsurprisingly, impairments of the NRF2–ARE signaling pathway leading to the reduced activity of this protective system can lead to more extensive post-TBI tissue damage, thus aggravating the secondary injury and worsening the outcome. Accordingly, the upregulation of NRF2 expression could be exploited to reduce post-TBI outcomes. TBI-induced brain damage provides a viable strategy to treat post-traumatic brain injuries, improve clinical outcomes, and reduce the risk of other neurological disorders by reducing OS and post-traumatic inflammatory responses [61-63].

1.11 Role of NRF2 in Blood-Brain Barrier Integrity, Traumatic Brain Injury, and Tobacco Smoke-induced Cerebrovascular Disorders

NRF2 (a member of the Cap-n-Collar family of basic leucine zipper proteins) as a ubiquitously expressed redox-sensitive transcription factor, primarily modulates the activation of biological systems encompassing anti-inflammatory molecules, antioxidants (such as thioredoxin, glutathione, and others), phase I & II drug metabolizing enzymes (such as cytochrome P450s), phase III enzymes (efflux transporters), and free radical scavengers [64-68]. Consequently, cell vulnerability to the detrimental effects of ROS and OS damage to mitochondrial function (leading to cell apoptosis) are enhanced by down-regulation or suppression of NRF2 activity [69]. Cellular OS initiates a sequence of biological responses so that NRF2 (residing in the cytoplasm at a low basal level) translocates into the nucleus [70], where it forms a heterodimer with small Maf proteins

(MafG, MafK, MafF). Coupling with Mafs endows NRF2 with a DNA-linking capacity to bind to the ARE sequence and initiate the transcription of ROS detoxification genes [71]. Since NRF2 is likely to control, modulate and sustain the expression of detoxification and antioxidative response elements and other types of protective elements (which include the ubiquitary iron exporter ferroportin 1, anti-apoptotic B-cell lymphoma 2, brain-derived neurotrophic factors, the peroxisome proliferator-activated receptor gamma coactivator 1-alpha (PGC-1α), the mitochondrial-nuclear respiratory factor 1 (NRF1), and the autophagic protein p62) [72,73], its activation plays a considerable role in counteracting acute injuries, effects of xenobiotics, inflammation, and many other stimuli that are promoted by OS [70]. Concerning OS being implicated in several pathologies, current research focuses on the pathogenic mechanisms leading to mitochondrial dysfunction and redox imbalance.

In the CNS, the vascular endothelium acquires specific characteristics and functions that differ from other vascular beds. This specialized endothelium which forms the BBB, becomes a dynamic functional interface between the blood and the brain, which strictly regulates the passage of substances, maintains the brain homeostasis, and protects the brain from pathogens as well as endogenous and xenobiotic substances [74]. According to numerous studies, there is a relationship between NRF2 and BBB relevant to cerebrovascular disorders, so NRF2 signaling plays a neurovascular protective role in conserving the BBB and CNS [64,67,75]. Concerning BBB endothelium, it has been emphasized that NRF2 upregulates the expression of tight junctional proteins (TJ), promotes redox metabolic functions, and produces ATP with mitochondrial biogenesis

[67,75-77]. Recently published data from side-by-side experiments investigating the impact of electronic cigarettes (EC) vs. TS on mouse primary brain microvascular endothelial cells (BMVEC) clearly showed that OS promoted by 24h exposure to EC extracts was not dissimilar from that induced by TS. NRF2 was similarly strongly activated and promoted upregulation of its downstream signaling molecule NAD(P)H quinone dehydrogenase 1(NQO-1) [78]. NQO-1 exerts acute detoxification and cytoprotective functions, and its activity may be compromised by chronic oxidative insults. These data suggested an overall impairment of BBB integrity confirmed increased permeability to paracellular markers and decreased trans-endothelial electrical resistance (TEER) [75,79]. In addition to the loss of BBB integrity, *in vivo* data also showed upregulation of inflammatory markers, including vascular adhesion molecules and pro-inflammatory cytokines, as well as blood hemostasis changes favoring blood coagulation and, therefore, risk of stroke. Recent preliminary data and work by others have also clearly demonstrated that NRF2 modulates mitochondrial biogenesis, redox metabolism, and antioxidant/detoxification functions, thus strongly suggesting that impairment of NRF2 activity can negatively affect mitochondrial biogenesis and function [77]. Altogether, these studies have shown that NRF2 plays a major role in critical BBB cellular functions ranging from modulation of barrier integrity, inflammatory responses, redox metabolism, and antioxidative responses [63,68,75,78,80-82]. In fact, cerebrovascular and neurodegenerative disorders such as subarachnoid brain hemorrhage, MS, ALS, AD, PD, Stroke, and Type-2 diabetes mellitus (TD2M) have been tied to dysfunctions of NRF2 activity [67,68,83]. Not surprisingly, the activation of the NRF2-

ARE system can be considered as a potential to prevent/reduce BBB impairments and, consequently, decrease brain injury [84]. Since vascular endothelial dysfunction and consequent CNS damages have been relevant to ROS [85-87] and OS-driven inflammation [88], NRF2 activation is likely to preserve the BBB by maintaining ROS homeostasis, which ultimately leads to a decrease in the risk of cerebrovascular, neurodegenerative and CNS disorders [84,89-92]. For instance, the well-known NRF2 promoter/activator Sulforaphane (SFN) has been shown to have neuroprotective characteristics that counteract OS by enhancing NRF2 activation [84,93-96] and regulating antioxidant reactions [71].

With respect to TBI, disruption in the normal brain function following TBI is one of the foremost causes of death, as well as severe emotional, physical, and cognitive impairments [4,74,97]. Despite the pathogenic role of the primary brain injury immediate to TBI, the post-traumatic secondary injury derived from OS, inflammation, excitotoxicity, enhanced vascular permeability, and BBB impairment can significantly worsen post-traumatic brain damage as well as the clinical outcome [17,18]. Excessive ROS generation following cell damage, neuronal cell death, and brain dysfunction result from several secondary biochemical and metabolic changes in the cells. According to recent studies, NRF2 plays a neuroprotective role in TBI, so NRF2 activation counteracts TBI-induced OS, loss of BBB integrity, etc. Not surprising, impairments of the NRF2-ARE signaling pathway leading to reduced activity of this protective system can result in more extensive post-TBI tissue damage, thus aggravating the secondary injury and worsening the outcome. Accordingly, promoting upregulation of NRF2 activity could be

considered a clinical pathway to reduce post-traumatic brain injuries, improve clinical outcomes and reduce the risk of other neurological disorders [61,98].

Cerebrovascular and BBB dysfunction promoted by TS are also associated with the initiation of various neurovascular and neurodegenerative diseases linked to dysregulation of NRF2 activity, such as stroke, vascular dementia, and previously noted neurogenerative disorders [75,89,99]. This is not surprising since TS contains over 7000 chemicals, including nicotine and ROS (e.g., H_2O_2, epoxides, nitrogen dioxide, peroxynitrite - $ONOO^-$, etc.), which cross the alveolar lung wall and raise systemic OS. At the cerebrovascular level, this promotes oxidative damage and BBB breakdown via tight junction (TJ) modification and activating proinflammatory pathways [67]. Under normal conditions, ROS are scavenged by endogenous antioxidants involving vitamins such as ascorbic acid and α-tocopherol or intracellularly converted into less reactive molecules by superoxide dismutase (SOD), catalase (CAT), and glutathione peroxidase. However, containing excessive pro-oxidant substances, chronic exposure to active and passive smoking can overwhelm these protective mechanisms. Furthermore, the protective nature of NRF2 may be altered in smokers through somatic mutation, epigenetic alteration, and accumulation of disruptor proteins, thereby promoting cell resistance and proliferation of cancerous cells as indicated by other studies[75]. According to several recent studies, NRF2 enhancers can counteract OS and possibly decrease the burden of neuropathologies, including ischemic and cerebral stroke [78,89,100]. Recently Prasad et al. have confirmed the upregulation of NRF2 upon acute TS/EC exposure and its impact on mitochondria biogenesis and bioenergetic functions at

the BBB. Their results confirmed the positive role of NRF2 in regulating the redox metabolic interplay that triggers the expression of antioxidative active elements and, ultimately, the protection of the BBB against OS damage [75]. NRF2 nuclear translocation and increased transcription of detoxifying enzymes and antioxidants effectively protect against chronic TS exposure [78]. However, they demonstrated impairment of NRF2 activity by chronic TS exposure resulting in a suboptimal antioxidative response and consequent cellular OS damage. In contrast, acute exposure to TS and vapors from EC initially enhances NRF2 expression and activation [67,75,76,89]. This facet of chronic TS and EC exposure and their effect on the NRF2-ARE system needs to be considered due to remaining early-stage former smokers at high risk of developing cerebrovascular disorders for years after quitting [99]. Similar results have been observed in our recent work confirming TS/EC induced cerebrovascular dysfunction and possibly other detrimental xenobiotics affects the BBB via OS [26] (see also Fig. 1.3).

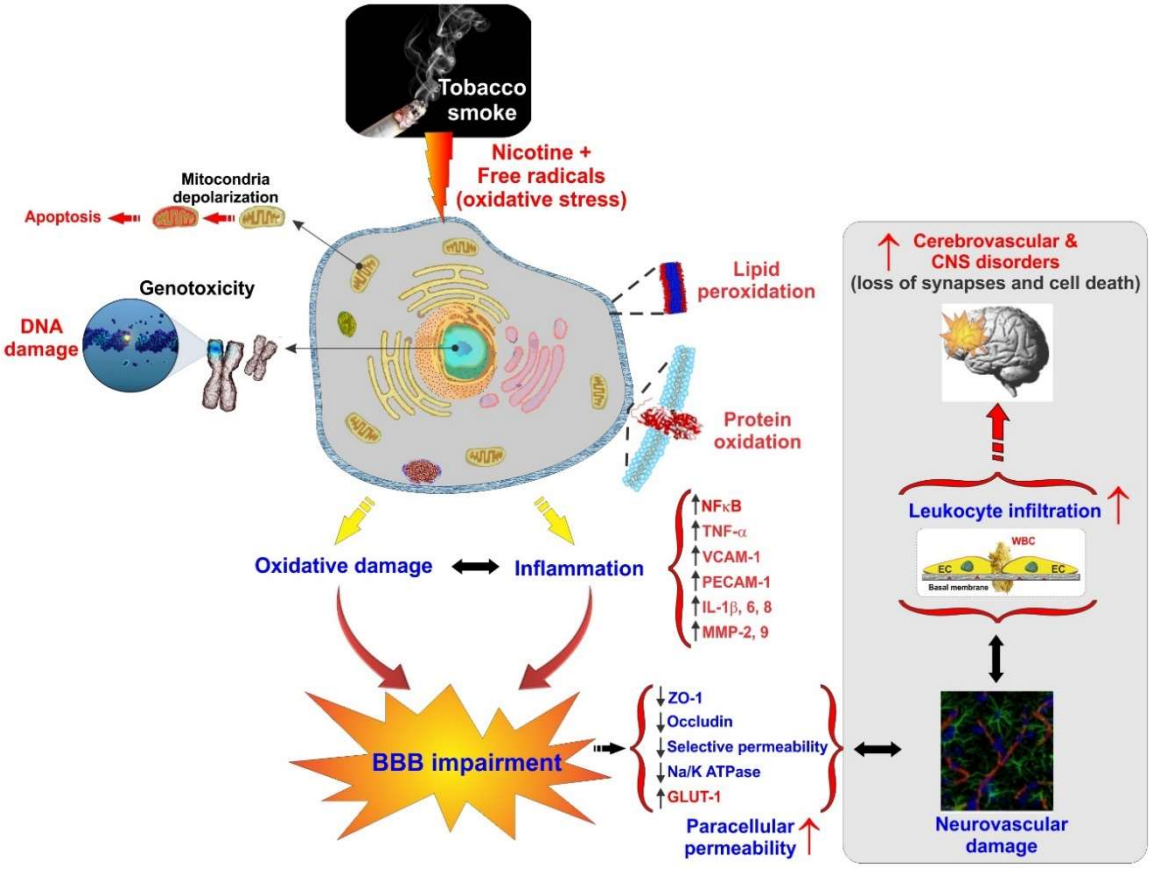

Figure 1.3 Schematic illustration of the impact of smoking on BBB impairment and the onset of cerebrovascular and CNS disorders [15].

1.12 NRF2 Enhancers for the Treatment of Cerebrovascular Disorders: Repurposing of Antidiabetic Drugs

Recent studies have provided several dietary and therapeutic agents currently approved for the treatment of non-vascular and non-neurodegenerative pathologies that, on the contrary, do possess protective effects against the initiation/progression of neurodegenerative [101] and cerebrovascular diseases [75,78]. Metformin (MF), an oral anti-hyperglycemic agent, not only enhances neurogenesis for the injured or degenerating neurovasculature, but also reduces BBB disruption and decrease/inhibit ischemic injury upon stroke and impairment in neurodegenerative disorders [102-106]. MF has been shown to activate counteractive mechanisms which drastically reduce OS toxicity at the cerebrovascular and BBB levels, such as those promoted by chronic TS exposure [75,79]. These beneficial effects are seemingly mediated by MF‘s activation of NRF2 [102] and include suppression of TJ proteins, downregulation and loss of BBB integrity by CS, reduction of inflammation and OS, a renormalization of the expression levels of the major BBB glucose transporter Glut-1 and that of the anticoagulant factor thrombomodulin. Both AMPK-dependent and independent mechanisms are known to be involved in the mechanism of action of MF [107]. According to a study by Montalvo et al., treatment with MF resulted in an increased lifespan of aging mice brought about by increased antioxidant property and AMPK activation. In addition, pre-treatment with MF has been discovered in distinct research to avoid ischemia-induced brain injury by activating the AMPK and NRF2 signaling pathways and promoting rearrangement with ZO-1, Occludin, and Claudin-5 [102,103]. Recently our team showed that pretreatment with MF *in vitro* prevented downregulation of the CSE-induced tight junction protein

(ZO-1 and Occludin) and induced activation of the NRF2 and AMPK signaling pathways, although our studies indicate that activation of NRF2 (upregulation and translocation to the nucleus) is not exclusively related to activation of AMPK [75].

MF also has shown a neuroprotective effect on TS-induced cerebrovascular/BBB impairments to diminish the cerebrovascular toxicity accounting for a functional role of NRF2 and NRF2-ARE signaling pathways in protecting BBB integrity in chronically TS-exposed human BBB microvascular endothelial cells [67,75,76,89,102]. A recent study also demonstrated that treatment with MF in TS-exposed mice restored NRF2 and NQO1 to control levels in a dose-dependent manner. Along with these effects, TJ proteins ZO-1 and Occludin levels were also restored [79]. In supporting the neuroprotective effect of anti-diabetic drug against OS in another study, Rosiglitazone (RSG) is a thiazolidinedione compound used for the treatment of TD2M that is well known to improve insulin resistance by regulating adiponectin gene expression. RSG is also considered a transcription factor peroxisome proliferator-activated receptor (PPARγ) agonist**.** Although the exact mechanism of action of RSG is not fully understood, recent studies have shown that this drug also possesses antioxidative features and can protect against OS damage and inhibit the inflammatory cascade through signaling inactivation by p38, JNK, and NF-κB [108,109]. Recently, Ceolotto et al. demonstrated that RSG protects endothelial cells against glucose-induced OS with an AMPK-dependent mechanism [26]. AMPK has been shown to promote NRF2 activity via nuclear accumulation, implying that RSG-mediated upregulation of PPARγ can also be associated with increased NRF2 activity[110]. In another study, Kadam et al. observed

upregulation of NRF2 and its downstream target HO-1 and downregulation of Toll-like receptor 4 (Tlr4) following RSG administration[111]. Activation of Tlr4 promotes NF-κB activity, followed by pro-inflammatory cytokine production and the innate immune system stimulation. A very recent study by our group has shown that RSG can seemingly mediate NRF2 upregulation and activation through upregulation of PPARγ expression[26]. Our data strongly suggest the possibility for a PPARγ-mediated mechanism of NRF2 upregulation/activation leading to the repairing of BBB integrity, decreased endothelial inflammatory responses and upregulation of NRF2 downstream signaling molecule NQO-1, which exert acute detoxification and cytoprotective functions [75]. Along this line, it is conceivable that other drugs presenting similar NRF2 enhancing effects could be repurposed to treat OS and pro-inflammatory-dependent cerebrovascular and neurological disorders.

CHAPTER TWO

CEREBROVASCULAR AND NEUROLOGICAL IMPACT OF CHRONIC TOBACCO SMOKING ON POST-TRAUMATIC BRAIN INJURY

2.1 Introduction

Despite the epidemiological and translational studies strongly suggesting activation of pathophysiological pathways by TS that exacerbate TBI outcome and influence recovery, determination and characterization of shared key modulators in BBB impairment due to TS and TBI lies unexplored. In fact, the underlying mechanisms and characterization of shared critical mediators of BBB impairment caused by TBI and TS have not been thoroughly evaluated. Identifying and then targeting these putative key modulators could help prevent the initiation of metabolic/cerebrovascular complications due to TBI in smokers. Thus, the goal of the present study was to characterize the pathogenic impact of chronic smoking on TBI and assess the post-traumatic exacerbation of TBI by studying key established pathological parameters leading to loss of BBB function and integrity. For this purpose, in this chapter, we investigated the effect of premorbid TS exposure on post-traumatic microvascular damage using an *in vitro* BBB endothelial traumatic injury model generated from Primary brain microvascular endothelial cells (mBMEC). We also used a well-established weight-drop TBI mice model to test the impact of premorbid TS exposure on post-TBI injury and recovery animals with or without chronic pre-exposure to TS. We believe that a better understanding of TS potential influence on TBI can facilitate the development of more

targeted and effective interventions to improve post-traumatic outcomes and reduce the impact of chronic smoking. This latter is of paramount importance for patients that cannot quit smoking. Furthermore, subjects who have recently stopped smoking remain at high risk of cerebrovascular disorders and worse secondary brain injury outcomes (due to the lingering effect of chronic smoking) for a relatively long period.

2.2 Methods

2.2.1 Reagents and Materials

Reagents and chemicals were purchased from Sigma-Aldrich (St. Louis, MO, USA) or Bio-Rad Laboratories (Hercules, CA, USA). All Quantikine ELISA kits were purchased from R & D systems; The antibodies used in this study were obtained from various sources: mouse anti-Claudin-5 (#352500), rabbit anti- NRF2 (#PA5-88084), rabbit anti-ZO-1 (#402200) and mouse anti-Occludin (#331500) were purchased from Invitrogen; mouse anti-PECAM-1 (#sc-376764), mouse anti-VCAM-1 (#sc-13160), mouse anti-NQO-1 (#sc-376023), mouse anti-HO1 (#sc-390991) and mouse anti-NFκB-p65 (#sc-(F-6)-8008) from Santa Cruz Biotechnology. Donkey anti-rabbit (#NA934) and sheep anti-mouse (#NA931) HRP-linked secondary antibodies were obtained from GE Healthcare (Piscataway, NJ, USA). Primary brain microvascular endothelial cells from C57 mice (C57BL/6-mBMEC, #C57- 6023) and complete mouse endothelial cell medium (M1168) were acquired from Cell Biologics (Chicago, Illinois, USA). Quantikine ELISA kits were obtained from R & D systems (Minneapolis, MN, USA). Subcellular Protein Fractionation and Pierce BCA Protein Assay Kits (respectively #78840 and #23225) were purchased from Thermo Scientific.

2.2.2 Cell Culture

mBMEC cells were seeded on 6-wells plates containing fresh supplemented medium with 10% FBS for a final total volume of 2 ml/well. All cell cultures were maintained in an incubator at 37 °C, 95% humidity, and 5% CO_2 [75]. Culture media was changed every 48 hours until the cells reached full confluency.

2.2.3 Soluble Cigarette Smoke Extract Preparation

Standardized 3R4F research cigarettes obtained from the National Institute on Drug abuse (NIDA) were used to prepare the soluble TS extract as previously described by our group using a computer-controlled Single Cigarette Smoking Machine (SCSM) acquired from CH Technologies Inc. (Westwood, NJ, USA) (35 mL puff volume, 2 s puff duration, 58 s intervals, 8 puffs per cigarette directly into phosphate-buffered saline (PBS), equivalent to full flavor brands containing 9.4 mg tar and 0.726 mg nicotine/cigarette) [26,75,112]. For each exposure cycle, freshly prepared TS extract was diluted to 5% (V/V) concentrations in culture medium containing 1% FBS.

2.2.4 Induction of Traumatic Endothelial Injury *in Vitro*

Confluent mBMEC-P5 cultures were manually scratched, as previously described in several published studies [6]. In brief, every 6-well plate was scratched manually using a sterile plastic pipette tip matching a 9 × 9 square grid with an inter-lines space of 4 mm. Without changing the media, cell cultures were then stored back in the incubator for another 24 hrs and maintained at 37 °C under normoxic conditions. Parallel uninduced cultures were prepared as controls.

2.2.5 *In Vivo* Experimental Design

The experiment protocol in this study was abided by the Institutional Animal Care and Use Committee, TTUHSC, Lubbock, Texas [75]. C57BL/6J male mice, ranging between 6–8 weeks old and a bodyweight of 20–22 g) were purchased from Jackson Laboratory. Mice were divided into four major groups (6 animals/group), including control, TBI, smoke (TS-exposed animals), and smoke + TBI. Animals were given three days for acclimatization post-arrival in the new location to recovery from the transport. All mice were given unlimited access to standard mouse chow and water. Of these mice, the smoke only and smoke + TBI test groups were chronically and simultaneously exposed (via direct inhalation) to sidestream smoke derived from 3R4F standardized research cigarettes (9.4 mg tar and 0.726 mg nicotine/cigarette equivalent to full flavor commercial products). Sidestream smoke was generated using a Single Cigarette Smoking Machines (SCSM, CH Technologies Inc., Westwood, NJ, USA) following previously published methods [75,79] (see also Fig. 2.1). Animals were exposed to TS mixed with oxygenated air six times/day; 2 cigarettes/hour, 6–8 h/day, seven days/week for three weeks according to the International Organization for Standardization/ Federal Trade Commission (ISO/FTC) standard smoking protocol. This consists of 35 ml puff volume, 2 s puff duration, 58 s intervals, and eight puffs per cigarette [112]. Control and TBI animal groups underwent the same operational procedure (to minimize the variability impact of the process itself on behavioral assessments) but were exposed to oxygenated air [79].

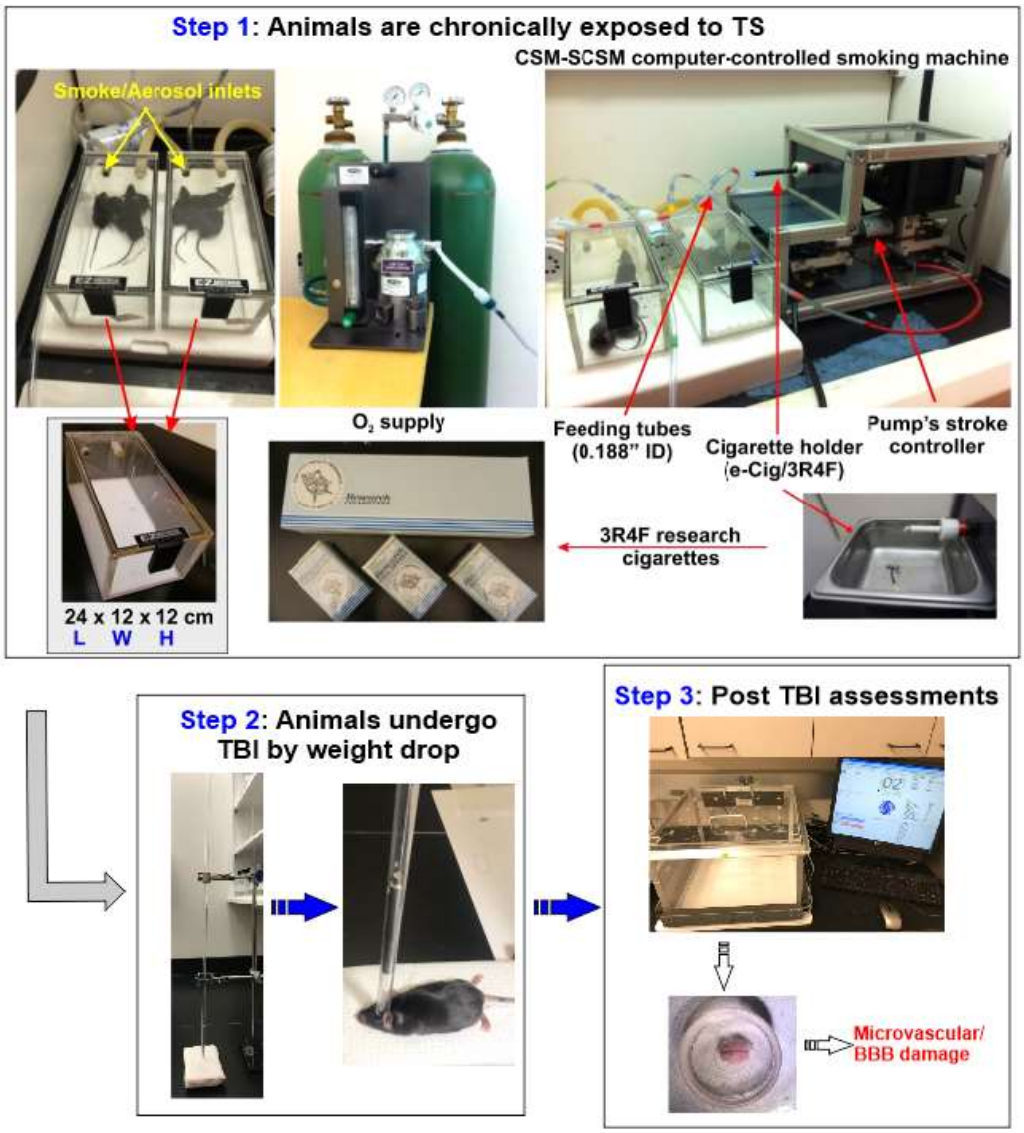

Figure 2.1 Experimental flow and setup, including cigarette smoke generation, animal exposure, induction of traumatic brain injury, and post-traumatic assessment of motor activity.C57BL/6J mice were chronically exposed to TS (full body side stream exposure) for three weeks using a computer-controlled single cigarette smoking machine using the FTC-approved smoking protocol. Test animals were subjected to TBI by head weight (30g) drop from an 80 cm height through a pre-positioned vertical guide. Physical activity and weight of the mice were analyzed before TBI and at 1h, 24h, and 72h after TBI using an open-field test. Finally, mice were sacrificed to collect blood and brain samples for subsequent biochemical and molecular analysis.

2.2.6 Induction of Head Injury in Mice

We used a weight-drop model of TBI [10]. This model was developed to mimic human closed head injury by a standardized weight-drop device inducing a focal blunt trauma over an intact skull without pre-injury manipulations. The impact triggers a robust neuroinflammatory response (highly reproducible), BBB breakdown, and neurological impairment. In brief, mice were first anesthetized by inhaling Isoflurane vapor for 3 to 5 minutes and then placed on a spongy platform under the weight-drop device. Head movements were allowed parallel to the injury plane at the induction time to mimic a mild- to moderate head injury. During the induction phase, mice were positioned to direct the trauma from the left anterior frontal area at the same distance between the eye and the ear. A hollow tube (with an internal diameter of 13 mm) was used as the guiding system for a metal weight (30 g) released in a free fall from the dropping point positioned 80 cm above the target (Fig. 2.1). The sham-injured mice underwent the same procedures with the exclusion of being subjected to head impact by weight drop.

2.2.7 Open Field Test

Open field test is a standard measure of rodents' exploratory behavior and general activity. Briefly, mice were housed in a 16″ × 16″ unobstructed glass chamber containing infrared sensors along the perimeter. Then the mice were monitored and recorded for one h. The first 30 min were excluded as the acclimatization period (Fig. 2.1). Automatic calculation of the activity (total distance traveled) and resting time of the animals was performed by Versamax software (Accuscan Instruments., Columbus, OH).

2.2.8 Blood Collection and Brain Isolation

Mice were sacrificed under terminal anesthesia three days after TBI to collect blood samples and brains for subsequent biochemical and molecular analysis. Blood samples were collected by cardiac puncture as described elsewhere. Briefly, mice were positioned on their back. All animals were anesthetized with inhaled isoflurane (4% induction; 1-1.5% maintenance) to minimize discomfort, distress, and pain. Then a V-cut was made through the skin and abdominal wall, and internal organs were moved to the side. The needle was inserted through the diaphragm and into the heart. Blood was collected by applying negative pressure on the syringe plunger. To isolate the brain, we cut at the nape and then extended along the midline from the dorsal cervical area to the tip of the nose. The skin was then pulled away from the skull laterally. The skull was cut and opened by placing the point of the scissors in the foramen magnum and cutting along the midline. After levering away the parietal bones from the brain and disrupting the nerve attachments at the brain stem and the optic chiasm, the brain was removed from the skull into the sterile medium [22,75].

2.2.9 Preparation of Protein Extracts and Western Blotting (WB)

We harvested total proteins by RIPA lysis buffer to determine the protein expression levels based on the manufacturer's guidelines. The total protein content was collected by centrifugation at 14000g for 30 mins. Samples were then aliquoted and stored at −80 °C for subsequent protein expression analysis by WB. Protein quantification was conducted using Pierce BCA Protein Assay Kit (Thermo Scientific, # 23225). Samples (30 μg for cell lysate and 90 μg for tissue lysates) were prepared as

previously described by us [26,67,75]. Briefly, denatured samples were run on SDS-PAGE (4–15% gradient gel) and transferred to polyvinylidene fluoride (PVDF) membranes or nitrocellulose membranes for further blotting. The membranes were washed with Tween-Tris-buffered Saline (TTBS) (10 mmol/l Tris-HCl, pH 7.4, 150 mmol/l NaCl containing 0.1% Tween-20), then blocked for one h with Tween-TBS (containing 5% non-fat dry milk) and incubated overnight at 4 C with primary antibodies prepared in TTBS containing 5% bovine serum albumin (BSA). The following day, cells were washed and incubated with the secondary antibody prepared in Tween-TBS containing 5% BSA for 2h. The protein band densities were visualized using chemiluminescent reagents according to the manufacturer's instructions. We used Image Studio Lite Ver 3.1 for protein quantification analysis. All protein quantifications were adjusted for the corresponding β-actin level and reported as fold changes vs. control.

2.2.10 Enzyme-Linked Immunosorbent assay (ELISA)

The analysis of cell culture supernatant and blood samples collected from mice was done using Quantikine ELISA kits to determine the levels of thrombomodulin and inflammatory cytokines IL-6, TNF-α, and IL-10, as described by the manufacturer.

2.2.11 RNA Extraction and Quantitative Real-Time Polymerase Chain Reaction (RT-PCR)

Quantitative RT-PCR was performed according to the protocol used in our previous work [113,114]. Briefly, the total RNA was extracted from the mBMEC cells using an RNeasy plus mini kit as described in the manufacture’s protocol (Qiagen Inc, Santa Clarita, CA). Complementary DNA (cDNA) was synthesized using a superscript III first-strand synthesis system (obtained from Life Technologies, Carlsbad, CA). Gene

expression was determined by qPCR using an SYBR green-based fluorescence procedure. The primer pairs (see sequences in Table 2.1) were designed based on PubMed GenBank and synthesized by Integrative DNA technologies (Coralville, IA, USA). The RNA targets were amplificated using a Bio-Rad CFX96 Touch Real-Time PCR detection system.

2.2.12 Immunofluorescence Imaging (IF)

Immunofluorescence imaging was performed according to a protocol used in our previous work [113,114]. mBMEC cells cultured in double-well chamber slides were fixed in 4% formaldehyde (methanol-free) and permeabilized at 25 °C by 0.02% Triton 100X for 10 min. The slides were then set in blocking buffer at 25 °C for 1 h incubated with primary antibodies at 4 °C overnight. The following day, the slides were washed and stained with Alexa Fluor R 488 or 555 conjugated goat antibodies at 25 °C and mounted with DAPI mounting medium to show the nuclei locations. Slides were then photographed using an our EVOS M5000 Imaging System (Thermo Fisher, #AMF5000) following previously published procedurees [67,75]

Table 2.1 Forward and Reverse Primer Sequences (5' -3') for Quantitative RT-PCR.

Target Gene	Forward	Reverse
NRF2	5'- GGC TCA GCA CCT TGT ATC TT -3'	5'- CAC ATT GCC ATC TCT GGT TTG -3'
NQO-1	5'- GAG AAG AGC CCT GAT TGT ACT G -3'	5'- ACC TCC CAT CCT CTC TTC TT -3'
HO-1	5'- CTC CCT GTG TTT CCT TTC TCT C -3'	5'- GCT GCT GGT TTC AAA GTT CAG -3'
NF-kB	5'- AGA CAT CCT TCC GCA AAC TC -3'	5'- TAG GTC CTT CCT GCC CAT AA -3'
Claudin-5	5'- GGT GAA GTA GGC ACC AAA CT -3'	5'- TTT CTC CAG CTG CCC TTT C -3'
Occludin	5'- CAG CAG CAA TGG TAA CCT AGA G -3'	5'- CAC CTG TCG TGT AGT CTG TTT C -3'
VCAM-1	5'- GAG GGA GAC ACC GTC ATT ATC -3'	5'- CGA GCC ATC CAC AGA CTT TA -3'
PECAM-1	5'- CAA CAG AGC CAG CAG TAT GA -3'	5'- TGA CAA CCA CCG CAA TGA -3'
ZO-1	5'- CAT TAC GAC CCT GAA GAG GAT G -3'	5'- AGC AGG AAG ATG TGC AGA AG -3'
B-Actin	5'- GAG GTA TCC TGA CCC TGA AGT A -3'	5'- CAC ACG CAG CTC ATT GTA GA -3'

2.2.13 Cell Viability Assay

Tetrazolium 3-(4, 5-dimethyl thiazolyl-2)−2, 5- diphenyltetrazolium bromide (MTT) assay was used to assess the cells' viability [75]. Briefly, 24 h after TBI induction, 5 mg/ml of MTT was added to the cells seeded on 6-well plates and incubated for 3 h at 37 °C. Metabolically active cells converted the yellow MTT to purple formazan crystals. The formazan compound was solubilized using 1ml of DMSO, and the absorbance was then measured using a Bio-rad plate reader at 570 nm.

2.2.14 Measurement of Intracellular Reactive Oxygen Species Generation

Intracellular ROS was analyzed using 2,7-dichlorodihydrofluorescein diacetate (2,7-DCFH-DA). Briefly, cultured cells on 6-well plates were rinsed with cold PBS and incubated in 25 uM DCFHDA for 45 min at 37°C in the dark. Cells were then rinsed thrice with PBS and transferred to a 96-well black plate by scarping the wells' surface. The intensity of dichlorofluorescein (DCF) fluorescence was measured with a Bio-rad plate reader at specific excitation (Ex: 485 nm) and emission wavelengths (Em: 535 nm).

2.2.15 Glutathione Levels Measurement

Tissue and cell lysate were analyzed by Quantification Kit for Oxidized and Reduced Glutathione (Sigma Aldrich, St. Louis, MO, USA) according to the manufacturer's guidelines. For the quantitative determination, samples were prepared by lysis of total cell protein in T-PER lysis buffer followed by dilution of 1:50 for GSH analysis. In brief, a serial dilution of reduced (GSH) and oxidized glutathione (GSSG) stock standards were prepared along with assay mixtures for detection of GSH and total GSH using 100 X Thiol green stock solutions, assay buffer, and GSSG probe. A one-step

fluorometric reaction of the sample with the respective assay buffer was incubated for 30 minutes. Fluorescence intensity was assessed at Ex/Em of 490/520 nm. GSSG was determined by subtracting GSH from the total GSH. Finally, GSH was plotted against GSSG to obtain the GSH/GSSG ratio.

2.2.16 Statistical Analysis

All collected data were expressed as mean, standard ± deviation (SD). The sample size was chosen based on previous work by us and others to generate 80% power and a type 1 error rate = 0.05. The blind analysis was performed by one-way ANOVA using GraphPad Prism 9 Software Inc. (La Jolla, CA, USA). Post multiple comparison tests were performed as with Tukey's or Dunnett's test recommended by the software. P values < 0.05 were considered statistically significant.

2.3 Impact of Chronic Smoking on Traumatic Brain Microvascular Injury: *In Vitro* Study

2.3.1 Evaluation of Cell Viability Through MTT Cytotoxicity Assay

MTT cytotoxicity assay was performed to evaluate TS and TBI's effects based on cell toxicity and viability. As indicated in Fig. 2.2A, the viability of TS-exposed and TBI-induced cells significantly decreased compared to control.

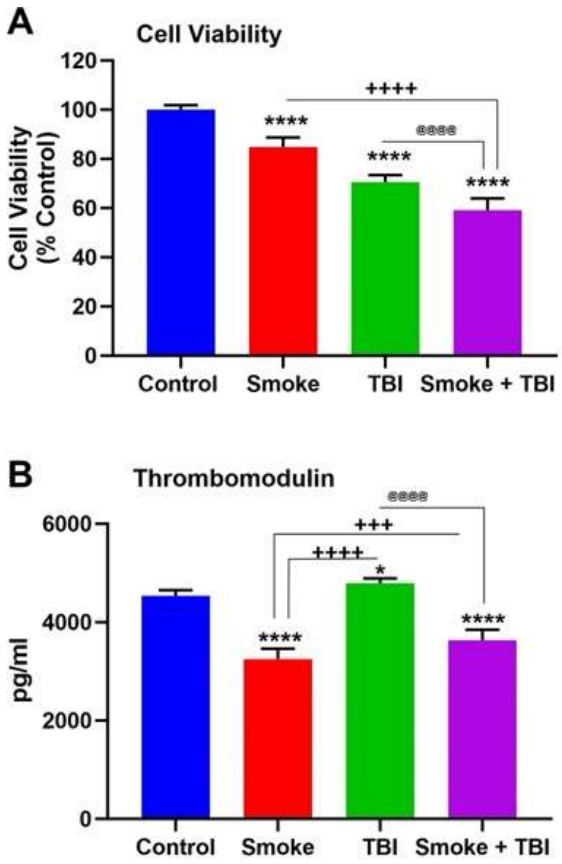

Figure 2.2 (A) MTT cytotoxicity assay for cell viability evaluation. (B) Effect of TS-exposure and TBI on level of Thrombomodulin.Levels of Thrombomodulin in the supernatants collected at 24h after TBI were measured by ELISA. TS-exposure promoted suppression of thrombomodulin and potentially impaired blood hemostasis. n = 6 biological replicates, *p < 0.05, **p < 0.01, ***p < 0.001, ****p < 0.0001 versus control. +p < 0.05, ++p < 0.01, +++p < 0.001, ++++p < 0.0001 versus smoked group. @p < 0.05, @@p < 0.01, @@@p < 0.001, @@@@p < 0.0001 versus TBI-induced group.

2.3.2 Tobacco Smoke-Exposure Increases the Inflammatory Endothelial Responses to Traumatic Injury While Possibly Affecting Blood Hemostasis

Chronic TS-exposure reduced the anticoagulant factor thrombomodulin expression level as previously recognized both *in vitro* and *in vivo* studies [75,79]. As shown in Fig. 2.2B, the TBI effect on the BBB endothelial cells was abolished by TS. This data suggests that TS can abolish the endothelial response to traumatic injuries and increase blood coagulation risk in TBI patients. We used a combination of WB, IF, and quantitative RT-PCR to assess changes in the expression levels of NF-kB (an essential modulator and inducer of inflammatory activities), inflammatory adhesion molecules, Platelet Endothelial Cell Adhesion Molecule 1 (PECAM-1), and Vascular Cell Adhesion Protein 1 (VCAM-1). As shown in Fig. 2.3A, we determined a remarkable NF-kB increase (protein expression and mRNA levels). In parallel, we also observed an increased expression of inflammatory cytokines, including IL-6 (Fig. 2.3B), IL-10 (Fig. 2.3C), and TNF-α (Fig. 2.3D). A similar trend was also noted when we assessed the expression levels of PECAM-1 (Fig. 2.4A) and VCAM-1 (Fig. 2.4B). Both TS and TBI as standalone stimuli can elicit an inflammatory response. However, this response was substantially enhanced in cell cultures exposed to co-stimulation (TBI + TS). This data suggests that TS exposure increases the vascular inflammatory response to traumatic injury.

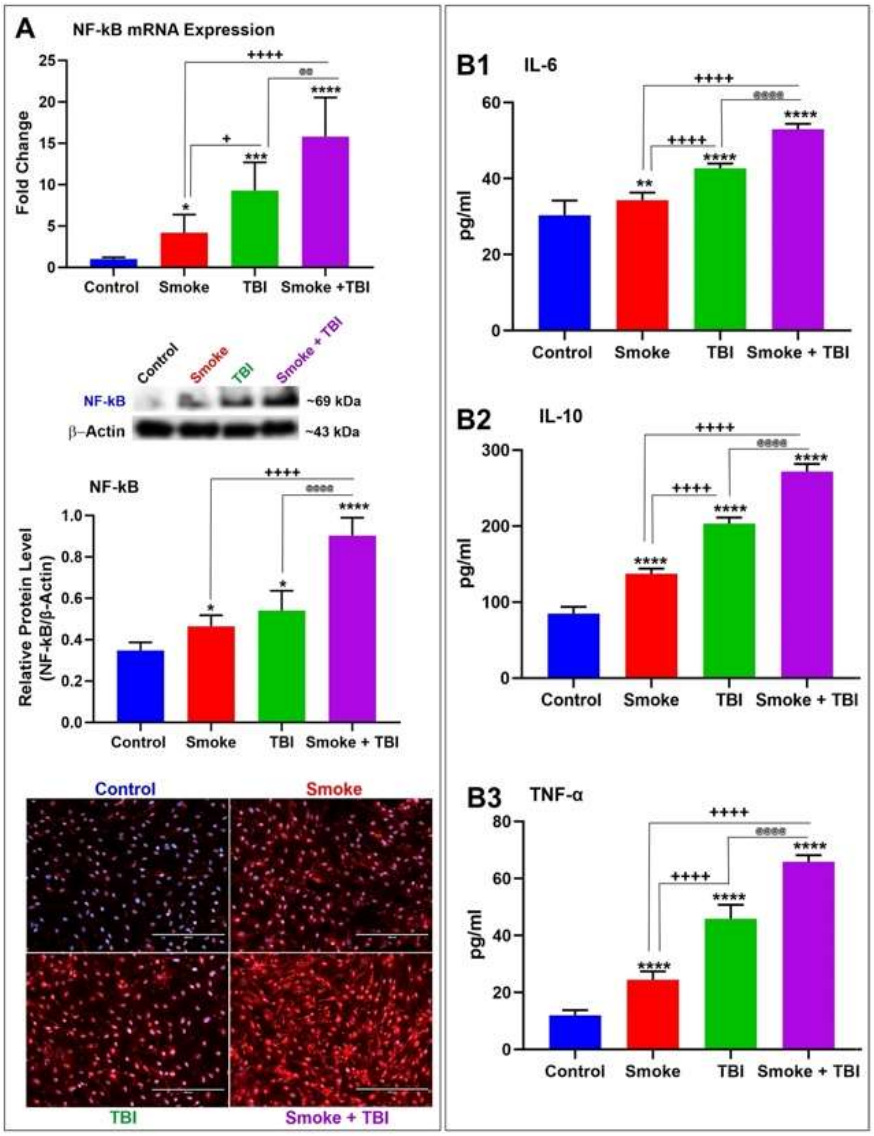

Figure 2.3 TS-exposure elicits a stronger inflammatory response at the BBB endothelium following traumatic injury.(A) TS-exposure and traumatic injury independently upregulated NF-kB. Also, note the combined effect of TS over Traumatic injury, which potentiated the inflammatory response. Results were assessed by WB, quantitative RT-PCR, and IF imaging. A similar trend was observed with respect to the expression levels of inflammatory cytokines (B1) IL-6, (B2) IL-10, and (B3) TNF-α. 24h after traumatic injury. n = 6 biological replicates, *p < 0.05, **p < 0.01, ***p < 0.001, ****p < 0.0001 versus control. +p < 0.05, ++p < 0.01, +++p < 0.001, ++++p < 0.0001 versus smoked group. @p < 0.05, @@p < 0.01, @@@p < 0.001, @@@@p < 0.0001 versus TBI-induced group. WB analyses express protein/β-actin ratios.

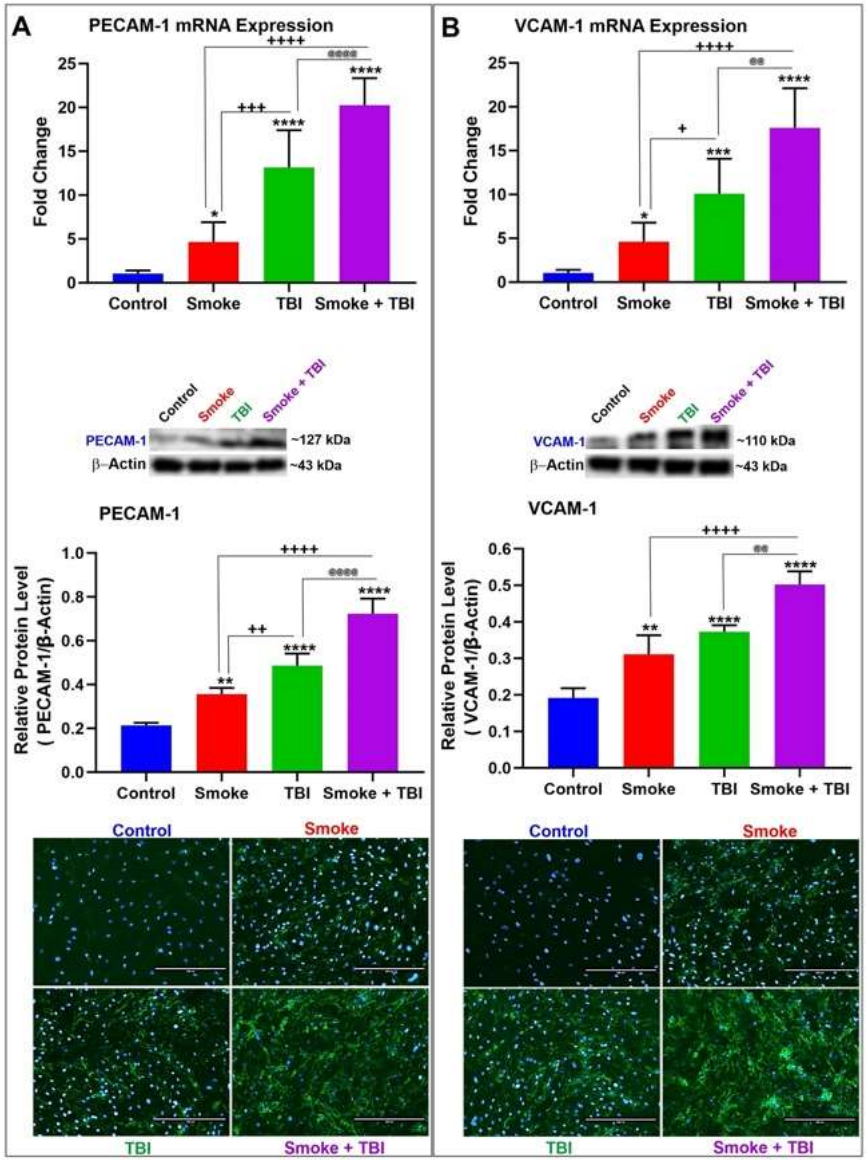

Figure 2.4 TS-exposure enhances the expression levels of inflammatory adhesion molecules PECAM-1 and VCAM-1 in BBB endothelial cells undergoing traumatic injury simulation.TS-exposure caused upregulation of PECAM-1 expression and was further enhanced by traumatic injury as shown by (A) WB, quantitative RT-PCR, and IF analyses. (B) A similar parallel trend was observed for VCAM-1. n = 6 biological replicates, *p < 0.05, **p < 0.01, ***p < 0.001, ****p < 0.0001 versus control. +p < 0.05, ++p < 0.01, +++p < 0.001, ++++p < 0.0001 versus smoked group. @p < 0.05, @@p < 0.01, @@@p < 0.001, @@@@p < 0.0001 versus TBI-induced group. WB analyses express protein/β-actin ratios.

2.3.3 Tobacco Smoke-Exposure Increases Reactive Oxygen Species Generation and Oxidative Stress

The intracellular ROS generation and glutathione levels were assessed to determine any possible relation between OS and cell-deteriorating effect. Measurements of total glutathione as GSH and GSSG (Total GSH + GSSG) were not different from controls across all the experimental settings (see Fig. 2.5A). However, as shown in Fig. 2.5B, intracellular ROS was significantly higher in TS-exposed samples and TBI-induced cultures. When TS pre-exposure was combined with traumatic injury, ROS generation reached the highest level measured across all the experimental settings. The effect was statistically significant compared to controls and TS and TBI as standalone conditions. The observed increase in intracellular ROS was paired with a substantial decrease in reduced glutathione (GSH, see Fig. 2.5C) and increased oxidated glutathione (GSSG, see Fig. 2.5D). This effect is noticeably in Fig. 2.5E showing the ratio of GSH/GSSG. Interestingly, TS-TBI co-stimulation produced a considerably higher amount of GSSG than either TS or TBI alone (Fig. 2.5D).

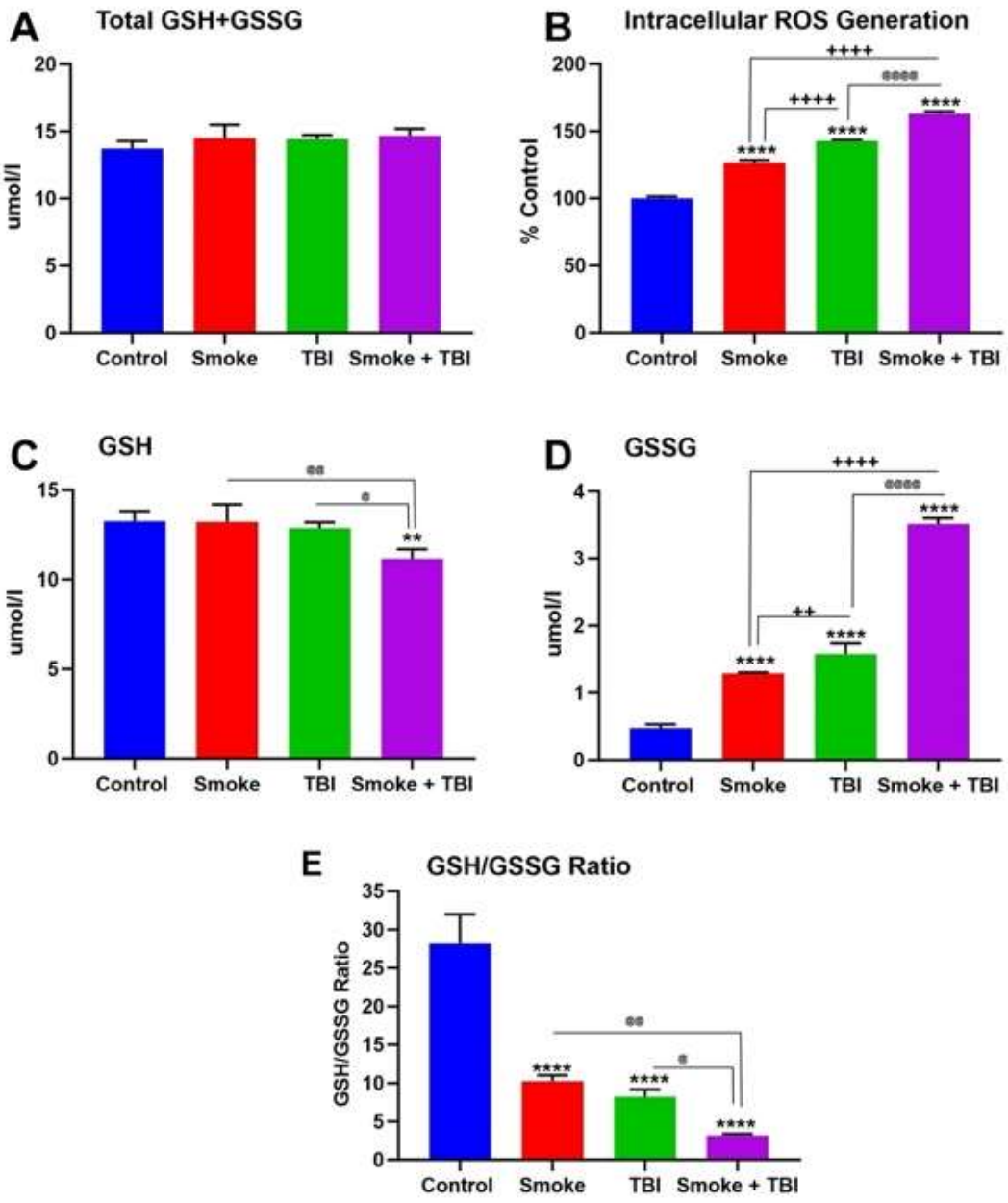

Figure 2.5 TS-exposure and TBI affected intracellular ROS generation and OS.(A) Total glutathione (GSH+ GSSG), (B) intracellular ROS generation, (C) reduced glutathione (GSH), (D) oxidized glutathione (GSSG) and (E) GSH/GSSG measured by plate reader. n = 6 biological replicates, *p < 0.05, **p < 0.01, ***p < 0.001, ****p < 0.0001 versus control. +p < 0.05, ++p < 0.01, +++p < 0.001, ++++p < 0.0001 versus smoked group. @p < 0.05, @@p < 0.01, @@@p < 0.001, @@@@p < 0.0001 versus TBI-induced group.

2.3.4 Tobacco Smoke-Exposure and Traumatic Brain Injury Downregulates NRF2 and its Detoxifying Effector Molecules HO-1 and NQO-1

The impact of TS-exposure and TBI on NRF2 expression was also investigated through a set of WB, IF, and quantitative RT-PCR analyses (see Fig. 2.6). Downregulation of NRF2 (protein and mRNA expression) as well as its immediate downstream detoxifying effector (see Fig. 2.6B & C) was indicative of impairment of the antioxidative response system (ARS) caused by chronic TS-exposure. Specifically, TS downregulated both Heme oxygenase-1 (HO-1; Fig. 2.6B) and NAD(P)H dehydrogenase [quinone] 1 (NQO-1; Fig. 2.6C). The effect was strong enough to counteract the cellular response to TBI, which produced a substantial upregulation of NRF2, but this response was significantly abrogated in cells previously exposed to TS.

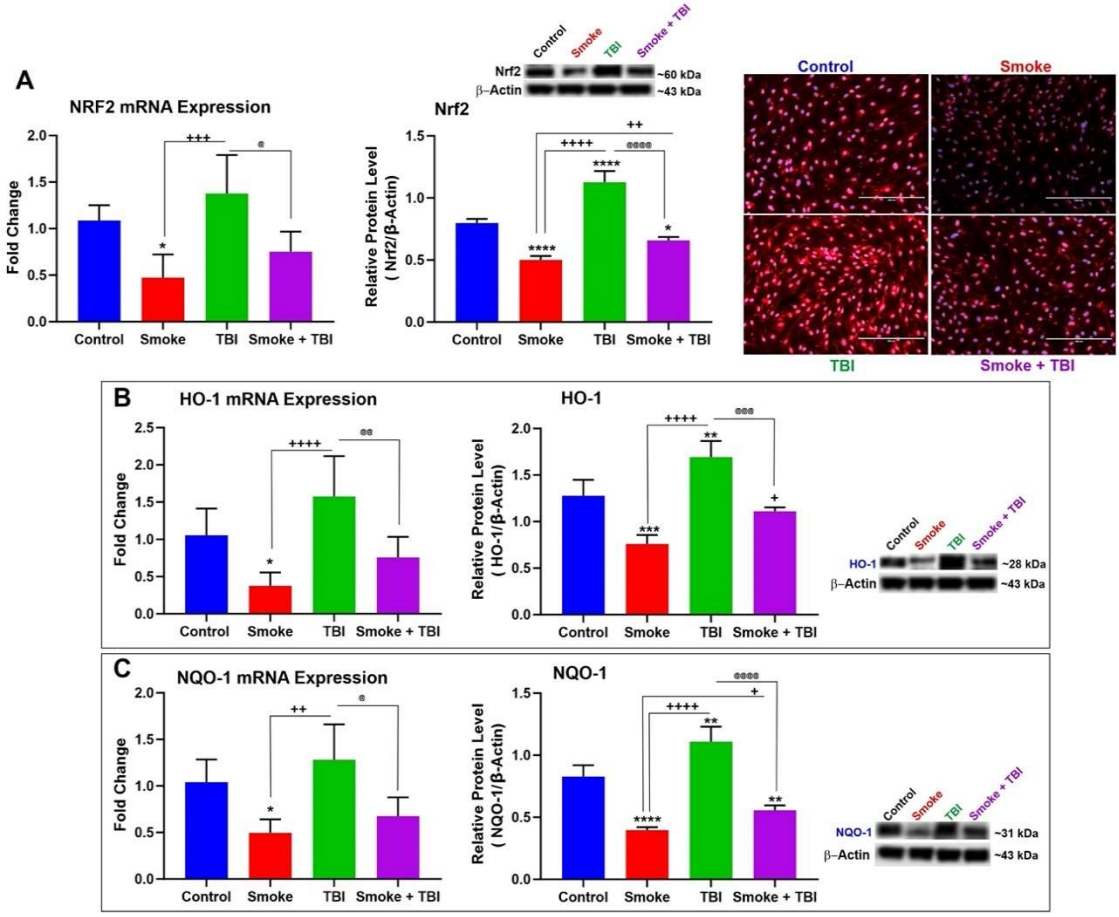

Figure 2.6 TS-exposure downregulated NRF2 and its downstream detoxifying effector molecules HO-1 and NQO-1 in BBB endothelial cells following traumatic injury simulation.(A) WB, quantitative RT-PCR, and (B) IF imaging analyses emphasized the role of chronic TS exposure in NRF2 expression level and synergism with TBI. Alternations in NRF2 expression levels were paralleled by corresponding changes of (B) HO-1 and (C) NQO-1. n = 6 biological replicates, *p < 0.05, **p < 0.01, ***p < 0.001, ****p < 0.0001 versus control. +p < 0.05, ++p < 0.01, +++p < 0.001, ++++p < 0.0001 versus smoked group. @p < 0.05, @@p < 0.01, @@@p < 0.001, @@@@p < 0.0001 versus TBI-induced group. WB analyses express protein/β-actin ratios.

2.3.5 Chronic Tobacco Smoke-Exposure Negatively Impacted Blood-Brain Barrier Integrity in Traumatic Brain Injury

We performed IF, WB, and quantitative RT-PCR analyses to assess TBI and TS exposure effect on BBB integrity. Particularly, we determine the expression level of zonula occludens-1 (ZO-1, a major BBB accessory protein) and tight junction (TJ) proteins primarily responsible for the low paracellular permeability of the BBB, such as Occludin and Claudin-5. Both the protein expression levels and the respective mRNAs were assessed. Exposure of mBMEC cells to TS downregulated ZO-1 expression and its mRNA when compared to controls (Fig. 2.7A). A similar trend was observed for Claudin-5 (Fig. 2.7B) and Occludin (Fig. 2.7C). Both protein levels and the respective mRNAs were considerably downregulated compared to controls. Although the TJ proteins expression was also slightly decreased by traumatic injury, our previous work supports the notion that TS is the main effector of the downregulation [67,75,112].

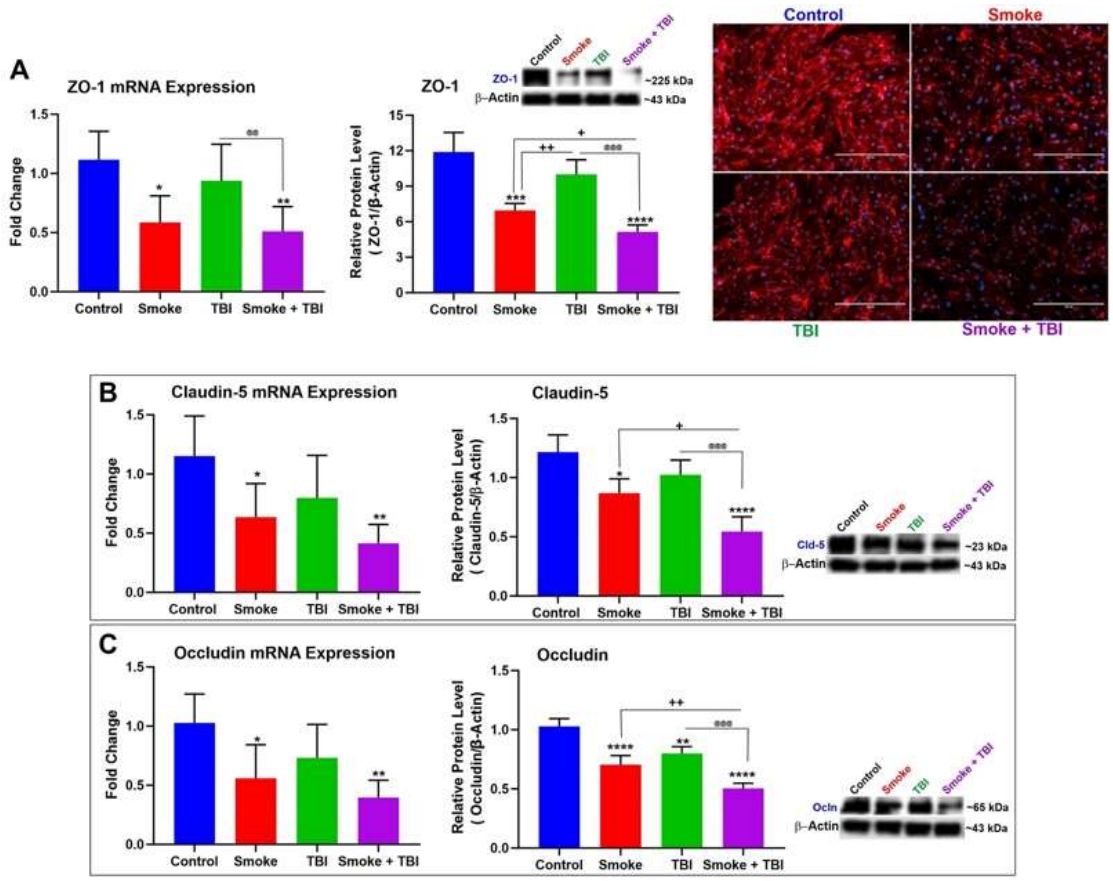

Figure 2.7 TS-exposure and TBI affected cytoplasmic accessory protein ZO-1 and TJ proteins Occludin and Claudin-5.(A) WB, quantitative RT-PCR, and IF imaging analyses demonstrate the downregulation of ZO-1 and its mRNA in cells exposed to TS and/or TBI. Data from WB and quantitative RT-PCR analyses demonstrated a similar downregulation of (B) Claudin-5 and (C) Occludin in cells exposed to TS and/or TBI. TBI as a standalone factor has a marginal effect compared to TS alone, thus suggesting TS's responsibility for TJ downregulation observed in TS-exposed cells subjected to TBI. n = 6 biological replicates, *p < 0.05, **p < 0.01, ***p < 0.001, ****p < 0.0001 versus control. +p < 0.05, ++p < 0.01, +++p < 0.001, ++++p < 0.0001 versus smoked group. @p < 0.05, @@p < 0.01, @@@p < 0.001, @@@@p < 0.0001 versus TBI-induced group. WB analyses express protein/β-actin ratios.

2.3.6 Discussion

The present work outlined the possible impact of chronic TS on the influence of TBI on brain microvascular endothelium. NRF2 is generally accepted as a key regulator of several protective responses that control the cellular redox status in response to detrimental stress. Normally NRF2 is confined in the cytoplasm by an NRF2 inhibitor known as Kelch-like ECH-associated protein 1 (Keap1). NRF2 is then ubiquitinated and processed for degradation. However, in response to oxidative/inflammatory stress conditions (endogenous and/or xenobiotics), it dissociates from Keap1 and translocates into the nucleus, where it binds to the antioxidant response element (ARE). NRF2 binding to the ARE stimulates the transcription of more than 500 genes. These genes include regulators of redox metabolism, phase 1 and 2 enzymes, antioxidative agents (such as NADH and glutathione), promoters of ATP production, and BBB TJs [77]. Promoting anti-inflammatory mediators, the proteasome's activity and other transcription factors modulating mitochondrial biogenesis are remarkable features of NRF2. Recent studies have shown that the downregulation of NRF2 activity and NRF2–ARE signaling pathway impairments aggravate the oxidative damage caused by TBI and post-traumatic neurological injuries. These findings crucially emphasize the prominent neuroprotective role of NRF2 in TBI and other cerebrovascular disorders [10,17]. Increased NRF2 activity help reduce the burden of TBI and improve TBI outcomes by protecting BBB integrity and reducing OS and inflammation [61-63,75,79,115]. The impact of premorbid TS-exposure and TBI on NRF2 and its effector molecules NQO-1 and HO-1 were evaluated according to these findings. Our *in vitro* data demonstrate that traumatic injury

activates the NRF2-ARE signaling pathway at the BBB endothelium (see Fig. 2.6). These data are consistent with previous studies, confirming TBI does indeed promote NRF2 expression and activity along with its downstream effectors NQO-1, and HO-1 [115,116]. In contrast, chronic TS exposure has the opposite effect [75,79]. This result further strengthens the notion of the beneficial role of NRF2 in preventing TBI exacerbation by TS. Our data suggest that NRF2 may provide a promising path toward developing more efficient therapeutic strategies against TBI. The sources of OS after TBI are cellular and molecular pathways getting activated in various cell types, including endothelial cells, microglia, and astrocytes [117,118]. The cumulative effect of ROS following TBI seems to promote brain damage, leading to neuron loss, propagation of inflammation, increased cerebral blood flow, and a loss of autoregulatory function [119]. Measurements of intracellular ROS production and levels of GSH and GSSG confirmed the relation between OS and TBI (see Fig. 2.5). The data revealed that TS-exposure is responsible for a statistically significant increase in intracellular ROS production (see Fig. 2.5B), as well as a substantial decline in GSH levels (see Fig. 2.5C). Besides, the combined effect of TS-exposure with traumatic injury leads to a much more sizable rise of intracellular ROS, coupled with a significant fall of reduced glutathione (GSH) and a surge of its oxidated form (GSSG) (see Fig. 2.5E). The GSH level in TBI does not decline significantly when compared to controls (see Fig. 2.5C), which might be caused by the TBI-responsive upregulation of NRF2 since GSH production depends on the NRF2 activity promoting glutathione synthesis and antioxidative effects [77]. Taken together, TS-exposure, as a comorbid stimulus combined with traumatic injury, abolishes the post-traumatic

activation/upregulation of NRF2 and prevents this physiological recovery system's activation. NRF2 downregulation is responsible for further impairment of the BBB. Recent studies have shown BBB impairment as an essential element of secondary brain injury affecting TBI outcomes. As shown by our data, TS substantially downregulates the expression levels of Occludin and Claudin-5. These TJ proteins are considered primarily responsible for maintaining the low paracellular permeability of the BBB. Thus, the downregulation of their expression levels can significantly impact the integrity of the endothelial barrier. Furthermore, these TJs are anchored to the cell cytoskeleton through ZO-1, which helps direct their distribution around the cell membrane. Hence, downregulation of ZO-1 can affect these TJs' cellular distribution, further compromising the integrity of the vascular endothelial layer of the BBB. BBB integrity is remarkably affected by OS. Unbalanced ROS production can alter TJ proteins expression, promote endothelium dysfunction, and reduce BBB integrity [120]. Moreover, inflammation has been linked to OS caused by TS through sequential events leading to NF-κB activation and the upregulation of inflammatory factors, including vascular adhesion molecules and cytokines [121]. Sustained and excessive inflammation promoted by inflammatory mediators that penetrate through the leaky BBB may interfere with the brain's normal restorative processes and promote subsequent neurological impairment [122]. On the other hand, inflammatory molecules can further impair the BBB's integrity by promoting the loss of Occludin/ZO-1 and other TJ proteins. Thus, it is unsurprising that OS and inflammation have been widely recognized as essential negative contributors to the TBI pathophysiology and post-TBI neuronal damage [33,51]. In this respect, TS prompted the

inflammatory transcription factor NF-kB overexpression along with inflammatory cytokines and vascular adhesion molecules (see Fig. 2.3) while downregulating the TJ proteins (see Fig. 2.7). These data well cope with the notion that TS-induced OS and inflammation will likely worsen the loss of vascular integrity and TBI outcome [33]. NRF2 reduces the OS imbalance and negatively modulates the redox-sensitive NF-κB signaling pathway that promotes neuroinflammation [55]. Consistent with the NRF2 - NF-κB interplay, pro-apoptotic mediators, are downregulated by the cytoprotective activity of NRF2 while are upregulated by NF-κB [123]. Other studies have shown enhanced NF-κB activation and the upregulation of pro-inflammatory cytokines in the brain and spinal cord injury in NRF2-/- mice compared to their wild-type $NRF2^{+/+}$counterparts. These data indicate a higher severity of post-traumatic endothelial injury in premorbid TS, which is consistent with the mechanisms boosting TBI's secondary brain injury. An additional risk factor for TBI patients is the effect of TS on blood hemostasis regulation. In response to vessel damage and/or inflammation, thrombomodulin (a key element of the anticoagulant protein C pathway) released by the endothelium blocks the prothrombinase complex's activity, thus arresting the undesired coagulation cascade. Therefore, a decreased release of this anticoagulant factor would inherently increase the risk for the coagulation cascade to run unchecked. Unwanted blood coagulation could further restrict local blood flow and increase the damage of the affected vascular district (and the surrounding undamaged areas). TS-exposure has been shown to boost downregulation of thrombomodulin [75,79]. Although reducing the risk of cerebral hemorrhage could be beneficial for TBI patients, the decreased ability to

control the blood coagulation cascade increases the risk for unwanted blood clot formation and stroke [79]. In future studies, we plan further our understanding of the underlying mechanisms through which TS affects TBI outcome and evaluate the effectiveness of NRF2 modulators to help reduce the burden of TBI. Overall, the development of timed interventions aimed at interfering with different aspects of the oxidative and inflammatory response systems would likely help developing new approaches to reduce the burden of secondary post-traumatic injuries.

2.4 Cerebrovascular and Neurological Impact of Chronic Smoking on Post Traumatic Brain Injury Outcome and Recovery: *In Vivo* Study

As shown in Fig. 2.1, TS generated by a CSM-SCSM cigarette smoking machine (CH Technologies, Westwood, NJ) was forced directly into two airtight smoking chambers measuring 24 L X 12 W X 12 H. The smoking inlet is dually connected to a feeding tube and a ventilator system supplying O_2 (2 L/min) at atmospheric pressure (1 bar). Mice were housed in the smoking chambers (4 mice/chamber), receiving an uninterrupted supply of normal oxygenated air between puffs. At each smoking cycle's end, mice were immediately transferred back to their regular housings with standard food and water supply.

2.4.1 Traumatic Brain Injury and Tobacco Smoke-Exposure Negatively Affect Body Weight

Weight analysis was regularly performed to assess whether smoke and/or TBI negatively impacted body weight. Animals were divided into four groups at day 0 (Fig. 2.8A), representing the four main test categories: Control (no smoke exposure and no TBI); Smoke (but no TBI), TBI (without smoke exposure), and smoke exposure followed

by TBI (Smoke + TBI). Each group consisted of 6 animals. As shown in Fig. 2.8B, we observed that chronic TS exposure alone was enough to reduce the growth rate of body weight over time. This data is consistent with published data likely conducible to an appetite suppressant effect as well as a moderate increase of metabolism promoted by TS [75]. Following TBI, we also observed a post-traumatic reduction in body weight in animals that underwent TBI with and w/o TS exposure (Fig. 2.8C). Note also that post-TBI animals did not receive any further TS exposure. The full longitudinal study data pattern has been reported in Fig. 2.8D.

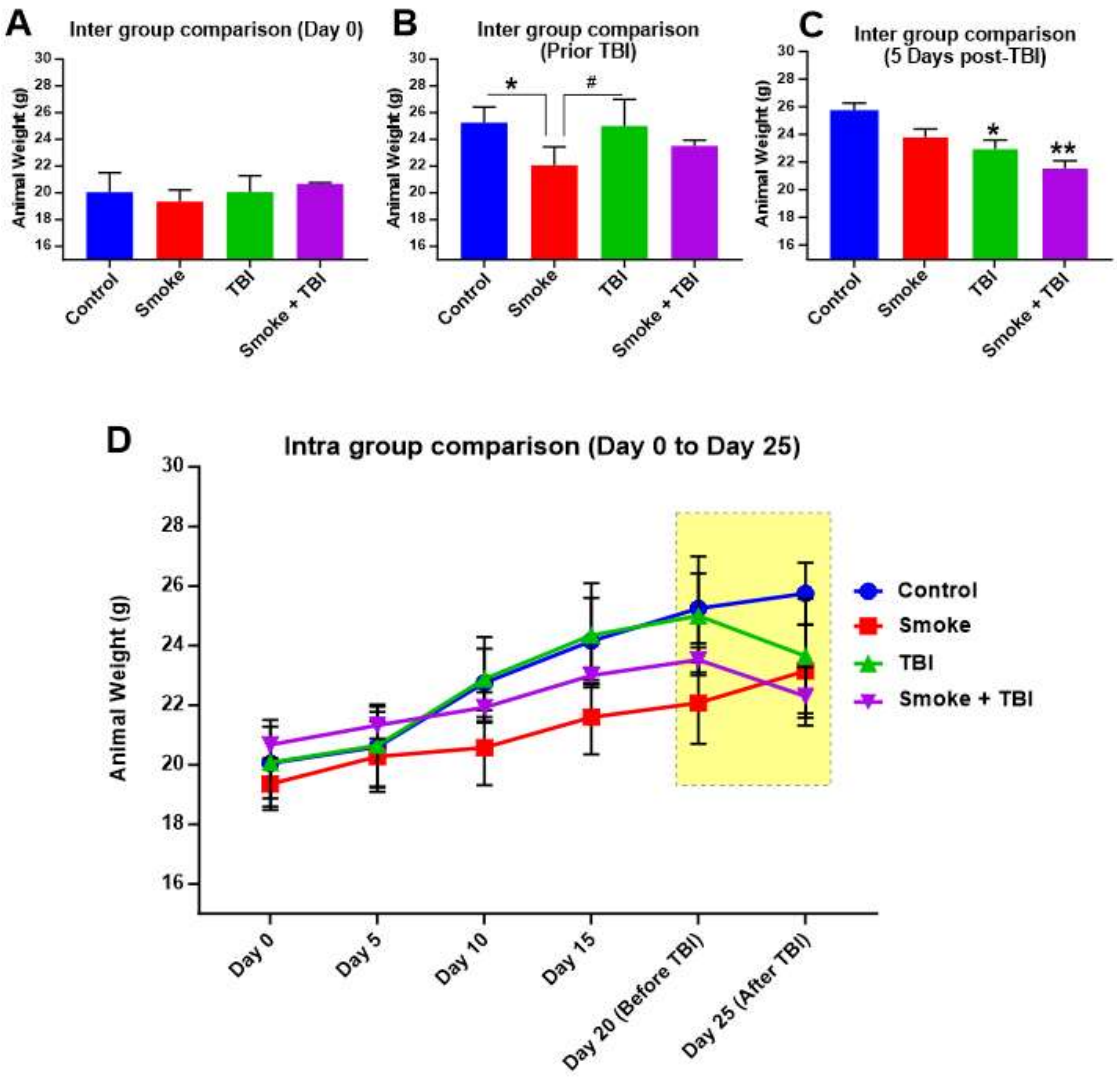

Figure 2.8 Effect of premorbid TS-exposure and TBI on body weight *in vivo*.(A) Measurements of animals' body weight do not show any significant difference between the tested groups at Day 0. However, at the end of the three weeks of exposure before TBI (B), animals exposed to TS showed a decreased body weight when compared to controls. (C) Three days after TBI, animals showed significantly decreased body weight compared to controls. (D) Longitudinal assessment of animals' body weight (all groups). n = 6 biological replicates for each experimental group. *$p < 0.05$ vs. control. # $p < 0.05$ 0001 vs. smoke.

2.4.2 Tobacco Smoke-Exposure and Traumatic Brain Injury Promote Vascular Inflammatory Responses and Potentially Impact Blood Hemostasis

Our primary hypothesis refers to the alteration in pro-inflammatory markers as one of the mechanisms that underlie the damage in the brains of TBI- induced mice. Hence, we evaluated the expression levels of inflammatory marker NF-kB, inflammatory adhesion molecules VCAM-1, and PECAM using WB and ELISA. As shown in Fig .2.9, WB analysis revealed a significant increase in the expression level of PECAM-1 (Fig .2.9A) as well as vascular adhesion molecules VCAM-1 (Fig. 2.9B) and NF-kB (Fig. 2.9C) in mice exposed to TS w or w/o TBI as well as mice undergoing TBI alone. As evident from the data analysis and the exemplative blots (Fig. 2.9D), both TS and TBI elicited an inflammatory response as standalone stimuli. However, the effect was significantly increased when the two stimuli were combined. Our results suggest a synergistic effect between TS and TBI. Furthermore, as shown in Fig. 2.10, the inflammatory activity of TBI and TS was confirmed by the analysis (via ELISA) of the pro-inflammatory cytokines IL-6 (Fig. 2.10A), IL-10 (Fig. 2.10B) and TNF-α (Fig. 2.10C) in blood samples collected 24h and 72h after TBI. Similar to NF-kB and the adhesion molecules, we observed a synergistic effect between TS and TBI. Of relevant interest, TS exposure decreased the expression level of the anticoagulant factor thrombomodulin (Fig. 2.11A&B). This effect has been previously observed *in vitro* and *vivo* [75,79]. Thrombomodulin was downregulated by TBI in animals pre-exposed to TS. The effect was statistically significant, even 72h (3 days) post-TBI (Fig. 2.11B).

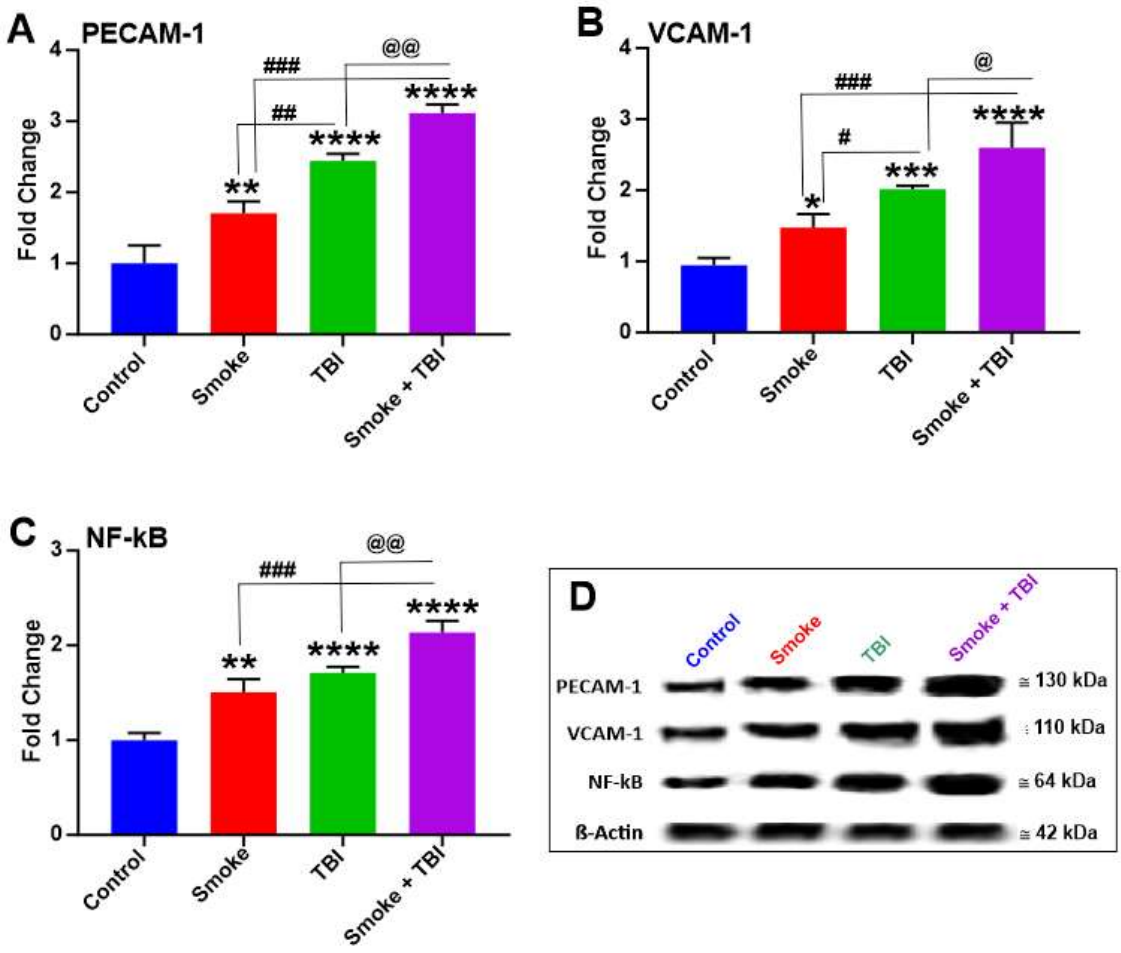

Figure 2.9 Effect of premorbid TS-exposure and TBI on vascular inflammatory responses.(A) The expression level of the inflammatory adhesion molecules PECAM-1 and (B) VCAM-1 and the pro-inflammatory regulator NF-kB (C), which were upregulated by TS-exposure and synergistically potentiated by TBI. n = 6 biological replicates for each experimental group. *p < 0.05, **p < 0.01, ***p < 0.001, ****p < 0.0001 vs. control. #p < 0.05, ##p < 0.01, ###p < 0.001 vs. smoke. @p < 0.05, @@p < 0.01 vs. TBI. WB analyses report protein/β-actin ratios.

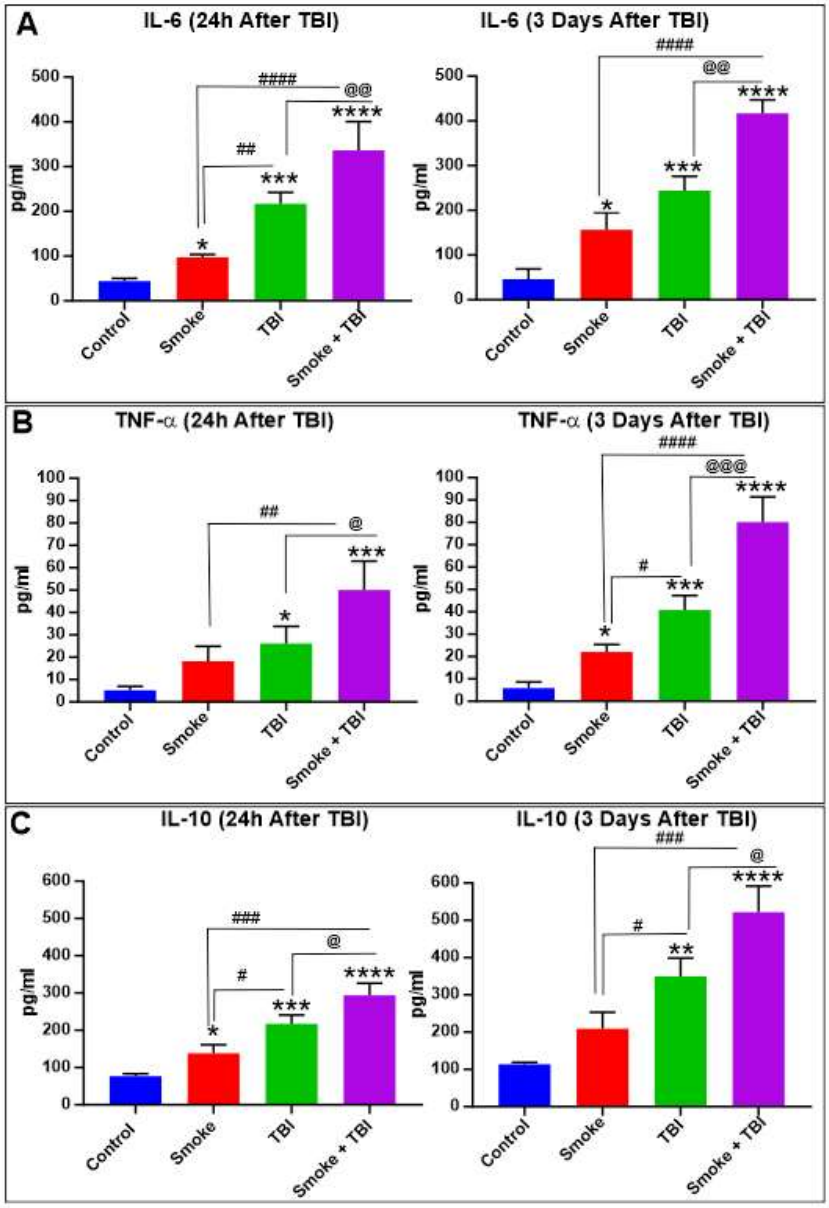

Figure 2.10 Effect of premorbid TS-exposure and TBI on pro-inflammatory cytokines IL-6, IL-10, and TNF-α.ELISA results of pro-inflammatory cytokines (A) IL-6, (B) TNF-α, and (C) IL-10 24h and 3 days after TBI. Our data show that TS exposure promotes inflammation and synergistically potentiates the cytokines upregulation induced by TBI. n = 6 biological replicates for each experimental group. *p < 0.05, **p < 0.01, ***p < 0.001, ****p < 0.0001 vs. control. #p < 0.05, ##p < 0.01, ###p < 0.001, ####p < 0.0001 vs. smoke. @p < 0.05, @@p < 0.01, @@@p < 0.001, @@@@p < 0.0001 vs. TBI.

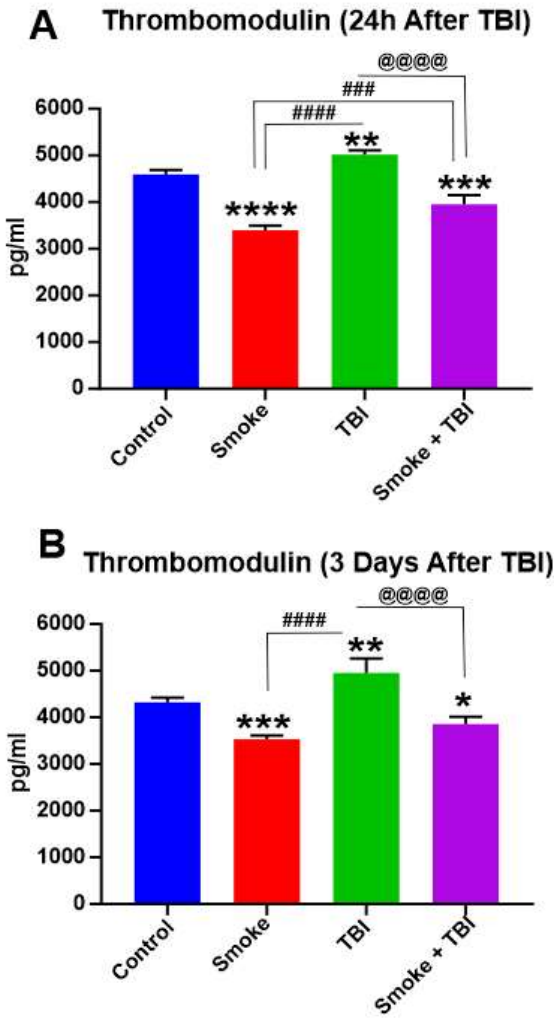

Figure 2.11 Effect of premorbid TS-exposure and TBI on Plasma Level of Thrombomodulin.ELISA measurement of thrombomodulin levels in the blood samples collected at (A) 24h after TBI and (B) 3 days after TBI. Note how TS exposure promotes downregulation of thrombomodulin, potentially impairing blood hemostasis, such as the control of the blood coagulation cascade. n = 6 biological replicates for each experimental group. *p < 0.05, **p < 0.01, ***p < 0.001, ****p < 0.0001 vs. control. ###p < 0.001, ####p < 0.0001 vs. smoke. @@@@p < 0.0001 vs. TBI.

2.4.3 Downregulation of NRF2 and its Downstream Effector NQO-1 and HO-1 by Tobacco Smoke-Exposure and Traumatic Brain Injury

The effect of TS-exposure and TBI on the expression of the antioxidative response NRF2 was also evaluated by WB analysis of whole-brain homogenate, as shown in Fig. 2.12. Consistent with our previous finding, chronic TS exposure significantly downregulated NRF2 expression (Fig. 2.12A) and that of its immediate downstream effector, including NAD(P)H dehydrogenase [quinone] 1 (NQO-1; Fig. 2.12B) and Heme oxygenase 1 (HO-1; Fig. 2.12C), thus suggesting impairment of the antioxidative response system. By contrast, TBI, as a standalone stimulus, had the opposite effect, were NRF2 was instead upregulated. These data are also evident from the WB shown in Fig. 2.12D. Although cellular localization (cytoplasmic vs. nuclear distribution) was not possible at this time, the fact that its immediate effectors were also similarly upregulated suggests that the activity of the NRF2 antioxidative response system was indeed increased following TBI but abrogated by TS exposure. This latter further confirms the detrimental impact of chronic smoking in post-TBI settings.

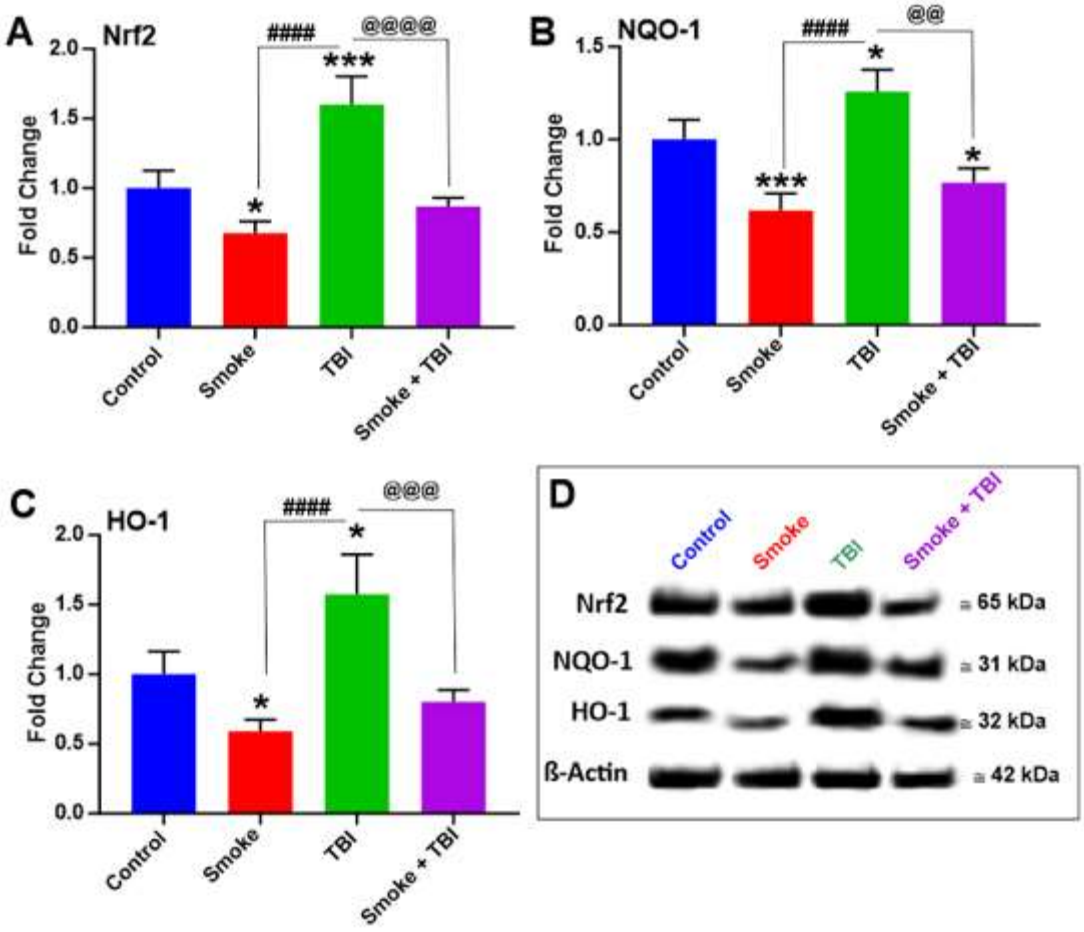

Figure 2.12 Effect of premorbid TS-exposure and TBI on the antioxidative response system.(A)WB analysis emphasizes the effect of chronic TS -exposure on NRF2 expression level as a standalone factor and synergism with TBI. (B & C) Changes in NRF2 expression levels were paralleled by corresponding changes of its downstream detoxifying effector molecules NQO-1 and HO-1. (D) Representative blot images of the analytes. n = 6 biological replicates for each experimental group. *p < 0.05, ***p < 0.001 vs. control. ####p < 0.0001 vs. smoke. @@p < 0.01, @@@p < 0.001, @@@@p < 0.0001 vs. TBI.

2.4.4 Synergistic Impact of Combined Chronic Tobacco Smoke-Exposure and Traumatic Brain Injury on Oxidative Stress

Our results show that, except for the smoke + TBI condition, the total glutathione levels are not significantly different from controls (Fig. 2.13A). Premorbid TS exposure as a standalone factor and the combination of TS premorbid condition with TBI promote a significant decrease in GSH levels (see Fig. 2.13B). In line with these results, GSSG levels (oxidated glutathione indicative of elevated OS responses) are significantly elevated in all the tested conditions compared to controls (Fig. 2.13C). In this setting, premorbid TS exposure coupled with TBI produces a substantially higher level of GSSG than either smoke or TBI (Fig. 2.13C). The impact of TS, TBI, and the combination of both on glutathione levels is also evident from the calculated GSH/GSSG ratio shown in Fig. 2.13D).

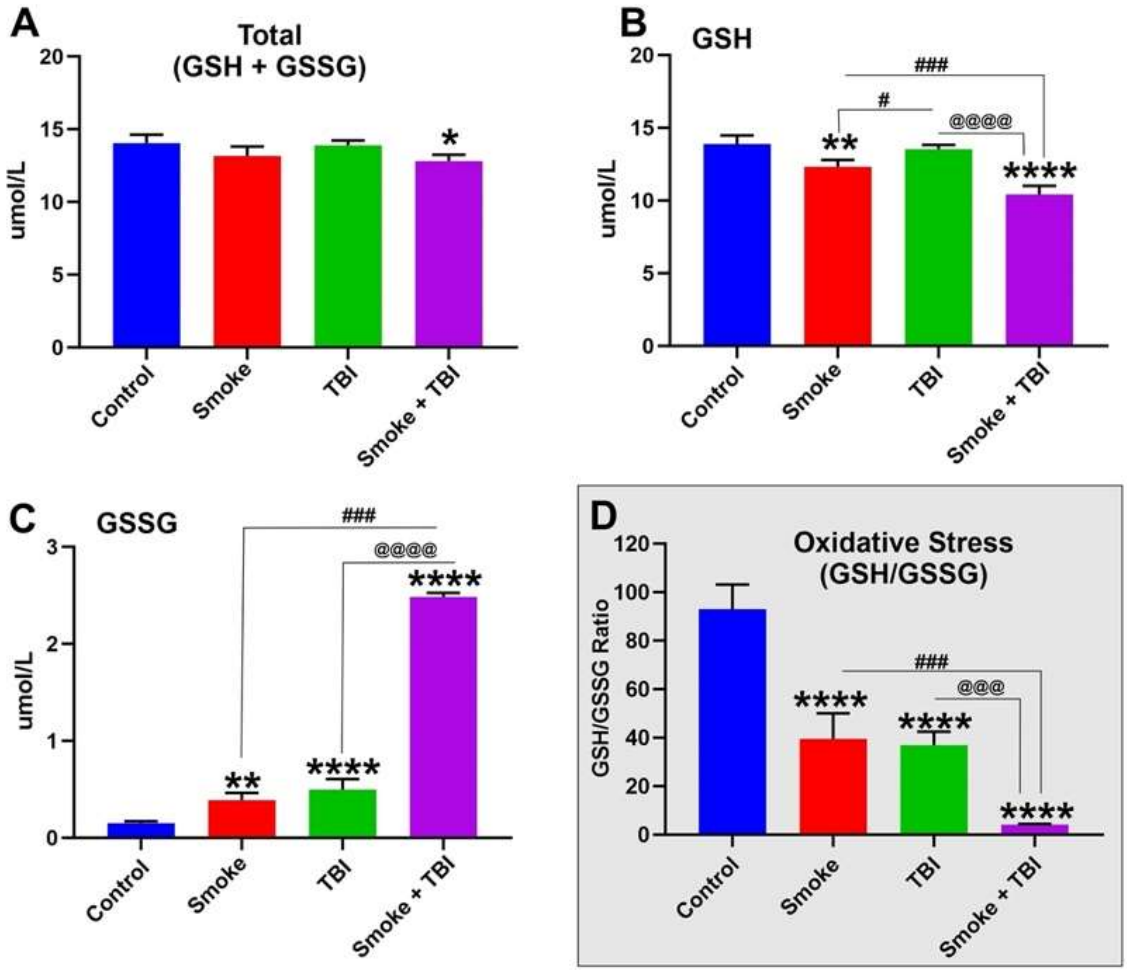

Figure 2.13 Effect of premorbid TS-exposure and TBI on glutathione levels *in vivo*.(A) total glutathione (GSH+ GSSG) (B) reduced glutathione (GSH), (C) oxidized glutathione (GSSG) and (D) GSH/GSSG measured by plate reader. n = 6 biological replicates for each experimental group. *p < 0.05, **p < 0.01, ***p < 0.001, ****p < 0.0001 vs. control. #p < 0.05, ##p < 0.01, ###p < 0.001, ####p < 0.0001 vs. smoke. @p < 0.05, @@p < 0.01, @@@p < 0.001, @@@@p < 0.0001 vs. TBI.

2.4.5 Chronic Tobacco Smoke-Exposure Hamper Blood-Brain Barrier Integrity in Traumatic Brain Injury

Additional experiments were performed to assess the effect of TS-exposure and TBI on BBB integrity. We evaluated the expression level of the BBB accessory protein zonula occludens-1 (ZO-1) and TJ proteins expression encompassing the primary regulator of BBB paracellular permeability Occludin and Claudin-5. As shown in Fig. 2.14, chronic TS-exposure significantly downregulated the expression of Occludin (Fig. 2.14A), Claudin-5 (Fig. 2.14B), and ZO-1 (Fig. 2.14C) when compared to controls (see also WB grouped in Fig. 2.14D). These results are consistent with previous work by our group, suggesting that TS acts as the main effector of TJ downregulation, thus promoting the loss of BBB integrity [67,75,112]. By contrast, TBI only has a significant impact on Occludin (which is a crucial regulator of BBB integrity). At the same time, the effect on Claudin-5 was marginal, and no effect was observed regarding the expression of ZO-1. However, when the stimuli are combined, we see a synergistic downregulation of Occludin, whereas that of Claudin-5 and ZO-1 is attributable uniquely to TS exposure. The critical point of these results is that in addition to inflammation, premorbid TS exposure promotes the onset of a pre-existing state of weakened BBB integrity, which TBI can more readily impact.

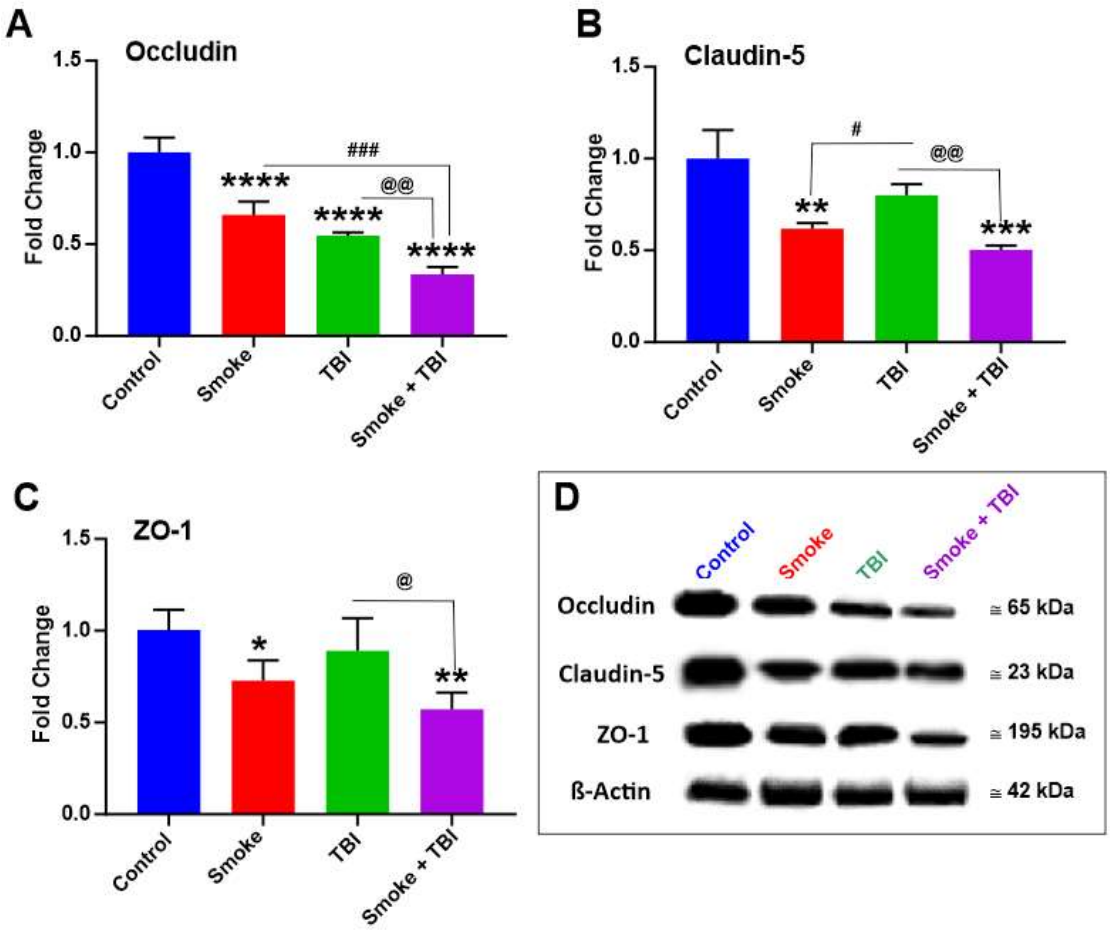

Figure 2.14 Effect of premorbid TS-exposure and TBI on BBB integrity.WB analysis demonstrated downregulation of TJ proteins Occludin (A), Claudin-5 (B), and accessory anchoring protein ZO-1 (C) in mice exposed to TS and/or TBI. Note that TBI per se had only a marginal impact on the expression levels of Claudin-5 and ZO-1. Therefore, with the exclusion of Occludin, which TBI significantly downregulated, TS seemed mainly responsible for the TJ downregulation observed in TBI mice chronically exposed to cigarette smoke. n = 6 biological replicates for each experimental group. *$p < 0.05$, **$p < 0.01$, ***$p < 0.001$, ****$p < 0.0001$ vs. control. #$p < 0.05$, ####$p < 0.0001$ vs. smoke. @$p < 0.05$, @@$p < 0.01$, vs. TBI.

2.4.6 Tobacco Smoke Promotes Increased Motor Activity in Mice but Aggravates Post-Traumatic Behavior in Mice Undergoing Traumatic Brain Injury

Exploratory behavior and general activity of the test mice were regularly recorded to evaluate the impact of smoke and TBI based on their motor activity before and after a mild traumatic injury induction. As shown in Fig. 2.15, we observed compared to both groups of TS- free mice, animals chronically exposed to TS demonstrated substantially higher motor activity expressed as the total distance traveled by the animals. This data is consistent with the metabolic effect of TS as well as a craving for TS itself (Fig. 2.15B1 to 2. 15B3). We expected that TBI would reduce the mice's motor activity (the effect was evident as early as 1h post-trauma and partially recovered later). Interestingly, behavior/activity was more significantly reduced in TBI mice chronically exposed to TS compared to TBI alone (see Fig. 2.15, panels B2 and B3). Furthermore, as shown in Fig. 2.15 panel C (yellow insert), TS exposure also negatively impacted motor recovery compared to TBI mice that were not exposed to TS and which returned to levels comparable to controls within three days post-TBI. Moreover, as shown in Fig. 2.16 (panels A through C), the rest time follows the opposite pathway of motor activity, where mice chronically exposed to TS exhibited a significantly reduced rest time compared to controls. Note also how the rest time significantly increases following TBI and renormalizes after 72 hours (see Fig. 2.16 panel D). Of significance is the fact that mice undergoing chronic premorbid TS exposure before TBI exhibited a significantly higher rest time 24 and 72h post-TBI injury.

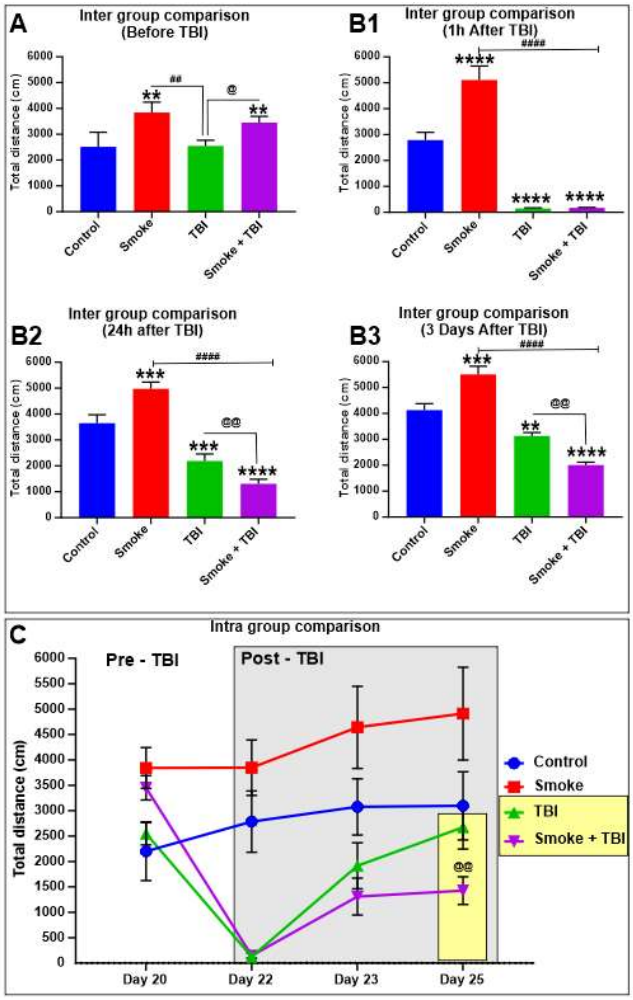

Figure 2.15 Effect of premorbid TS-exposure and TBI on exploratory behavior and general motor activity.(A) Measurements of totaled distance traveled by mice do not show any significant difference between the tested groups at day 0 before TBI. However, mice undergoing chronic TS exposure w/o TBI demonstrated significantly higher motor activity (B1). Note also that both TBI and TS-exposed mice undergoing TBI displayed a significant reduction in motor activity. Measurements performed at 24 and 72 hours post-TBI clearly show that TS further aggravated TBI injury as denoted by the significant reduction of motor activity compared to the TBI mice group (B2 and B3). (C) Longitudinal assessment of the animals' response to injury w/wo TS exposure clearly shows that animals chronically exposed to TS experienced a significant delay in motor activity recovery compared to TBI animals that were not exposed to TS. N = 6 biological replicates for each experimental group. *p < 0.05, ***p < 0.001, ****p < 0.0001 vs. control. ##p < 0.0, ####p < 0.0001 vs smoke. @p < 0.05, @@p < 0.01 vs. TBI.

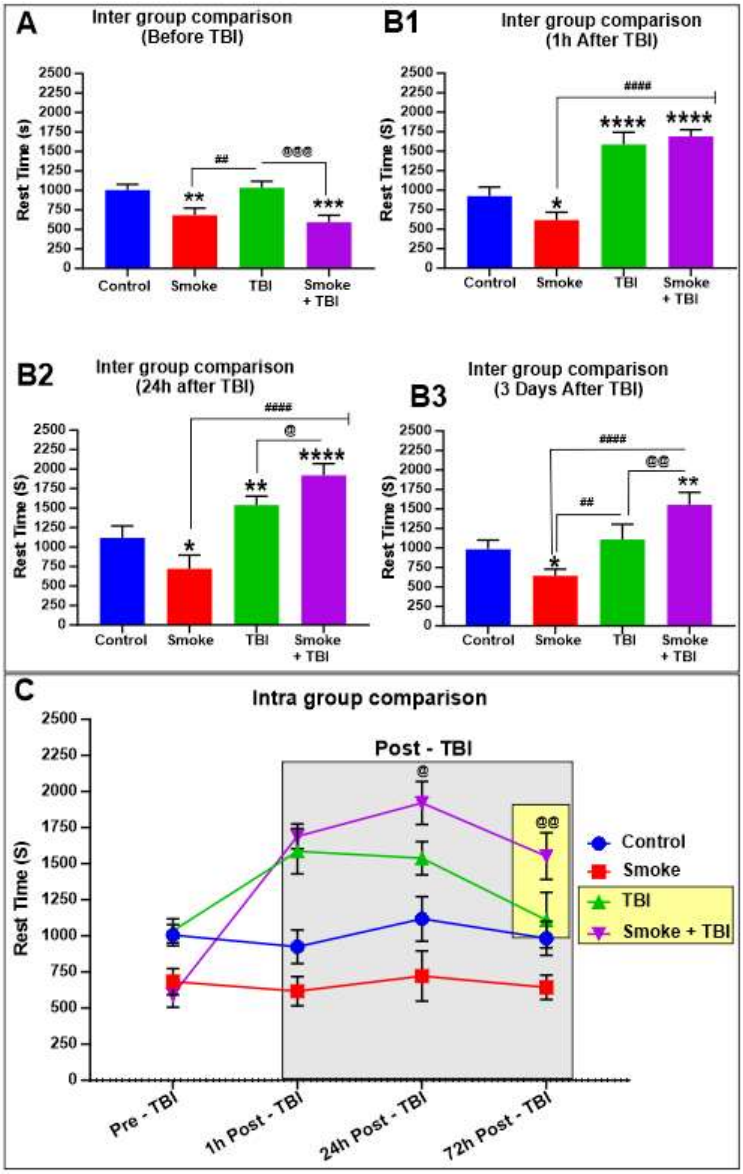

Figure 2.16 Additional effects of premorbid TS-exposure and TBI on general motor activity such as resting time.(A) Intergroup rest time comparison prior to TBI shows the effect of chronic TS exposure on motor activity. In this case, the increased rest time observed in smoke and smoke + TBI animal groups well match the increased motor activity (distance traveled) previously assessed. (Panel B1 to B3) TS increasesthe rest time of animals undergoing TBI at 24- and 72-hours post injury compared to TBI alone. (Panel D) Side by side longitudinal assessment of rest time between the 4 test groups. N = 6 biological replicates for each experimental group. *p < 0.05, **p < 0.01, ***p < 0.001, ****p < 0.0001 vs. control. ##p < 0.0, ####p < 0.0001 vs. smoke. @p < 0.05, @@p < 0.01, @@@p < 0.001 vs. TBI.

2.4.7 Discussion

In the present study, we evaluated the potential influence of chronic tobacco smoking on pathophysiological mechanisms underlying the exacerbation of TBI and retardation of post-TBI recovery using a weight-drop mice model. This model releases a fixed weight for a free fall based on a defined path and height. The weight and the height from which the weight is dropped determine the severity of the injury, which can range from mild to severe. This model was chosen because of its ability to simulate traumatic head injuries comparable to those observed in road accidents or falls [10]. Based on our results, both groups of smoked mice demonstrated a loss of body weight compared to the control, confirming the common metabolic stimulatory effect of TS. Longitudinal body weight increase was also significantly dampened after TBI induction, which is consistent with the well-observed reduced appetite after TBI. In line with these findings, the behavioral analysis confirmed similar changes in the state of consciousness and *awareness* immediately after TBI and during recovery. While TS was consistently associated with an increase in motor activity as a standalone stimulus, when combined with TBI (see Fig. 2.15) is further depressed motor activity when data were compared to TBI mice that were not exposed to TS. The post-traumatic motor recovery was also significantly reduced when compared to the same group. These data are consistent with the increased severity of post-TBI promoted by TS and well correlated with the analysis of inflammatory biomarkers and BBB integrity. Moreover, systemic and microenvironmental effects of neuroinflammation induced by TBI can affect neurotransmission and especially the dopaminergic pathways. This latter plays a

significant role in secondary injury and behavioral and cognitive dysfunction following TBI [45,51,124]. Previous studies suggested that dopamine dysregulation may have a substantial role in behavioral deficit after TBI, possibly due to alterations in proteins regulating dopamine [125]. Dopamine release is suppressed after TBI, and a higher substance dosage has been necessary to maintain the behavior. Moreover, alterations in dopaminergic pathways have also been evidenced by increases in tobacco abuse after TBI since nicotine is the principal component of TS that underlies the addictive properties of cigarette smoking. [126,127]. In chronic smokers, nicotine increases dopamine release by stimulating nicotinic cholinergic receptors (nAChR) in multiple brain regions. Cravings and aberrant behaviors may be initiated and promoted because of the enhanced dopamine release after a long-standing TS experience. On the other hand, higher nicotine exposure may cause rapid nAChR desensitization, which induces nAChR function loss [128]. Thus, chronic tobacco smoking leads to addiction, which is linked to dysfunctions in the DA transmission system [128]. NRF2, a basic region-leucine zipper (bZip) redox-sensitive transcription factor, is the master regulator of multiple cytoprotective responses, which controls the redox state of cells in harmful stresses [22]. Under normal conditions, NRF2 is localized in the cytoplasm by its inhibitor, Kelch-like ECH-associated protein 1 (Keap1). Nevertheless, under oxidative or xenobiotic stress conditions, the cysteine residues of Keap1 become oxidized, and NRF2 dissociates from Keap1. The free NRF2 then translocates into the nucleus, binding to the antioxidant response element (ARE), thus promoting gene transcription. This latter includes over 500 genes encompassing phase 1 and 2 enzymes, regulators of redox metabolism, production of ATP and

antioxidative agents (including NADH and glutathione), and TJ proteins expression at the BBB [15,77]. Based on valid evidence, NRF2 also promotes anti-inflammatory mediators, the activity of the proteasome, and other transcription factors involved in mitochondrial biogenesis. According to recent studies, suppression of NRF2 activity and impairments of the NRF2–ARE signaling pathway exacerbate TBI-induced oxidative damage as well as post-traumatic neurological deficits. This data strongly suggests that NRF2 plays a significant neuroprotective role in TBI and neurodegenerative disorders [10,17]. Since the upregulation of NRF2 activity reduces the burden of TBI-induced brain injury, it is plausible that positive modulation of NRF2 could improve TBI outcomes through reducing OS, inflammation, and protection of BBB integrity [61-63,75,79,115,129]. In line with these findings, we assessed the impact of premorbid TS-exposure and TBI on NRF2 expression levels, as well as its downstream effector molecules NQO-1 and HO-1, known for exerting acute detoxification and cytoprotective functions. Our *in vivo* data show that the NRF2-ARE system is activated in response to TBI (see Fig. 2.12). This effect could be due to a direct modulatory activity toward NRF2 expression and the sequential activation of the NRF2–ARE signaling pathway in response to trauma. Our findings are in line with the results obtained in a previous study by Li et al., indicating significantly enhanced NRF2, NQO-1, and HO-1 protein expression following TBI [115]. However, chronic TS exposure as a standalone stimulus has the opposite effect (see Fig. 2.12A), which also agrees with previous *in vitro* and *in vivo* observations recently published by our group [27,75,79]. The OS impact of premorbid chronic smoking and TBI (as standalone or combined factors) was also

confirmed by measurements of GSH as well as GSSG (see Fig. 2.13). Our data show that TS exposure as a standalone factor is responsible for a statistically significant decrease in the levels of GSH (see Fig. 2.13B). The combined effect of premorbid TS exposure with TBI also causes a substantial drop in GSH combined with a significant increase in its oxidated form GSSG (see Figs. 2.13B-D). These data well reflect the impact of TS on the NRF2 system previously analyzed and further supporting the notion of a synergistic effect. Noteworthy is the concurrent effect of TS and TBI, which negatively impact the total level of glutathione (GSH + GSSG; see Fig. 2.13A). This latter suggests that there is a higher turnover of GSH, and its overall production is decreased. GSH production is dependent upon the activity of the NRF2 system, which promotes glutathione synthesis, among other antioxidative effects [77]. The modest yet significant increase of GSSG observed in TBI (see Fig. 2.13C) and also evident from the calculated GSH/GSSG ratio (see Fig. 2.13D) is also indicative of OS, which in this case is solely mediated by inflammation as shown in Fig. 2.10. The fact that the level of GSH in TBI does not seem to be diminished when compared to controls (see Fig. 2.13B) is also in agreement with our results showing upregulation of NRF2 in response to injury, which promotes GSH synthesis in response to an acute stressor. As a comorbid stimulus, when TS exposure is combined with TBI, it abrogates the post-traumatic activation/upregulation of NRF2 that follows brain trauma, thus preventing this physiological recovery system from being activated. The downstream impact of NRF2 downregulation includes further impairment of the BBB (significantly less severe in TBI animals not exposed to TS; see also Fig. 2.14) and upregulation of post-traumatic inflammatory responses. This latter (including

overexpression of the pro-inflammatory transcription factor NF-kB, cytokines, and vascular adhesion molecules; see Figs. 2.10 and 2.11) further aggravates vascular integrity and worsens TBI outcome. These findings are consistent with the analysis of post-traumatic motor activity, showing that animals chronically exposed to TS before TBI fared significantly worse than those undergoing traumatic injury but were not exposed to TS (see Figs. 2.15 and 2.16). In this specific case, the overall cerebrovascular/BBB impairment promoted by TS before TBI could explain the phenomenon. The BBB is a complex dynamic interface between the blood and the CNS, which strictly maintains brain homeostasis and controls the passage of substances in and out of the brain environment. Among the various control functions of the BBB, the inter-endothelial TJs rigidly control the paracellular pathways blocking the passage of polar molecules (including ions) from moving between adjacent endothelial cells [3]. The most critical TJ proteins modulating the extremely low BBB permeability to polar molecules are Occludin and Claudins (specifically Claudin-5), forming homotypic bonding with their corresponding counterparts on adjacent endothelial cells. ZO-1 plays the critical function of anchoring this TJ protein to the cell cytoskeleton, thus allowing the cell to direct the distribution of these TJ proteins around the membrane. Recent findings have demonstrated that BBB impairment is a crucial component of post-TBI secondary brain injury and can significantly affect the outcome. Additional evidence also indicates that inflammation is an essential contributor to the TBI pathophysiology exacerbating neuronal damage during post-traumatic brain injury. Therefore, sustained and excessive inflammation through the secretion of proinflammatory mediators can increase

subsequent neurological impairment [130]. This process involves resident microglia and astrocytes, peripheral leukocytes penetrating through the leaking BBB, and inflammatory mediators, including cytokines that interfere with normal restorative processes of the brain, thus promoting neuronal cell death [33,51]. Proinflammatory cytokines like IL-6, IL-10, and TNF-α are increased in post-traumatic blood samples. Furthermore, the synthesis of chemokines, prostaglandins, and expression of cell adhesion molecules like VCAM-1 and PECAM-1 on the surface of the cerebrovascular endothelium is also increased. This latter process can favor the extravasation of inflammatory cells from the blood into the brain [33]. There is also a growing consensus that all these processes are the principal promoters of the secondary brain damage associated with TBI, including dysfunction of astrocytes and microglia, as well as BBB impairment contributing to the increased paracellular permeability and the loss of neurons. Proinflammatory molecules play a supplementary role in increased BBB permeability related to loss of Occludin/ZO-1 and other tight junctions. It is also well described that BBB integrity is deeply affected by OS, so enhanced ROS production leads to redistribution and/or altered expression of tight-junction proteins, endothelium dysfunction, and increased BBB permeability [120]. Inflammation is also linked to OS, whereas ROS (such as those released within TS) are considered among the most potent inflammatory mediators [121]. OS caused by TS has been widely recognized as a negative contributing factor to neurological outcomes following brain injury [63], where TS modulates a cascade of events leading to the activation of NF-κB and the expression of pro-inflammatory cytokines and vascular adhesion molecules. This has been observed in glial cells and neurons following TBI and

is associated with long-term inflammatory processes [78]. Mettang et al., using an experimental model of closed-head injury promoted neuronal cell death, demonstrated the repression of the NF-κB inhibitor system exacerbating the neurological outcome and increasing post-traumatic mortality rate [55]. In the contest of NRF2 - NF-κB interplay, recent studies confirmed the cytoprotective activity of NRF2, which promotes the downregulation of pro-apoptotic mediators such as Bax, BAD, and others. These pro-apoptotic factors are instead upregulated by NF-κB [123]. NRF2reduces ROS levels and affects the redox-sensitive NF-κB signaling pathway involved in neuroinflammation. Moreover, in a recent study, it has been reported that $NRF2^{-/-}$ mice have greater NF-κB activation and generation of pro-inflammatory cytokines in the brain and spinal cord injury compared to their wild-type $NRF2^{+/+}$counterparts. Relevant to our study is the fact that chronic TS exposure dampened NRF2 activity in TBI mice. Thus, the cascading effect of NRF2 downregulation well fit the slowed recovery, and overall, worse outcomes observed in TBI animals chronically exposed to TS when compared to TBI mice that were not exposed to smoke. An additional risk factor for TBI patients that is associated with chronic smoking may be derived from the impact of smoking on blood hemostasis. Thrombomodulin is a critical component of the anticoagulant protein C pathway, which ensures control over the process of blood-coagulation. This anticoagulant system acts by blocking the activity of the prothrombinase complex and promoting fibrinolysis. This control system is activated following activation of the coagulation cascade in response to vessel injury and/or inflammation. Inflammatory cytokines inhibit thrombomodulin activity; thus, blocking NF-kB activation can effectively prevent cytokine-induced

downregulation of this anticoagulant factor. Mediated by its pro-inflammatory activity, TS-exposure has been previously shown to promote thrombomodulin downregulation and to increase the risk of blood clot formation and stroke [79]. While this may seem of potential benefit for TBI patients, whereas a significant risk of mild TBI is hemorrhage, impairment of blood coagulation related to the inability to control it would be a very undesirable effect. Thrombomodulin is essential to block the activity of the prothrombinase complex and therefore arrest the coagulation cascade. Reduced activity or production of this anticoagulant factor would lead to an uncontrolled coagulation cascade that could extend beyond the damaged area, affecting other (undamaged) vascular districts and restricting local blood flow with consequent ischemic damages and more damage to the blood vessels. A shortcoming of this study is the exclusive use of male mice rather than a mixed-gender population of animals. Given the "early stage" nature of this study assessing the impact of TS on TBI damage and post-TBI recovery, we felt that it was necessary to minimize the variability of physiological responses (including behavioral) caused by gender-related hormonal differences. However, recent previous studies by our group have highlighted possible gender-specific cellular responses to chronic TS exposure [27] affecting the expression levels of Phase-II enzymes as well as the iron transporters. Although the physiological implications of these differential responses to TS are not clear, they do suggest that gender is a potential risk factor and needs to be investigated. Therefore, we plan to use a mixed gender animal population in follow up studies to determine further pieces of evidence (if any) of a gender-specific impact on TS on TBI and post-TBI recovery. Another limitation of the

study is that we have only two sampling points, at 24 and 72 hours. This experimental choice, unfortunately, limits the ability to profile the inflammatory activity and antioxidative responses post-injury since a comparison can be made only in respect of the treatments and only between the sampling window. Although outside the scope of this work, future experiments will focus on further detailing the concurrent underlying mechanisms through which TS impacts TBI. We will also focus on assessing the impact of gender as an additional risk factor in the TS-TBI interplay and expand further to evaluate the effects of vaping on TBI. Targeting NRF2 to prevent TBI exacerbation by TS and other vascular comorbidities could provide a possible path toward the development of more effective treatments. This latter is of paramount importance for patients that either cannot quit smoking or those that recently stopped but will remain at high risk of developing CNS disorders for a significant amount of time (years) before full renormalization. Crucial consideration must be extended to several other factors that may hinder this renormalization process, including number and type of cigarette smoked per day, years spent smoking, and age of the subject when entirely quit. It is also possible that gender may play a significant role, as well. Although the therapeutic window of BBB regulation after TBI remains unknown, further understanding of the dynamics regulating BBB dysfunction post-TBI would provide essential data to support the development of novel therapeutic approaches, including more selective therapeutic agents, and timing of treatment.

2.5 Summary

Chronic TS is among the preeminent causes of preventable mortality in the USA. [131]. Yearly, TS has affected the life of about six million people globally, and more than half a million people in the USA are killed by TS [21,132]. Smoking increases the onset and progression of major neuroinflammatory and cerebrovascular diseases through excitotoxicity, OS, cerebral edema formation, neuroinflammation, and impairment of BBB endothelial physiology. In this work, we assessed the effect of TS on TBI- induced damage of the BBB endothelium using an *in vitro* traumatic injury cell culture model based on mBMEC cells, and the exacerbation of TBI and retardation of post-TBI recovery was investigated using a weight-drop model. Our data suggest that TS exacerbates brain microvascular endothelial damage caused by traumatic injuries. The detrimental effects of TS are driven by the impairment of the ARS primarily controlled through NRF2. These effects manifest as increased cellular OS, inflammation, and downregulation of TJs, leading to BBB integrity loss. Our data provide further evidence verifying the damaging role of premorbid TS in exacerbating post-TBI injuries. Considering all the data presented, we showed that TS promotes TBI exacerbation of cerebrovascular injuries and impairs post-TBI healing. Our data suggest that the effects of premorbid TS are consequential to the abrogation of physiological antioxidative and anti-inflammatory response to TBI worsening impairments of the BBB, OS damage, and inflammation. The overall result is that premorbid TS may exacerbate the risk of post-traumatic brain damage and slower recovery.

CHAPTER THREE

PROTECTIVE EFFECT OF ROSIGLITAZONE AGAINST SMOKE-INDUCED CEREBROVASCULAR TOXICITY

3.1 Introduction

Smoking is responsible for many deaths worldwide based on the knowledge of its effect on vascular health [26]. EC may be considered a safer product than TS (since they contain no tobacco and do not involve combustion, users may avoid several harmful constituents usually found in TS, such as ash, tar, and carbon monoxide.). However, recently published data from side by side experiments investigating the impact of EC and TS clearly showed similar OS-dependent impact on 24 h EC/TS exposed mBMEC [133,134]. There is now a wealth of evidence suggesting the major role of OS caused by TS/EC in endothelial dysfunction in the cerebrovascular level. In our group's recent work, the involvement of common pathogenic modulators of BBB impairment was confirmed so that chronic cigarette smoking and HG carried similar risks for cerebrovascular diseases and stroke, sharing similar pathogenic mechanisms [67,135]. This result accounts for the possible application of anti-diabetic drugs to reduce BBB damage promoted by chronic TS exposure. RSG is a member of the thiazolidinedione family that can improve insulin resistance through modulating adiponectin gene expression. RSG is also considered a transcription factor PPARγ agonist which is a nuclear receptor that regulates numerous genes implicated in glucose homeostasis, and fatty acid metabolism [136]. Despite the unknown mechanism of RSG, numerous studies and our previous work have confirmed the protective effect of RSG on ameliorating

oxidative damage [26,137]. Thus, this chapter's main aim is to investigate RSG's role in activating counteractive antioxidative mechanisms to reduce TS and EC toxicity at the BBB through *in vitro* and *in vivo* studies.

3.2 Methods

3.2.1 Materials and Reagents

Reagents and chemicals were purchased from Sigma-Aldrich (St. Louis, MO, USA) or Bio-rad laboratories (Hercules, CA, USA). Sterile culture wares were purchased from Fisher Scientific (Pittsburgh, PA, USA), Mouse primary brain microvascular endothelial cells (C57BL/6- mBMEC, #C57- 6023) and completed mouse endothelial cell medium kit (M1168) were obtained from Cell Biologics (Chicago, Illinois, USA). Gel electrophoresis was carried out using Mini-Protean®TGXTM gels 4–15% (#456–1084) from Bio-Rad laboratories (Hercules, CA, USA). Fluorescein isothiocyanate (FITC)-dextran (3000–5000 MW; #FD4) and Rhodamine B isothiocyanate (RITC) - dextran (70,000 MW; #R9379) were obtained from Sigma-Aldrich (St. Louis, MO, USA). Rosiglitazone (RSG # A00183, MW: 357.4) was obtained from Adipogen. The antibodies used in this study were purchased from various sources: rabbit anti-ZO-1 (#402200), mouse anti-Occludin (#331500), and mouse anti-Claudin-5 (#352500), from Life Technologies; rabbit anti- NRF2 (#sc-722), mouse anti-NQO-1 (#sc-376023), mouse anti-PECAM-1 (#sc-376764), mouse anti-HO1 (#sc-390991) and mouse anti-NFκB-p65 (#sc-(F-6)-8008) from Santa Cruz Biotechnology. Rabbit anti-PPARγ (#PA3-821A) from Invitrogen; Sheep anti-mouse (#NA931) and Donkey anti-rabbit (#NA934) secondary antibodies were obtained from GE Healthcare (Piscataway, NJ, USA); goat anti-rabbit

(#A11008, A21428) conjugated to Alexa Fluor® 488 and 555 respectively, and anti-mouse (#A11001, A21422) conjugated to Alexa Fluor® 488 and 555 respectively from Invitrogen (Camarillo, CA, USA).

3.2.2 Cell Culture

Mouse primary brain microvascular endothelial cells (mBMEC-P3- C57BL/6J) were seeded on gelatin-coated cell culture flasks and glass chamber slides, cultured in supplemented medium (M1168) along with 10% FBS, and maintained at 37 °C with 5% CO2 exposure [75]. The culture medium was changed every other day until the cells reached confluency. The monolayer integrity of mBMEC cells at confluency was confirmed by phase contrast microscopy and the expression of characteristic phenotypic markers.

3.2.3 Soluble Cigarette Smoke Extract Preparation

Soluble TS and EC extract were prepared according to the FTC standard smoking protocol from 3R4F research cigarettes (35 mL puff volume, 2 s puff duration, 58 s intervals, 8 puffs per cigarette directly into phosphate buffered saline (PBS), equivalent to full flavor brands containing 9.4 mg tar and 0.726 mg nicotine per cigarette; University of Kentucky) and EC containing 2.4% nicotine (35 mL puff volume, 4 s puff duration, 17 s intervals, 8 puffs per cigarette directly into phosphate buffered saline (PBS))) using a Single Cigarette Smoking Machine (SCSM, CH Technologies Inc., Westwood, NJ, USA) following previously published methods [75,76]. TS/EC extract solutions were prepared fresh for each cycle and were then diluted to 5% concentrations in low serum media.

3.2.4 Transwell Cell Culture Set-up

mBMEC cells were seeded on the luminal side of Treated polyester transwell inserts (Corning® Transwell® polyester membrane cell culture inserts, 12 mm, 0.4 μm pore membrane insert; #3460) and grown in the supplemented culture medium, as mentioned above [75,138]. The confluence and integrity of the cell monolayers were confirmed by phase contrast microscopy and trans-endothelial electrical resistance (TEER) measurement (baseline value ≈ 10 Ω.cm2).

3.2.5 Cell Viability

MTT cell viability study was conducted to evaluate the appropriate RSG pretreatment dose for *in vitro* studies [75]. Briefly, cells cultured in a 96-wells plate were pre-treated with varying concentrations of RSG (20 μM to 2000 μM) for 24 h. Parallel RSG untreated controls were also evaluated for cell viability. Cells were stained with 10 μl of 5 mg/ml tetrazolium MTT (3-(4, 5-dimethylthiazolyl-2)−2, 5- diphenyltetrazolium bromide) for 3 h at 37 °C, after which 100 μl of DMSO (solubilizing agent) was added. The absorbance was read on a Bio-rad plate reader at a wavelength of 570 nm.

3.2.6 Treatment

mBMEC cells were incubated in the low serum media containing supplemented culture medium (as mentioned earlier) and 1% FBS with no growth factors for 24 h. In all analyses, RSG was first dissolved in DMSO at a concentration of 100 mM and then freshly diluted with supplemented culture medium to the appropriate concentrations. The final concentration of DMSO was <0.1%. Culture medium with DMSO served as the control in each RSG-treating experiment. The cells were then pretreated with RSG (20

μM based on our cell viability results) and exposed to 5% TS/EC extract solution for 24 h [67]. Parallel controls (without EC/TS and /or RSG) were also provided.

3.2.7 *In Vivo* Experimental Design

The animal study was conducted based on the animal protocol approved by the Institutional Animal Care and Use Committee, TTUHSC, Lubbock, Texas [75]. Twenty male C57BL/6J mice (in the range of 8–10 weeks old and body weight between 20–25 g) were purchased from Jackson Laboratory. After the animals arrived at the laboratory, they were given three days of recovery from the transport and for acclimatization to the new location. All animals were given unrestricted access to water and standard mouse chow. They were divided into five groups, as shown in Table 3.1. Test animals were chronically exposed (via direct inhalation) to side stream cigarette smoke (CS) derived from 3R4F research cigarettes (9.4 mg tar and 0.726 mg nicotine/cigarette) 6 times a day, 2 cigarettes/hour/8 animals every day for 2 weeks. Cigarette exposure was set to meet the International Organization for Standardization/ Federal Trade Commission (ISO/FTC) standard smoking protocol (35 ml puff volume, 2 s puff duration, 58 s intervals, 8 puffs per cigarette) [26,75]. CS was generated using a Single Cigarette Smoking Machines (SCSM, CH Technologies Inc., Westwood, NJ, USA) following previously published methods [112]. RSG was injected intraperitoneally and at the beginning of the day. Two weeks of CS exposure and Drug injection was selected as the time course due to the reduction of possible inflammation caused by DMSO.

Table 3.1 Experimental Design.

	Group 1	Group 2	Group 3	Group 4	Group 5
Saline	✓	-	-	-	-
Saline+DMSO	-	✓	-	✓	✓
RSG 10 mg/kg	-	-	-	✓	-
RSG 20 mg/kg	-	-	-	-	✓
TS-Exposure	-	-	✓	✓	✓

3.2.8 Drug Injection

RSG was dissolved in DMSO/ sterile saline (1:10) and administered daily via intraperitoneal injections of dose levels of 10 or 20 mg/kg with a dose volume of 20 ml/kg to mice either exposed to TS (mixed with oxygenated air) or oxygenated air alone (controls) for 2 weeks as earlier mentioned. An equal volume of DMSO/Saline (1:10) was used for the control group, which received either oxygenated air or TS [137].

3.2.9 Tissue Preparation

Mice were sacrificed one day after the last day of the TS exposure cycle to collect their brains for subsequent biochemical and molecular analysis. Briefly, a cut was made at the nape and extended along the midline from the dorsal cervical area to the tip of the nose. After pulling the skin away from the skull laterally, a cut through the spine at the base of the skull was made using a dedicated pair of sterile brain harvest scissors. The skull was opened by placing the point of the scissors in the foramen magnum and cutting along the midline. The parietal bones were levered away from the brain through the flat end of the scissor blade. The nerve attachments at the brain stem and the optic chiasm

beneath the brain were disrupted using the closed point of thumb forceps. The brain was then dropped from the skull into a sterile medium [75].

3.2.10 Preparation of Protein Extracts and Western Blotting

To lyse homogenized brain tissues and cells to harvest the proteins, either RIPA lysis buffer or subcellular protein fractionation kit for cultured cells (Thermo scientific, #78840) as per manufacturer's guidelines was used so that total proteins were collected by centrifugation at 14000g for 30 mins. Samples were then aliquoted and stored at −80 °C until needed for protein expression analysis by WB. Proteins quantification was conducted using Pierce BCA Protein Assay Kit (Thermo Scientific, # 23225). Samples (15–30 µg for cell lysates and 60–90 µg for tissue lysates) were then prepared according to the following method described in our previous lab report so that denatured samples were run on SDS-PAGE (4–15% gradient gel) and transferred to PVDF membranes for further blotting [67,75]. The membranes were then washed with Tris-buffered saline (TBS) (10 mmol/l Tris-HCl, pH 7.4, 150 mmol/l NaCl) containing 0.1% Tween-20 (TBS-Tween), blocked for 1 h with TBS-Tween containing 5% non-fat dry milk, and incubated with primary antibodies prepared in TBS-Tween containing 5% bovine serum albumin (BSA) for overnight at 4 °C. The following day, for immunodetection, cells were washed and then incubated with the secondary antibody prepared in TBS-Tween containing 5% BSA for 2h. The protein Band densities were analyzed through Image Studio Lite Ver 3.1 and calculated as fold change/ percentage change over control protein expression. To confirm loading of equal amounts of protein and unchanged levels of protein by the

different treatment conditions, all quantifications were adjusted for the corresponding β-actin level.

3.2.11 Immunofluorescence Imaging

mBMEC cells were seeded and grown in four-well chamber slides, as mentioned previously. Cells were fixed using 16% methanol-free formaldehyde diluted 1 in 4 in 1X PBS, then washed and permeabilized using 0.02% Triton 100X. Cells were then blocked with blocking buffer (5% goat serum in PBS) at 25 °C for about 1h and incubated with primary antibodies prepared in blocking buffer overnight at 4 °C. The following day, cells were washed, stained with Alexa Fluor® 488 or 555 conjugated goat anti-rabbit or anti-mouse antibodies or vice-versa at 25 °C and then mounted with DAPI in prolonged gold anti-fade mounting media (Invitrogen, OR, USA). The following day, mounted slides upon overnight drying were examined under EVOS digital inverted fluorescence microscope. As negative controls, cells stained with only secondary antibodie were prepared [67,75].

3.2.12 ELISA

Tissue lysates from mice were analyzed by Quantikine ELISA kits (R & D systems, Minneapolis, MN, USA) for the quantitative determination of TNF-α and IL-6 according to the procedure following the manufacturer's protocol.

3.2.13 Blood-Brain Barrier Integrity Analyses

BBB integrity was evaluated as previously described by us elsewhere. Briefly, a mixture of labeled dextrans in PBS (FITC ~4 kDa, 10 mg/ml and RITC ~70 kDa, 10 mg/ml) was added to the luminal compartment of the transwells after 24 h of the last time

of the treatment and exposure to TS/EC extract solution. Then, 50 µl of media sample was collected from the abluminal compartment at 0, 15 and 30 min and replaced with equal volumes of new media to maintain appropriate sink conditions. Fluorescence was measured at specified excitation and emission wavelengths to determine the concentration of each fluorescent dye in the sample (FITC: 485 nm excitation/535 nm emission; RITC: 544 nm excitation/ 576 nm emission). Under normal conditions, the baseline permeability coefficients for FITC and RITC were approximately 2.1×10−4 cm/s and 5.8×10−4 cm/s. The permeability measurements were reported as the percentage of controls by considering the appropriate controls, such as media samples without dextran and that from abluminal compartments of cell-free inserts with dextran added to the luminal compartment. To confirm the findings, we also measured TEER (Ω.cm2) using EVOM 2 (World Precision Instruments, Sarasota, FL, USA). TEER measurements (baseline value) of cell-free inserts were used to determine the baseline values to subtract from the experimental readings.

3.2.14 Intracellular Reactive Oxygen Species Measurement

To measure the amount of intracellular ROS, we used 2,7-dichlorodihydro fluorescein diacetate (2,7-DCFH-DA) as described elsewhere. Briefly, seeded mBMEC cells on the 96-well plate were washed with 100 µL/well of PBS once. 12.5 ul of 20,70-dichlorofluorescein diacetate (DCFHDA) 20 mM (in DMSO) was diluted in PBS to final concentration (25 µM). 100 µl of DCFHDA was added and incubated in the dark at 37 °C for 45 min. Cells were then washed thrice with PBS, and 100 µl of PBS was added to each well. The intensity of dichlorofluorescein (DCF) fluorescent measurements in the

supernatant was taken at specified excitation and emission wavelengths (485 nm excitation and 535 nm emission). The ROS generation was calculated as the percentage change over control.

3.2.15 Nicotine and Cotinine Measurements in Brain and Plasma

Nicotine and cotinine concentrations in plasma and brain tissue were assessed previously described by our group [139]. Once the last smoking cycle on the last day was completed, we collected (within 30 minutes) a 100µL blood sample by cardiac puncture. The sample was centrifuged at 1300g for 10 minutes to obtain the plasma stored at -80°C. Following decapitation, the brain was removed and divided into 2 equal samples. One part was stored at -80°C for further molecular and biochemical analyses; the other part was instead homogenized in water (1:10 ratio) and used immediately for cotinine and nicotine quantification using a rapid, sensitive, and very specific UHPLC-MS method developed and validated by our group [139]. This method allows for simultaneous quantification of nicotine and cotinine in mouse plasma and brain homogenate.

3.2.16 Statistical Analysis

Data from all experiments were expressed as mean ± standard deviation (SD) and analyzed by one-way ANOVA using GraphPad Prism 6 Software Inc. (La Jolla, CA, USA). Post multiple comparison tests were performed with Tukey's or Dunnett's test as suggested by the software. P values < 0.05 were considered statistically significant.

3.3 Protective Effect of Rosiglitazone against Tobacco Smoke and Electronic Cigarette Induced Oxidative Stress Damage at the Blood-Brain Barrier: In Vitro Study

To evaluate appropriate RSG dosing based on its impact on cell toxicity and viability, an MTT cytotoxicity assay was used. As shown in Fig. 3.1, compared to control, the viability of cells treated with different RSG doses (20 μM to 2000 μM) did not show any significant difference except for the highest concentration tested, which resulted toxic to cell viability. Therefore, based on these results and literature evidence, the RSG working dose for all our *in vitro* studies was finalized at 20 μM.

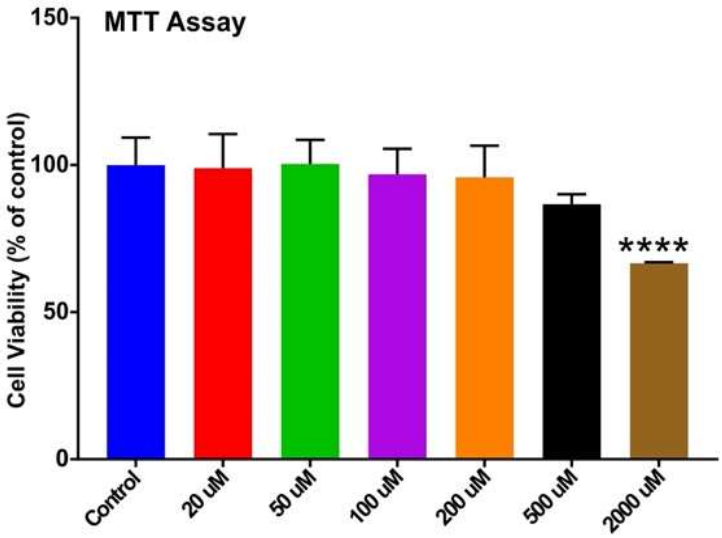

Figure 3.1 MTT cytotoxicity assay for RSG dose evaluation. n= 4 biological replicates; **** $p < 0.0001$ vs control.

3.3.1 Rosiglitazone Significantly Decreases Intracellular Reactive Oxygen Species Generated in Response to Tobacco Smoke /Electronic Cigarette Treatment as well as Their Pro-inflammatory Activity

To measure whether the cell-damaging effect of TS/EC was related to OS, we measured the intracellular ROS generation in RSG-treated and untreated cells for 24 h. As shown in Fig. 3.2A, a significant increase in intracellular ROS in the untreated TS/EC-exposed samples was observed. In addition to reducing OS, RSG decreased TC/EC pro-inflammatory activity, as demonstrated by the reduced expression of PECAM-1 (Fig. 3.2B) and NF-kB (Fig. 3.2C). RSG treatment significantly decreased ROS levels, and the effect parallels PPARγ upregulation and NRF2 activation (Fig. 3.3).

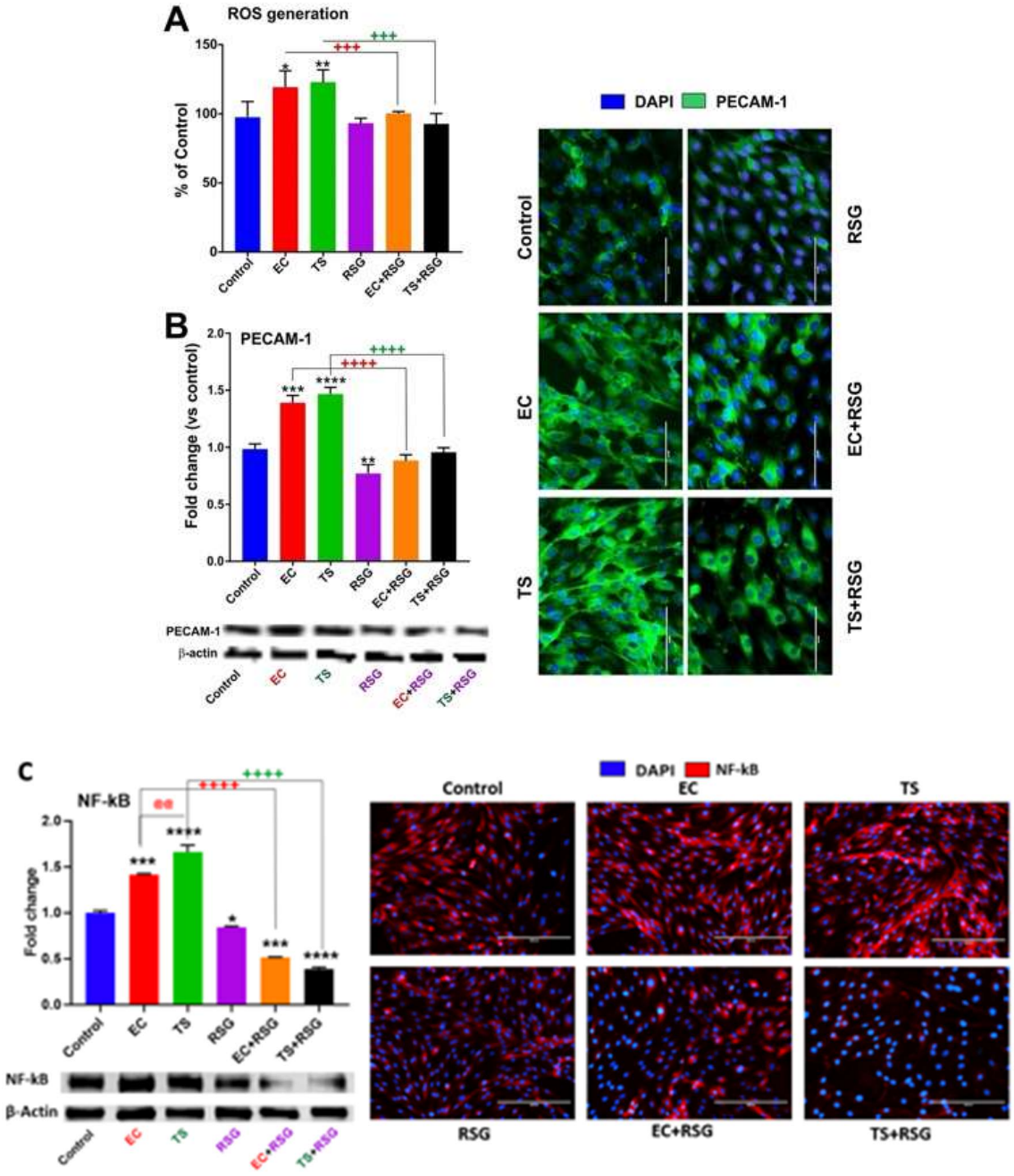

Figure 3.2 RSG decreases intracellular ROS generation and inflammation by TC/EC.A) Intracellular ROS generation measured by flow cytometry. B and C) expression level of the inflammatory markers PECAM-1 and NF-kB, which was increased in cells treated with TS/EC, was downregulated by RSG. n=3 to 4 biological replicates; * $p < 0.05$, ** p

< 0.01, *** p < 0.001, **** p < 0.0001, vs. control; +++ p < 0.001, ++++ p < 0.0001, TS/EC vs. TS/EC+RSG.

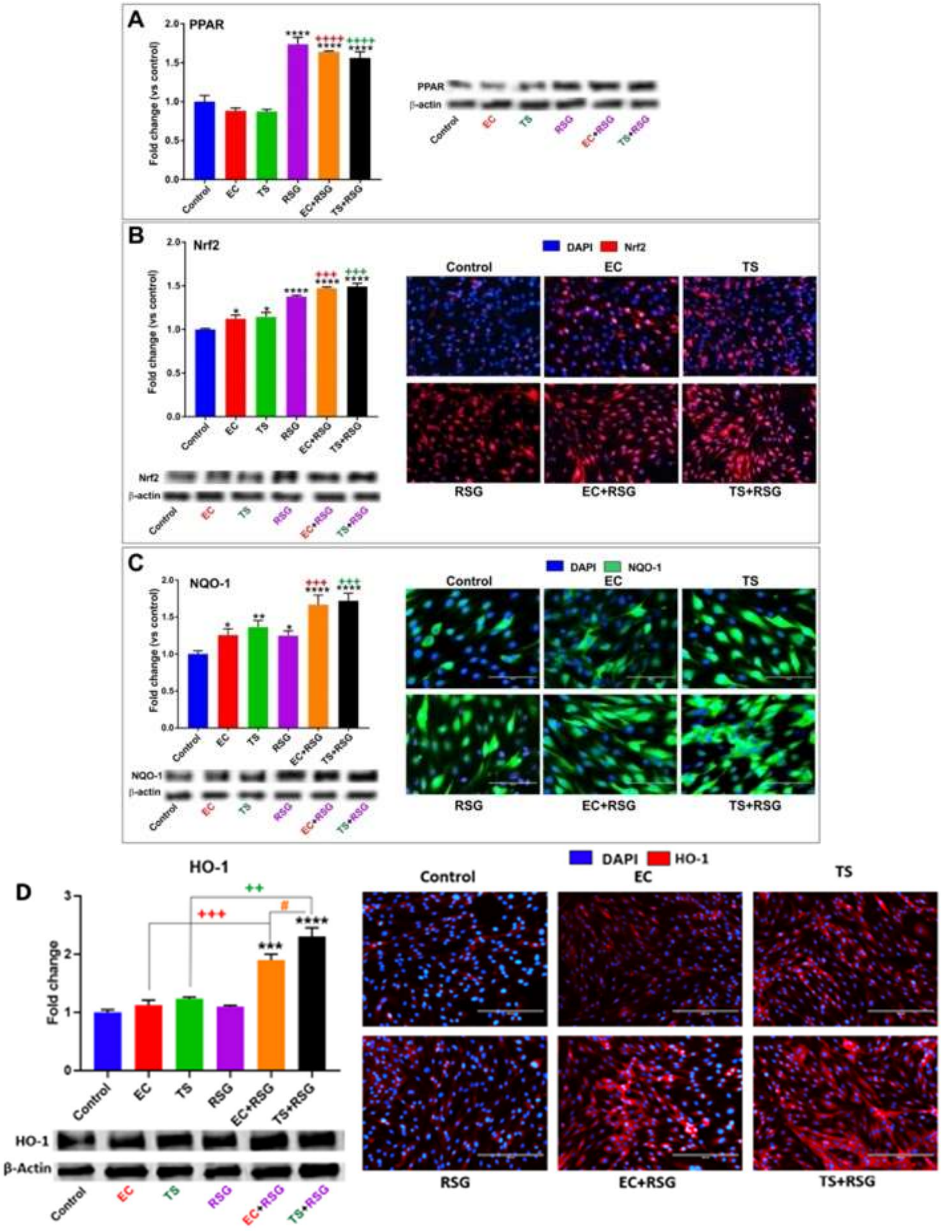

Figure 3.3 Protective effects of RSG against TS/EC-induced OS.A) IF and WB analysis emphasizes activation of the NRF2 signaling pathway. B) IF and WB analyses emphasize RSG's effect on the activation of peroxisome proliferator-activated receptor (PPARγ). C and D) Concurrently, the overexpression level of downstream detoxifying molecules NQO-1 and HO-1 in the cells, including RSG, was detected. n=3 to 4 biological replicates. * $p < 0.05$, ** $p < 0.01$, **** $p < 0.0001$, vs control; +++ $p < 0.001$, ++++ $p < 0.0001$, TS/EC vs TS/EC+RSG. WB analyses report protein/β-actin ratios.

3.3.2 Rosiglitazone Upregulates PPAR Expression as well as NRF2 and its Downstream Effector NQO-1 and HO-1

The effect of TS/EC on the expression of the NRF2 and PPARγ was also evaluated. As shown in Fig. 3.3A, the total expression levels of NRF2 in TS/EC exposed cultures were slightly more than control. Fig. 3.3 showed that treatment of the cells with RSG significantly stimulated the expression of PPARγ (Fig .3.3A) and increased the expression of NRF2 (Fig. 3.3B) as demonstrated by WB and IF analyses. Measurements also support increased expression/activity of NRF2 (both WB and IF analyses) of its downstream effector NQO-1 and HO-1, as demonstrated in Figs. 3.3C and 3.3D.

3.3.3 Rosiglitazone Decreases Tobacco Smoke/Electronic Cigarette -Induced Endothelial Inflammation and Loss of Barrier Integrity

To assess the effect of RSG on BBB integrity, IF, WB, TEER measurement and labeled dextrans permeability analyses were conducted. As shown in Figs. 3.4A, D, and E, exposure of mBMECs to TS/EC downregulated their expression of TJ accessory protein ZO-1 and TJ proteins Occludin and Claudin-5 compared to controls. Notably, these adverse changes were countered by RSG pretreatment. From a functional point of view, TS/EC negatively impacted barrier integrity as demonstrated by TEER measurements (Ohm cm^2) shown in Fig. 3.4B. RSG significantly reduced the negative impact of both TS and EC on BBB integrity. Results were further confirmed by parallel permeability assays using labeled FITC and RITC dextrans, demonstrating increased permeability (vs. control) in TS/EC exposed cultures which were reverted following RSG treatment (see Fig. 3.4C) [135].

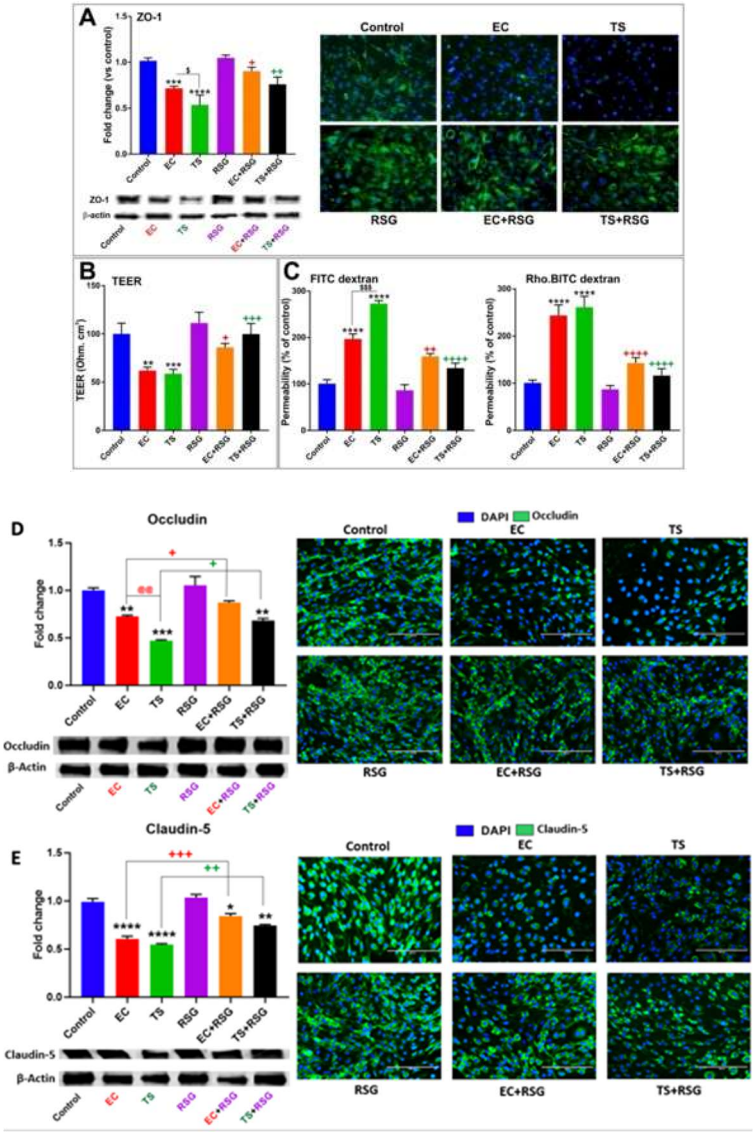

Figure 3.4 Protective effects of RSG against TS/EC-induced endothelial inflammation and loss of barrier integrity.IF and WB analyses demonstrate downregulation of TJ proteins A) ZO-1, D) Occludin and E) Claudin-5 in cells treated with TS/EC and increased expression of that in the cells including RSG. B) TEER measurement after treatments demonstrated a significant loss of BBB integrity in cells treated with TS/EC, while RSG prevented the decrease in TEER. C) Increase in dextran permeability measurements emphasizing the loss of BBB integrity in cells treated with TS/EC was prevented by RSG. n=3 to 4 biological replicates. ** $p < 0.01$, *** $p < 0.001$, **** $p < 0.0001$ vs control; + $p < 0.05$, ++ $p < 0.01$, +++ $p < 0.001$, ++++ $p < 0.0001$ TS/EC vs TS/EC+RSG; \$ $p < 0.05$, \$\$\$ $p < 0.001$ EC vs TS. WB analyses report protein/β-actin ratios.

3.3.4 Discussion

Excessive ROS production (endogenous and exogenous) can provide a state of redox imbalance causing cellular and tissue damage which are the main prodromal factors in the onset and progression of several cerebrovascular and neurodegenerative diseases such as stroke, amyotrophic lateral sclerosis (ALS), Parkinson's disease (PD), Alzheimer's disease (AD and aging. Chronic exposure to TS and EC is a risk factor for vascular endothelial dysfunction. The impact on BBB viability has been recently reported to be primarily linked in a dose-dependent and causative manner primarily linked to ROS, nicotine, and inflammation. The current scientific opinion suggests that ROS/OS plays a pivotal role in the pathogenesis of cerebrovascular disorders. NRF2, a ubiquitously expressed redox-sensitive transcription factor and the key regulator of redox homeostasis in cells, exerts cytoprotective functions encompassing anti-oxidative and anti-inflammatory responses under physiological conditions. NRF2 is a pivotal upstream transcription factor responsible for regulating redox balance so that downregulation or suppression of NRF2 activity enhances the cell susceptibility to the detrimental effects of ROS and pro-inflammatory stimuli leading to cell apoptosis [140]. Although under normal conditions, NRF2 is sequestered in the cytoplasm by its inhibitor Keap1, once activated, it translocates to the nucleus and dimerizes with another member of the Cap'n'Collar family of transcription factors which finally leads to activation of transcription by binding to an antioxidant response element (ARE) located in the promoters of several antioxidant genes. Our previous findings have shown that NRF2 regulates BBB endothelial tight and adherence junction protein expressions. In contrast,

chronic exposure to TS and EC adversely impacts NRF2 activity/levels and negatively influences BBB integrity and function [135]. Similarly to chronic smoking/vaping, downregulation of NRF2 worsens the diabetic phenotype, and the impairment in endothelial glucose uptake leads to the downregulation of TJ proteins expression and loss of BBB integrity. The results from our previous reports also support an additive release pattern of angiogenic and inflammatory factors by BBB endothelial cells in response to hyperglycemia (HG) with simultaneous exposure to cigarette smoke extracts, suggesting the involvement of common pathogenic modulators of BBB impairment. RSG, as a member of the thiazolidinediones (TZDs) family, which is the ligand of the PPARγ, has been currently investigated for diseases where insulin resistance may be an important factor. For example, Ceolotto et al. tested the effect of RSG on quenching OS initiated by high glucose by preventing and reducing NAD(P)H oxidase activation. They demonstrated that RSG activates AMPK, preventing hyperactivity of high glucose-induced NAD(P)H oxidase, possibly by PKC inhibition and thus, protecting endothelial cells against glucose-induced OS with an AMPK-dependent and a PPARγ-independent mechanism. AMPK has been demonstrated to promote nuclear accumulation and thus the activity of NRF2, thus implying that increased expression of PPAR by RSG can be linked to increased activity of NRF2 and its downstream effectors such as NQO-1 as shown in our work. In another study, Hwang et al. demonstrated that RSG has the potential to reduce vascular OS rapidly through mechanisms not depending on the correction of major diabetic metabolic derangements. Furthermore, Sayan-Ozacmak et al. evaluated the possible impact of RSG on chronic cerebral hypoperfused rats regarding the levels of

OS, reduced glutathione, and hippocampal neuronal damage. Their findings confirmed the beneficial effect of RSG on hypoperfusion-induced hippocampal neuronal damage due to the inhibition of OS. Lee et al. investigated the molecular mechanisms underlying apoptosis initiated by chlorpyrifos (CPF)- mediated OS, and finally, they suggest that RSG may employ an anti-apoptotic effect against CPF-induced cytotoxicity by the reduction of OS and also inhibition of the inflammatory cascade using inactivation of signaling by p38 and JNK, and NF-κB. In a separate study, Kadam et al. observed elevated expression of HO-1 and NRF2 and downregulated expression of Tlr4 receptor in response to RSG administration compared to the control group. RSG also prevented preterm birth by downregulating inflammation and upregulating the antioxidant factors NRF2 and HO-1 [137]. Although these studies clearly prove the protective effects of RSG against some other causes of OS, this drug's possible therapeutic use in reducing ROS and BBB integrity prodromal to cerebrovascular disorders could be investigated. Thus, in this preliminary focused study, we assessed the effectiveness of RSG treatment in preventing and reducing BBB damage and OS in response to chronic TS/EC exposure. The results of our study showed that the appropriate RSG dosing based on its impact on cell viability by MTT cytotoxicity (Fig. 3.1) notably inhibited TS/EC exposure-induced intracellular ROS production confirming cytoprotective effects of RSG (Fig. 3.2). In order to examine the mechanism underlying the antioxidant effect of RSG, we also detected the effect of RSG on the expression of NRF2, as one of the major transcription factors regulating the antioxidant defense response and its effector protein downstream signaling molecule NQO-1 which exert acute detoxification and cytoprotective functions

[75]. Although TS/EC exposures caused a slight increase in the expression of NRF2 and also promoted loss of BBB integrity and cellular inflammation (Fig. 3.3), RSG significantly induced NRF2 signaling pathway activation and increased the expression of NQO-1 [141]. These results might be due to an antioxidant role of RSG in a PPARγ-dependent manner, leading to the activation of NRF2 and NQO-1. Our results correlate very well with previous studies by Wang et al. demonstrating that inhibition of PPARγ markedly reduced the protective activity of RSG by preventing NRF2 activation of the antioxidative response system. Concerning the specific impact on the BBB, our *in vitro* data (Fig. 3.4) clearly show that TS/EC exposure decreases ZO-1 expression in mBMEC cells leading to cerebrovascular impairment in terms of loss of TJ proteins which RSG prevented. As expected, loss of ZO-1 following TS/EC exposure was paralleled by a significant TEER decrease and concomitant increase of paracellular permeability to both 4 and 10 kDa labeled dextrans (Fig. 3.3). Like for ZO-1 expression, Impairments of BBB integrity including loss of TEER and increased permeability to dextrans was reverted by RSG (Fig. 3.4). Moreover, RSG reduced the expression of the pro-inflammatory adhesion molecule PECAM-1 resulting from TS/EC exposure when compared to untreated TS/EC exposed cultures. This and the protective effect on BBB integrity suggests that RSG could be used to protect the cerebrovascular system from exogenous oxidative stimuli (like those promoted by TS/EC exposure). This preliminary work provides support for further *in vivo* studies aimed at validating our results and assesses the effectiveness of RSG in more realistic clinical settings (e.g., vascular inflammatory disorders and stroke).

3.4 Use and Effect of Rosiglitazone as Anti-diabetic Countermeasures Against Tobacco Smoke-Dependent Cerebrovascular Toxicity: *In Vivo* Study

In-vivo studies are performed to evaluate and validate the protective effect of RSG against BBB damage and cerebrovascular dysfunctions caused by TS exposure. As shown in Fig. 3.5A TS generated by a CSM-SCSM cigarette smoking machine (CH Technologies, Westwood, NJ) was forced directly into two airtight smoking chambers (Dimension- 24 L X 12 W X 12 H) housing the mice (4 mice/cage). The smoking inlet is dually connected to a feeding tube and a ventilator system supplying O_2 (2 L/min) at atmospheric pressure (1 bar). During the interval between puffs, animals received an uninterrupted supply of normal oxygenated air. Following each smoking cycle's end, animals were immediately transferred back to their regular housing with food and water supply. Mice received a daily intraperitoneal injection of RSG before the first smoking cycle.

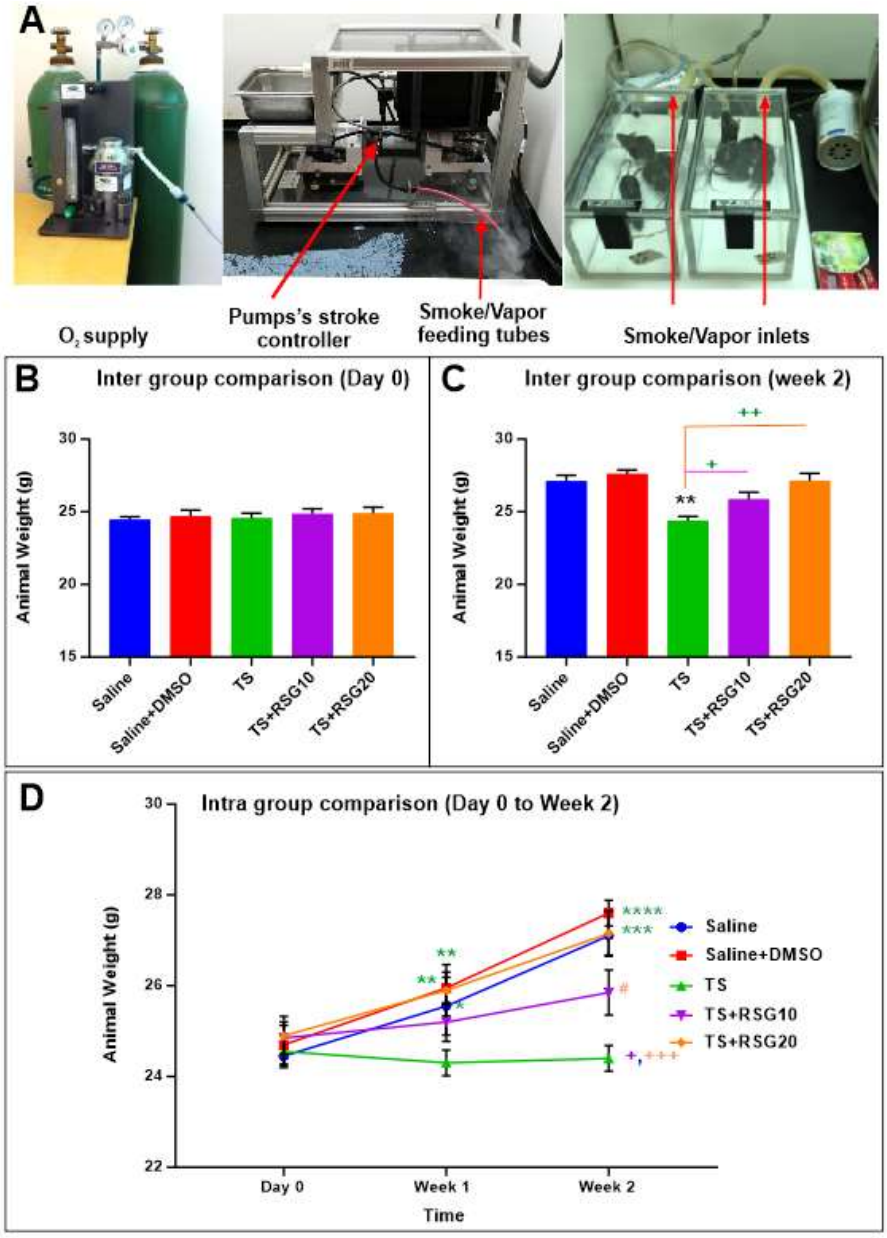

Figure 3.5 Effect of Saline/DMSO/RSG treatments with/without TS exposure on body weight *in vivo*.A) Set-up of the exposure of mice with chronic exposure to the TS. Test mice also received a daily intraperitoneal injection of RSG. At the end of the experiment, brain tissue was collected, homogenized, and processed for biochemical and molecular preparations. n = 3 to 4 biological replicates. *$p < 0.05$, **$p < 0.01$, ***$p < 0.001$, ****$p < 0.0001$ vs Saline. +$p < 0.05$, ++$p < 0.01$, +++$p < 0.001$ vs. TS. #$p < 0.05$ TS+RSG 20 vs TS+RSG 10. N=4 biological replicates.

3.4.1 Decreased Harmful Effect of Tobacco Smoke on Body Weight by Rosiglitazone

Weight analysis was regularly performed to evaluate whether RSG dosing negatively impacted body weight. As shown in Fig. 3.5B and 3.5C we observe a slight decrease in body weight in the group of untreated TS-exposed mice at the end of the two weeks of experimental testing. The concomitant administration of RSG reduced the effect of TS on body weight in a dose-dependent manner (see Fig. 3.5C and in Fig. 3.5D) demonstrating the lowered detrimental effect of TS by RSG accounts for the harmful effect of TS and the protective effect of RSG on the body weight.

3.4.2 Result for Nicotine and Cotinine Measurements

Plasma and brain levels of nicotine and cotinine in the mouse following two weeks of chronic exposure are shown in Fig. 3.6A. Data shows that nicotine and cotinine concentrations in plasma and the brain were comparable between all the experimental groups. This indicates that each group of animals was subject to a very similar level of TS exposure. As previously reported, our exposure methods allow achieving the physiological concentration of nicotine and cotinine that are comparable to those observed in a heavy chronic smoker [75,139]. In Fig. 3.6B, we reported the calculated plasma-to-brain ratio of nicotine and cotinine. As expected, we did not observe any significant difference between the experimental groups. The data also reflect the poor brain permeability of cotinine compared to nicotine.

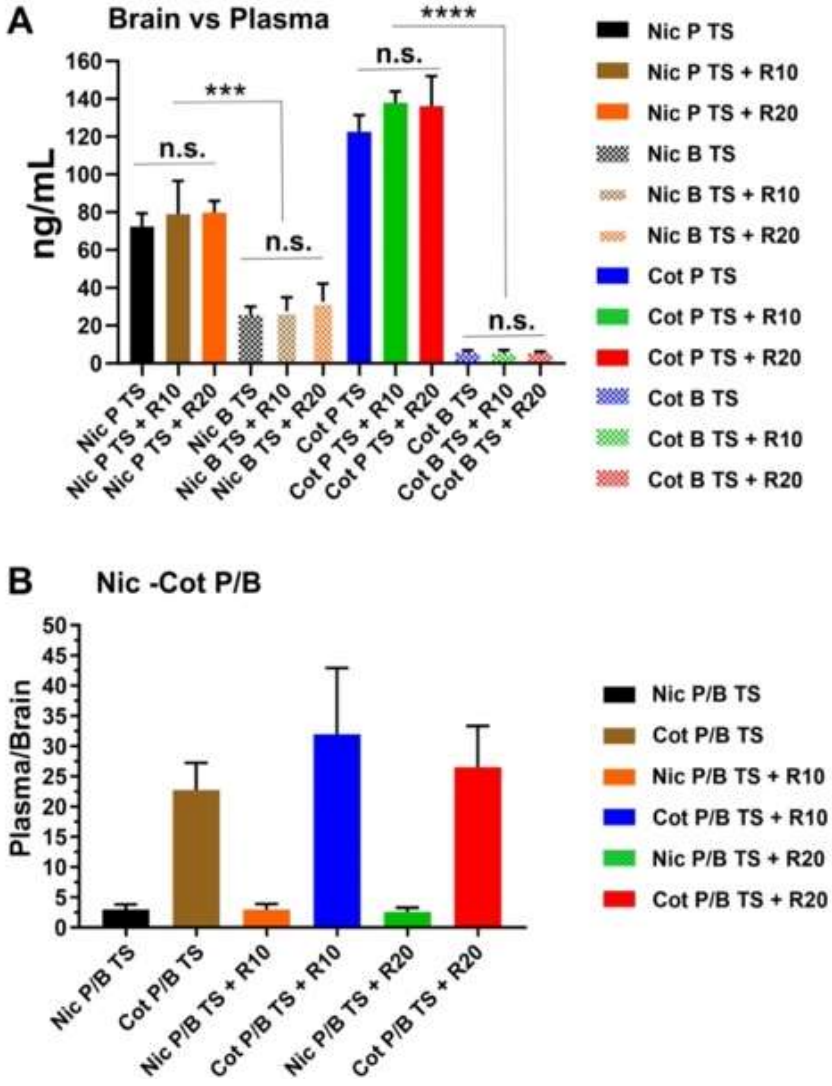

Figure 3.6 Plasma and brain levels of nicotine and cotinine in the mouse.(A) Side by side comparison of plasma "P" vs. brain "B" levels and (B) plasma/brain ratio of nicotine and cotinine across the main experimental groups, including TS exposed mice with and without RSG treatments. Note that nicotine and cotinine levels achieved across the various groups are not statistically different, thus indicating that levels of TS exposure achieved at the end of the 2 weeks among the test animals were very similar. Note also that differences in Brain concentration between nicotine and cotinine correctly reflect the reduced BBB permeability of cotinine vs. nicotine. "****" = $p<0.0001$; N=4 biological replicates.

3.4.3 Upregulation of PPAR Expression as well as NRF2 and its Downstream Effector NQO-1 and HO-1 in a Dose-Dependent Manner

The effect of TS on the expression of the NRF2 and PPARγ was also evaluated. as demonstrated by WB analysis in Fig. 3.7, treatment with RSG not only significantly stimulated the expression of PPARγ in a dose-dependent manner (Fig. 3.7A) but equally enhanced that of NRF2 (Fig. 3.7B1). As shown in Fig. 3.7B2 and 3.7B3, increased expression of NRF2 translated to similar upregulation of its downstream effector NQO-1 and HO-1 as assessed by WB analyses. This data demonstrated that RSG increases the overall activity of the NRF2-ARE system.

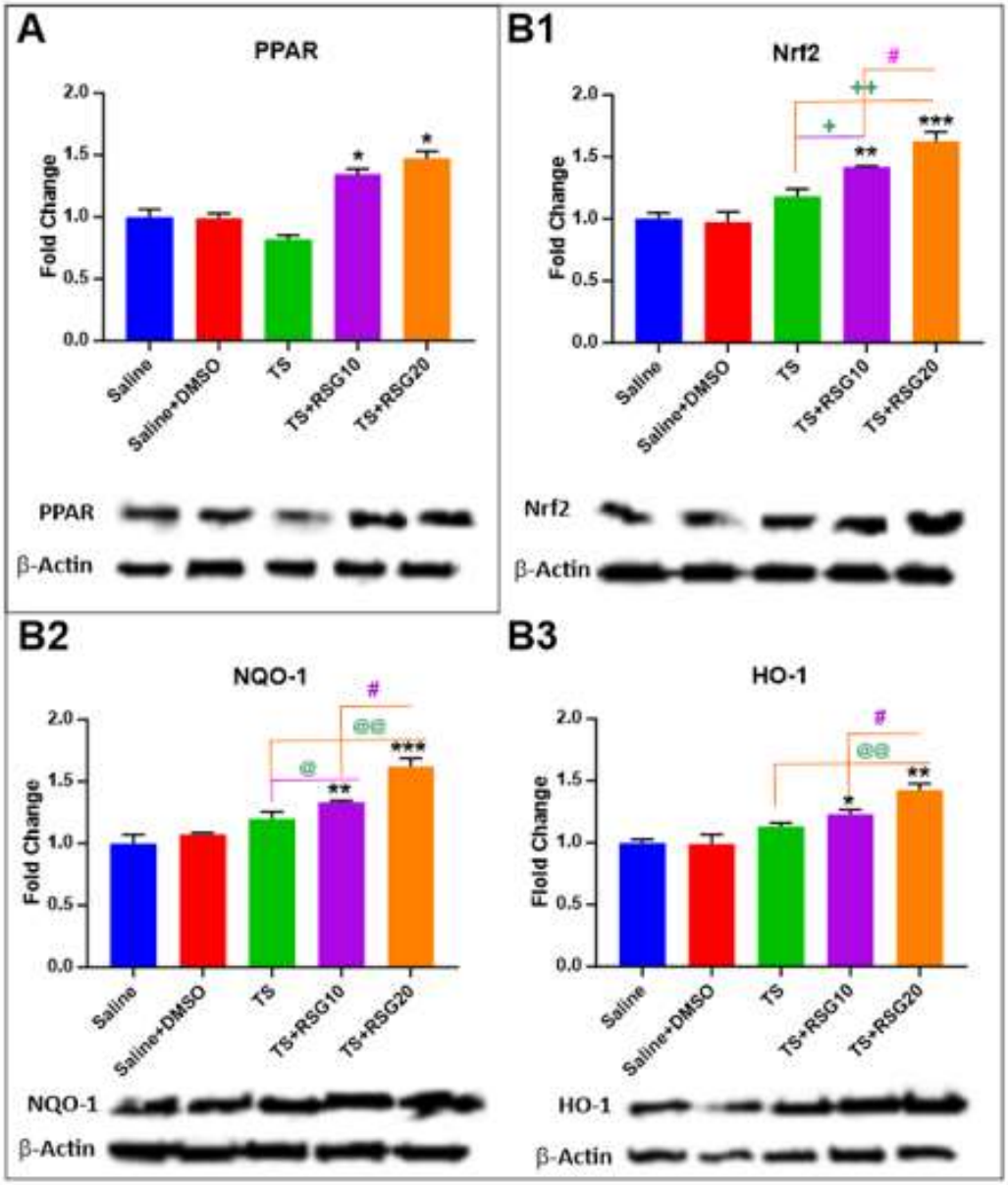

Figure 3.7 Dose-dependent protective effects of RSG against TS-induced OS.A) WB analysis emphasizes RSG's effect on activation of the transcription factor peroxisome proliferator-activated receptor (PPARγ). B1) WB analysis emphasizing activation of the NRF2 signaling pathway. B2, B3) Parallel to RSG's increased NRF2 expression levels, we also observe comparable upregulation of downstream detoxifying molecules NQO-1 and HO-1. n = 3 to 4 biological replicates. *p < 0.05, **p < 0.01, ***p < 0.001 vs Saline. @p < 0.05, @@p < 0.01, vs. TS. #p < 0.05 TS+RSG 20 vs TS+RSG 10. WB analyses report protein/β-actin ratios.

3.4.4 Rosiglitazone Decreases Tobacco-Induced Loss of Blood-Brain Barrier Integrity

Previous work by our group has shown that upregulated activity of the NRF2 system is also accompanied by increased expression of TJ proteins and decreased BBB permeability both *in vitro* and *in vivo* [67,75,79,135]. Similarly, we assessed whether increased expression of NRF2 by RSG also translated into upregulation of TJ protein expression using whole brain tissue homogenate. As demonstrated in Fig. 3.8, chronic exposure to TS significantly downregulated the expression of zonula occludentes-1 (ZO-1); a TJ accessory protein (Fig. 3.8C). Further, the expression level of main TJ proteins including Occludin and Claudin-5 (Fig. 3.8A & B) were also significantly downregulated when compared to controls. Notably, concurrent treatment with RSG counteracted the effect in a dose-dependent manner. TJ expression improvement by RSG over TS untreated mice was in strong accordance with that of NRF2 as previously shown.

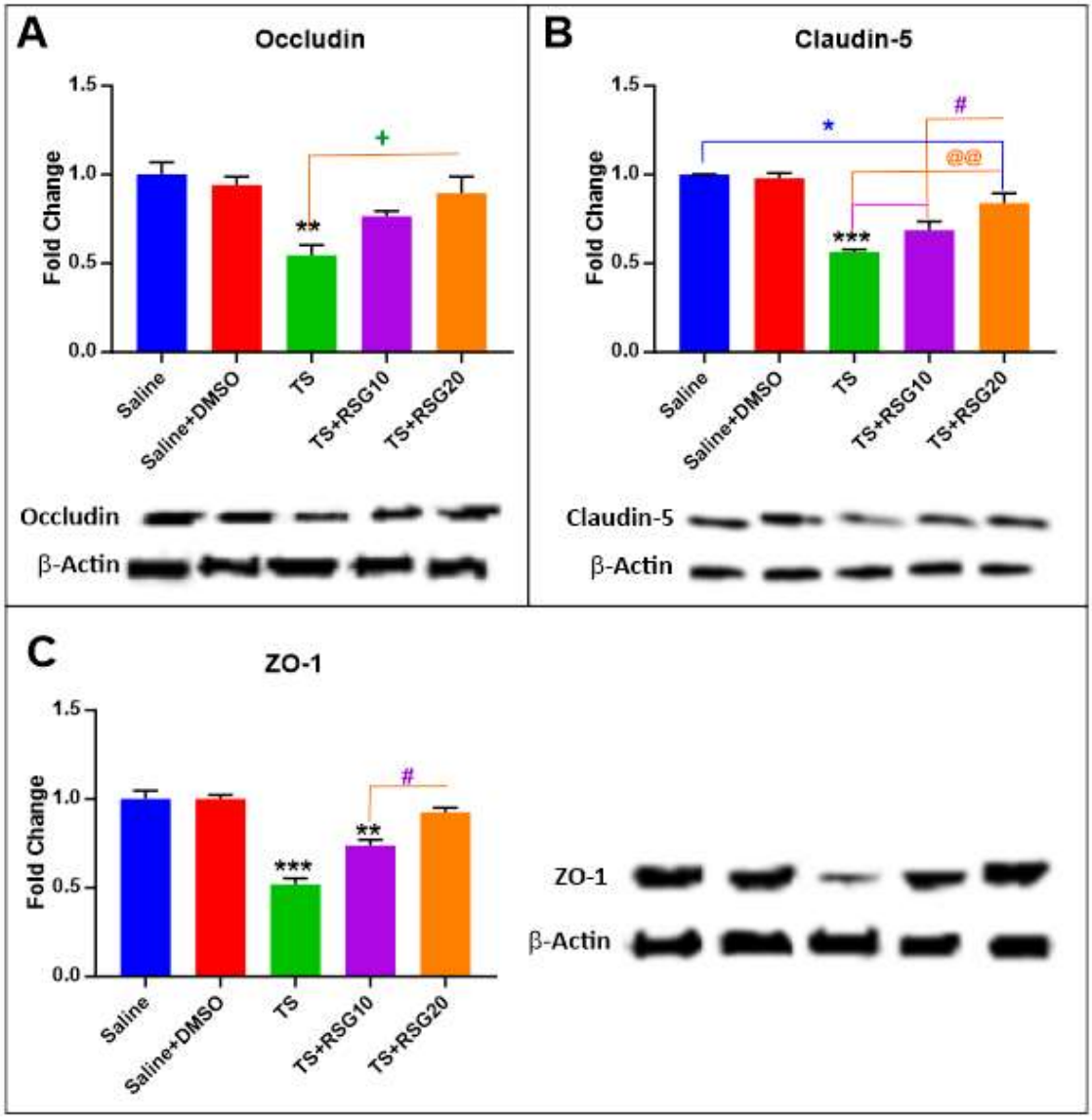

Figure 3.8 Dose-dependent protective effects of RSG against TS-induced loss of barrier integrity.WB analysis demonstrated the downregulation of TJ proteins ZO-1, Occludin, and Claudin-5 in animals exposed to TS. The effect was mitigated by RSG treatment in a dose-dependent manner. N = 4 biological replicates. *$p < 0.05$, **$p < 0.01$, ***$p < 0.001$ vs Saline. +$p < 0.05$, @@$p < 0.01$ vs. TS. #$p < 0.05$ TS+RSG 20 vs TS+RSG 10. WB analyses report protein/β-actin ratios. N=4 biological replicates.

3.4.5 Decreased Pro-inflammatory Effect of Tobacco Smoke-Exposure by Rosiglitazone

TS not only generates OS but also promotes inflammation linked to oxidative stimuli. Decrease and/or overwhelmed NRF2 activity following chronic TS exposure become less efficient in contrasting OS stimuli, thus leading to increased inflammation. In this respect, RSG provided an effective countermeasure to the pro-inflammatory activity of TS. As shown in Fig. 3.9A and Fig. 3.9B, WB revealed a significant increase in the expression level of PECAM-1 and nuclear factor kappa-light chain-enhancer of activated B cells (NF-κB); a master regulator of inflammatory responses [78]. By contrast, RSG treatment decreased inflammation when compared to untreated TS-exposed animals. Specifically, our data show a reduction in the expression level of NF-κB (Fig. 3.9A) and PECAM-1 (Fig. 3.9B). The effect was also dose-dependent. The analysis of pro-inflammatory cytokines by ELISA also revealed that RSG decreased TNF-α and IL-6 release in a dose-dependent manner in response to TS exposure (see Fig. 3.9C and Fig. 3.9D).

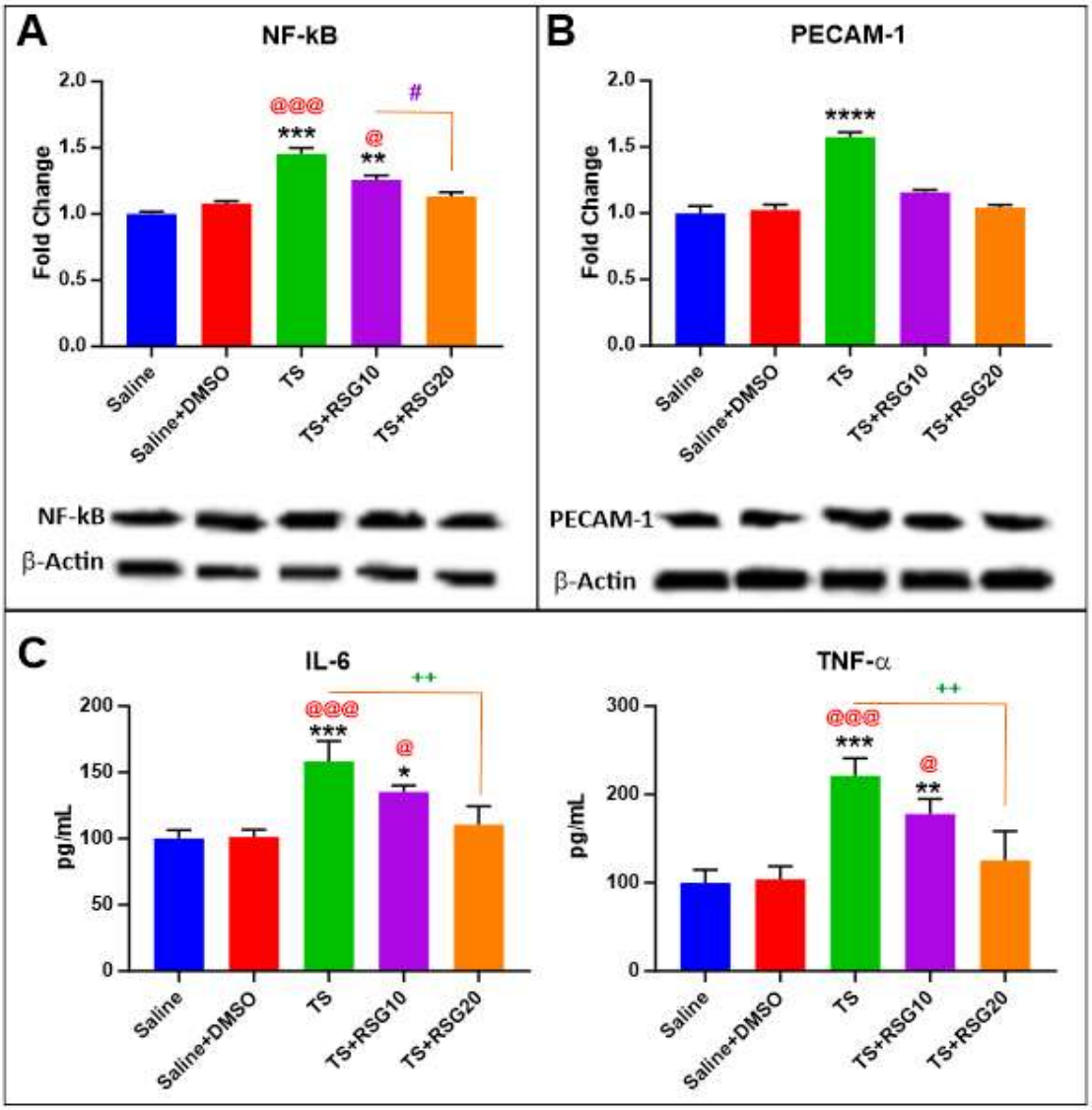

Figure 3.9 RSG decreases intracellular inflammation induced by TS.A) Expression level of the inflammatory marker NF-kB which was increased in cells treated with TS, was downregulated by RSG. B) Expression level of the inflammatory marker PECAM-1, which was increased in cells treated with TS, was downregulated by RSG. C, D) ELISA of pro-inflammatory cytokines TNF-α and IL-6. RSG reduced TS-induced TNF-α and IL-6 release. N = 4 biological replicates; *$p < 0.05$, **$p < 0.01$, ***$p < 0.001$, ****$p < 0.0001$ vs Saline. @$p < 0.05$, @@@$p < 0.001$, ++$p < 0.01$ vs. TS. #$p < 0.05$ TS+RSG 20 vs TS+RSG 10. WB analyses report protein/β-actin ratios.

3.4.6 Discussion

OS, the redox imbalance caused by highly ROS, which are either free oxygen radicals or reactive anions containing oxygen atoms, leads to cellular and tissue damage such as lipoperoxidation of polyunsaturated fatty acids in membrane lipids, protein oxidation, RNA oxidation, mitochondrial depolarization, DNA strand breakage, and apoptosis and finally serves as an essential role in propagating neuropathogenesis in numerous cerebrovascular and neurodegenerative diseases such as stroke, amyotrophic lateral sclerosis (ALS), Parkinson's disease (PD), Alzheimer's disease (AD) and aging [68,135]. OS is an early, initiator and a potential late by-product of neurodegeneration in these disease states. Recent evidence has suggested that chronic exposure to TS is associated, in a dose-dependent manner, with dysfunction of normal endothelial physiology and subsequently in the pathogenesis of cerebrovascular disorders [112,142]. NRF2, a basic region-leucine zipper (bZip) transcription factor is the master regulator of multiple cytoprotective responses and a key regulator of redox homeostasis in cells [78]. Under basal conditions, NRF2 is sequestered in the cytoplasm by its inhibitor Kelch-like ECH-associated protein 1 (Keap1). In OS conditions, the cysteine residues of Keap1 become oxidized, releasing NRF2, which is now free to translocate to the nucleus, which leads to it binding to the antioxidant response element (ARE) present in the regulatory regions of over 500 genes, allowing transcription of antioxidants. Based on valid evidence NRF2 also enhances anti-inflammatory mediators, the activity of the proteasome, and other transcription factors involved in mitochondrial biogenesis. Recent studies from our group and other groups have highlighted the critical neuroprotective role

of NRF2 in defense mechanisms against OS and regulation and maintenance of BBB integrity and function [68,76,135]. Similarly, to chronic smoking, upregulation of NRF2 diminishes the diabetic phenotype and the impairment in endothelial glucose uptake, causing the upregulation of TJ protein expression and restoration of BBB integrity. The results from our previous reports also suggested the pathological commonalities between hyperglycemia and cigarette smoking at the BBB. The PPARγ agonist and a member of the thiazolidinediones (TZDs) family has been currently assessed for the diseases associated with insulin resistance. PPARγ is a member of a family of nuclear receptors that plays a pivotal role in regulating a huge number of genes implicated in glucose homeostasis and fatty acid metabolism. Jimenez et al. demonstrated the potentiality of PPARγ activation in attenuating high glucose-induced OS in endothelial cells and diabetic rats associated with the involvement of NRF2 [136]. They emphasized that PPARγ plays a vascular protective role against hyperglycemia-induced OS with the subsequent induction of HO-1 and upregulation of the NRF2 [136]. Numerous studies confirmed that independent of their metabolic actions, RSG as a PPARγ agonist has a protective effect against OS caused by high glucose in diabetes and hypoperfusion [136,137]. As a member of the nuclear hormone receptor family, PPARγ is involved in adipogenesis and metabolic regulation and exerts pleiotropic anti-inflammatory effects such as enhancing the transcription of anti-inflammatory and antioxidant genes (several of which also up-regulated by NRF2). In addition, PPARγ trans-represses key proinflammatory transcription factors, including NF-κB, STAT6, and AP-1. Interestingly, the work of Cho and associates has identified a novel regulatory loop through which

PPARγ may, in turn, regulate the expression of NRF2. Specifically, the authors identified a putative PPAR response element in the NRF2 promoter, whereas silencing of PPARγ blocked up-regulation of NRF2 induced by hyperoxia. These results imply that NRF2 and PPARγ might reciprocally reinforce the expression of one another (see also Fig. 3.10). Moreover, the possible therapeutic use of this drug in the reduction of ROS and restoration of BBB integrity was investigated in our previous *in vitro* work. In this preliminary study, we investigated the effect of RSG treatment on the prevention and reduction of BBB damage and OS in response to chronic TS/EC exposure. Despite unknown mechanism of RSG, the previous study revealed that RSG could promote counteractive protective mechanisms primarily associated with the enhancement of NRF2 activity through activation of the PPARy and BBB protection against TS/EC exposure, including reduced inflammation, OS, TJ proteins downregulation and loss of BBB integrity [26]. In line with these findings, in the present work, we evaluate the protective effect of RSG against TS-dependent cerebrovascular toxicity using a rodent model of chronic smoking previously developed and validated by our group [79,139]. Our results indicate that control mice receiving either Saline or Saline+DMSO followed a regular trend on the increase in body weight which accounts for lack of the harmful effect of DMSO as a solvent for RSG.

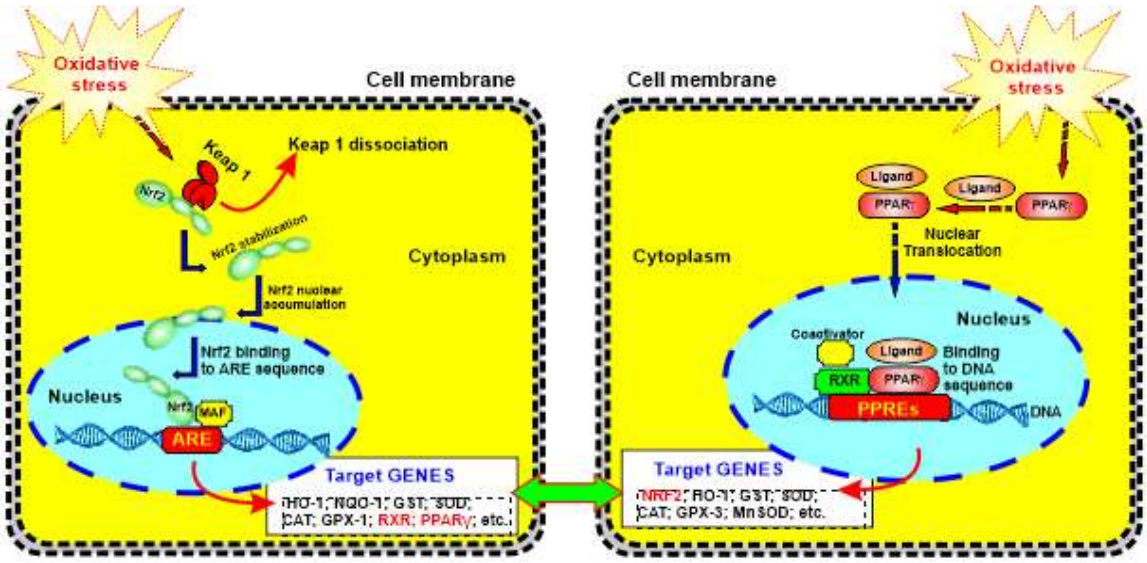

Figure 3.10 Schematic representation of crosstalk between NRF2 and PPARγ signaling pathways in relation to OS and inflammation.Recent data by others suggests that NRF2 and PPARγ might reciprocally reinforce the expression of one another, thus synergistically boosting the antioxidative response system.

The TS group demonstrated a loss of body weight compared to the control, which is also consistent with the well know metabolic stimulatory effect of TS. Loss of body weight was partially mitigated by RSG treatment in a dose-dependent manner. In contrast, RGS at the highest tested dose was not dissimilar from controls (Fig. 3.5). To confirm the *in vitro* protective effects of RSG, we assessed the impact of RSG on NRF2 expression levels, as well as its downstream effector molecules NQO-1 and HO-1 which are known for exerting acute detoxification and cytoprotective functions. Despite a slight increase in NRF2 level in untreated TS exposed mice receiving RSG alongside TS showed improved NRF2 expression/activity vs. their untreated counterparts (Fig. 3.7). Specifically, RSG-enhanced NRF2 activation/expression was paralleled by a similar

increase in the expression levels of NQO-1 and HO-1. The effect could be due to a direct modulatory activity toward NRF2 and/or PPARγ expression. Although it is impossible to dissect out each target's relative contribution at this time, our data corroborate the findings of Jimenez et al., who demonstrate the upregulation of HO-1 (protective factor against vascular OS) in response to PPARγ activation [136]. Moreover, Cho et al. showed antioxidant effects of NRF2 and PPAR-*γ* and PPAR*γ* modulation by NRF2, thus suggesting a positive role of PPAR-*γ* agonist in counteracting oxidative damage. Components of tobacco smoke trigger a complex pro-inflammatory response by recruiting the leukocytes to the site of inflammation and promoting the adhesion and binding of monocytes to the endothelial wall of blood vessels. This leads to an increase in the expression of selectins, pro-inflammatory and intercellular adhesion molecules. NF-κB is a rapid response factor that is kept in a resting state by the Inhibitor of κB (IκB) proteins. OS stimulates cell surface receptors by triggering the activation of the IκB kinase complex, leading to phosphorylation, ubiquitination, and degradation of IκB proteins, which leads to the release and translocation of NF-κB dimers to the nucleus, where it binds to specific DNA sequences and promotes the transcription of target genes to counteract OS and cellular damage [78]. As prevention of TS-induced progressive upregulation of PECAM-1 and NF-kB was observed at the cerebrovascular level in TS-exposed mice treated with RSG (Fig. 3.8). These results are in line with the earlier reported *in vivo* work by Prasad et al. wherein an increase in systemic inflammation was observed upon chronic TS exposure in mice [75]. These also support our previous *in vitro* results wherein RSG reduced the expression of the PECAM-1 and NF-kB resulting

from TS/EC exposure compared to untreated TS/EC exposed cultures [26]. Existing evidence also suggests that TS exposure induced the up-regulation and release of pro-inflammatory cytokines and decreased the release of cytokines could be indicative of reduced OS and inflammatory activity elicited by RSG (Fig. 3.8). Capillaries found in the CNS are different from those found in the rest of the body due to the BBB which is a significant filter that protects the brain. BBB include TJ proteins such as Occludin, Claudins attaching together the cerebral endothelial cells and also scaffolding proteins such as ZO-1, ZO-2 and ZO-3 anchoring the TJ proteins in the endothelial cell. the well-studied mechanisms for disruption of the BBB from OS are via matrix metalloproteinase (MMP) activation, NADPH oxidases, the toxicity of circulating free iron. It is widely described that BBB integrity is deeply affected by OS so that enhanced ROS generation leads to endothelium dysfunction and increased BBB permeability [143]. These alterations are mainly associated with the redistribution and/or altered expression of TJ proteins [143]. As demonstrated in Fig. 3.9, down-regulation of ZO-1, Claudin-5, and Occludin were observed in response to TS exposure, thus confirming previous results [26,75,76]. Pre-treatment with RSG exhibited a protective effect against TS-induced loss of BBB TJs in a dose-dependent manner. The effect was not dissimilar to that of another oral antidiabetic drug such as MF, which also exhibited the ability to upregulate NRF2 expression/activity [75]. Together, these novel data clearly highlight that RSG can prevent TS-induced cerebrovascular dysfunction. Our results in the present work correlate very well with our previous *in vitro* study and strongly support previous observations. In the future, we plan to dissect out the mechanistic interrelationship

between RSG, PPARγ signaling pathway, and NRF2 activity. Needless to mention that our experimental setting can only partially recapitulate the harmful effects produced by TS in chronic smoker over a period of years of decades. Ideally longer exposure periods could be used to reduce the gap to some extent. In addition, mice metabolism relative to nicotine conversion to cotinine is significantly faster than humans. However, this difference was partially compensated by the exposure rate which allowed us to closely mimic the steady-state concentration of these compounds observed in heavy chronic smokers. One more limitation is the nature of this study that was aimed at validating our previous *in vitro* observations rather than dissecting out the specific mechanism of action.

3.5 Summary

In summary, at the cerebrovascular level, cigarette smoking can cause oxidative damage, trigger a strong inflammatory cascade, and severely impair endothelial physiology, thus leading to the onset and/or progression of several major cerebrovascular disorders. In this study, the protective effect of RSG against TS/EC-induced damages was investigated in a rodent model with the scope to validate *in vitro* results. The key role of NRF2 in maintaining BBB functional integrity and endothelial structure was indirectly confirmed, thus supporting previous evidence *in vitro* and *in vivo*. The pivotal role of NRF2 in maintaining the BBB endothelial functional integrity and healthy cerebrovascular conditions was successfully emphasized. Our data and previous studies suggest that both TS and EC significantly impair the endothelial function and cerebrovascular condition through the enhanced load of OS caused by impaired NRF2 signaling [75,133,134]. RSG notably counteracts these TS/EC- induced adverse effects

through modulation of NRF2, possibly via upregulation of PPARγ expression, whereas NRF2 upregulation was paralleled by the restoration of BBB integrity and reduced endothelial inflammatory responses. In summary, our data suggest that RSG could have promising therapeutic potential to prevent cigarette-induced cerebrovascular dysfunction and possibly other xenobiotic substances which may impact the BBB via OS-mediated effects.

CHAPTER FOUR

ANTIDIABETICS DRUGS REDUCE TOBACCO SMOKE-ENHANCED CEREBROVASCULAR DAMAGE AFTER TRAUMATIC BRAIN INJURY

4.1 Introduction

Recently published *in vitro* and *in vivo* findings from our group strongly suggested that BBB impairment and increased severity of TBI following chronic TS exposure likely develop in response to common modulators such as OS, neuroinflammation, and alterations of the endogenous ARE regulated by NRF2. In recent years, the regulation of post-traumatic responses leading to elevated antioxidative and alleviated inflammatory responses has been reported to promote neuroprotective effects in TBI models [144-149]. Despite recent advances in TBI research, clinical trials have been less promising, and huge challenges to developing effective treatments remain unresolved [150]. We have recently shown that chronic TS and hyperglycemia carry similar risks for cerebrovascular diseases through sharing the same pathogenic mechanisms that involve common modulators of BBB impairment [135]. Furthermore, we demonstrated that antidiabetic drugs like MF and RSG prevent/reduce BBB impairment caused by chronic TS exposure. Our data suggested that MF and RSG can effectively support counteractive antioxidative response mechanisms, drastically reducing TS-induced OS toxicity by activating the NRF2-ARE signaling pathway [22]. Although the exact mechanism of MF and RSG is not fully understood, numerous studies have revealed that MF and RSG can potentially ameliorate oxidative damage [102,109,136,151]. Thus, the major objective of this chapter is to explore the

effectiveness of MF and RSG to prevent/reduce the loss of BBB function and integrity and protect the brain from post-TBI exacerbation in response to chronic TS exposure and assess the key biological targets involved in the process.

4.2 Methods

4.2.1 Reagents and Materials

Reagents and chemicals were purchased from Sigma-Aldrich (St. Louis, MO, USA) or Bio-rad Laboratories (Hercules, CA, USA). Primary mouse brain microvascular endothelial cells (mBMEC) from C57BL/6 male mice (#C57- 6023) and complete mouse endothelial cell medium (M1168) were acquired from Cell Biologics (Chicago, Illinois, USA). Quantikine ELISA kits were obtained from R & D systems (Minneapolis, MN, USA), Thermo Fisher Scientific (Waltham, CA, USA), and MyBioSource (San Diego, CA, USA). Pierce BCA Protein Assay Kit (#23225) was purchased from Thermo Fisher Scientific. Gel electrophoresis was performed using Mini-Protean®TGXTM gels 4–15% (#456–1084) from Bio-Rad Laboratories. Rosiglitazone (RSG # A00183, MW: 357.4) was obtained from Adipogen, and Metformin (MF #PHR1084, MW:165.6) was obtained from Sigma-Aldrich. Anti-Claudin-5 (#352500). Rabbit anti-NRF2 (#PA5-88084) was purchased from Invitrogen, while the rest of the antibodies were purchased from other sources, as mentioned elsewhere [116].

4.2.2 Cell Culture

Mouse brain microvascular endothelial cells (mBMEC; P5) were seeded on 6-wells plates containing fresh supplemented medium including 10% FBS for a final total

volume of 2 ml/well and incubated at 37 °C. The culture medium was changed every two days until the cells reached full confluency.

4.2.3 Treatment of mBMEC Cells with Rosiglitazone and Metformin

mBMEC cells were incubated in the low serum media containing supplemented culture medium (as mentioned earlier) and 1% FBS with no growth factors for 24 h. RSG was first dissolved in DMSO at a concentration of 100 mM and then freshly diluted with supplemented culture medium to the final concentration of 20 μM. The final concentration of DMSO was <0.1%. MF was also dissolved in cold PBS at the concentration of 1 mM and then freshly diluted with supplemented culture medium to the final concentration of 10 μM. The mBMEC cells were treated daily with RSG (20 μM) or MF (10 μM) for a total of three days [67]. Parallel controls (without RSG and MF) were also provided (see Table 4.1).

4.2.4 Soluble Cigarette Smoke Extract Preparation

Soluble TS extract was prepared according to the International Organization for Standardization/ Federal Trade Commission (ISO/FTC) standard smoking protocol (35 mL puff volume, 2 s puff duration, 58 s intervals, 8 puffs per cigarette directly into PBS) from 3R4F research cigarettes obtained from the University of Kentucky [26]. It is equivalent to full flavor brands containing 9.4 mg tar and 0.726 mg nicotine/cigarette. The mBMEC cells were exposed daily to fresh 5% TS extract ((V/V) concentration in a low serum culture medium) for three consecutive days [67]. The resulting TS concentration does not impact cell viability.

Table 4.1 *In Vitro* Experimental Design.

	TBI Control	TBI+TS	TBI+MF	TBI+RSG	TBI+TS+ MF	TBI+TS+ RSG
TBI	✓	✓	✓	✓	✓	✓
TS-Exposure	-	✓	-	-	✓	✓
MF 10 μM	-	-	✓	-	✓	-
RSG 20 μM	-	-	-	✓	-	✓

4.2.5 Induction of Traumatic Endothelial Injury *In Vitro*

6-well plates containing confluent mBMEC cells were manually scratched as described in our previous published papers [6,152]. In brief, every well was scratched manually using a sterile plastic pipette tip matching a 9 × 9 square grid with an inter-lines space of 4 mm. The culture plates were then incubated for another 24h at 37 °C under normal conditions without changing the media.

4.2.6 *In Vivo* Experimental Design

In this study, all experimental procedures performed on the mice were approved by the Institutional Animal Care and Use Committees (IACUC), OU, Rochester, MI. Thirty-Six C57BL/6J male mice (ranging between 6–8 weeks old and body weight between 20–22 g) were purchased from Jackson Laboratory and group-housed in a temperature-controlled environment under a 12/12-h light/dark cycle with free access to food and water. Mice were divided into six major groups (6 mice/group), including TBI Control, TBI+TS, TBI+TS+MF100, TBI+TS+MF200, TBI+TS+RSG10, and TBI+TS+RSG20 (see also Table 4.2). Mice were given one-week post-arrival for acclimatization in the new housing for recovery upon transport. All the groups, except

TBI Control, were chronically and simultaneously exposed to sidestream smoke derived from 3R4F research cigarettes via direct inhalation. Side stream smoke was generated using SCSM following previously published methods [79] (see also Fig. 4.1). Mice were exposed to TS mixed with oxygenated air six times/day; 2 cigarettes/hour, 6–8 h/day, seven days/week for a total of three weeks, according to the ISO/FTC standard smoking protocol.

4.2.7 Induction of Head Injury in Mice

TBI was induced by a standard weight-drop procedure [10,153]. This model mimics human head injury by a standardized weight-drop device inducing a focal blunt trauma over an intact skull without pre-injury manipulations. The impact stimulates a robust neuroinflammatory response, BBB breakdown, and neurological impairment. In brief, anesthetized mice were placed on a spongy surface under the weight-drop device.

Table 4.2 *In Vivo* Experimental Design.

	TBI Control	TBI+TS	TBI+TS+ MF100	TBI+TS+ MF200	TBI+TS+ RSG10	TBI+TS+ RSG20
TBI	✓	✓	✓	✓	✓	✓
TS-Exposure	-	✓	✓	✓	✓	✓
MF 100 mg/kg	-	-	✓	-	-	-
MF 200 mg/kg	-	-	-	✓	-	-
RSG 10 mg/kg	-	-	-	-	✓	-
RSG 20 mg/kg	-	-	-	-	-	✓

Head movements were allowed parallel to the injury plane at the induction time to mimic a mild- to moderate head injury. During the induction phase, mice were positioned to direct the trauma from the left anterior frontal area at the same distance between the eye and the ear. Then a metal weight of 30 g was allowed to free fall from 80 cm above the head through a vertical hollow tube (with an internal diameter of 13 mm) as the guiding system (see also Fig. 4.1). The sham-injured mice underwent the same procedures, excluding being subjected to head injury by weight drop.

4.2.8 Rosiglitazone and Metformin Treatment in Vivo

Mice were treated with RSG or MF following TBI (no pre-TBI treatment). Drugs were dissolved in DMSO/ sterile saline (1:10) and sterile saline, respectively, and administered daily via intraperitoneal (IP) injections for final dose levels of 10 or 20 mg/kg for RSG and 100 or 200 mg/kg for MF with final dose volume of 20 ml/kg for consecutive 7 days after TBI [137].

4.2.9 Fasting Blood Glucose Level Analysis

A tail pinprick was conducted on the anesthetized mice to determine the mice's fasting blood glucose levels. The glucose level was measured using a contour next blood glucose meter obtained from Bayer Healthcare (Indiana, USA).

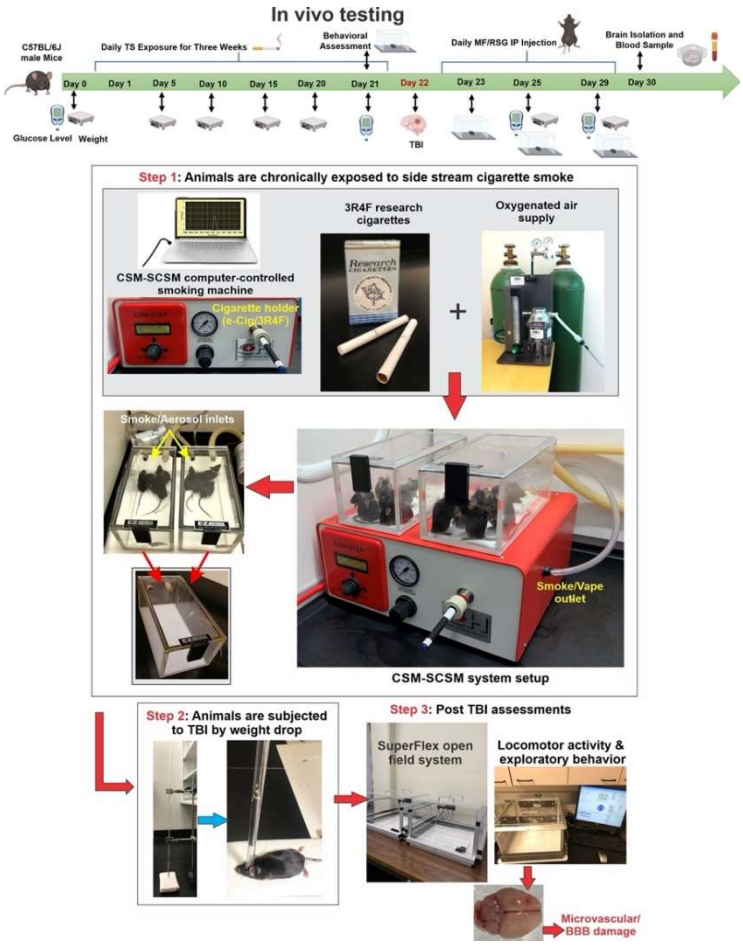

Figure 4.1 (A) Timeline of the *in vivo* study. The mice were divided into six groups (6 mice/group), including TBI Control, TBI+TS, TBI+TS+MF100, TBI+TS+MF200, TBI+TS+RSG10, and TBI+TS+RSG20.Mice were exposed to TS for a total of three weeks. On day 22, all groups were subjected to TBI. Following TBI, MF/RSG was administered to the corresponding groups for 7 days. As indicated, behavioral analyses, fasting blood glucose levels, and body weight measurements were performed. On day 30, mice were sacrificed, and the brain tissues and blood samples were extracted for subsequent biochemical and molecular assessments. (B) Experimental flow and setup, including cigarette smoke generation, TS mice exposure, induction of TBI, and post-traumatic assessment of motor activity. C57BL/6J male mice were chronically exposed to TS (full body side stream exposure) for three weeks using a computer-controlled single cigarette smoking machine using the FTC-approved cigarette smoking protocol. Test animals were subjected to TBI by a drop of the head weight (30 g) from an 80 cm height through a pre-positioned vertical guide. The physical activity of the mice was analyzed before TBI and at 24 h, three days, and seven days after TBI using an open-field test. Finally, mice were sacrificed to collect blood and brain samples for subsequent biochemical and molecular assessments.

4.2.10 Open Field Test

As a standard measure of exploratory behavior and general activity in rodents, open field tests were performed using a SuperFlex system (Omnitech Electronics, Columbus, OH) [154]. Briefly, mice were housed in 16″ × 16″ acrylic chamber containing infrared photosensors. Then the mice were monitored and recorded for 1 h. The first 30 min of 1 h were excluded as the acclimatization period (Fig. 4.1). Automatic analyses of the total activity of the mice were performed through Fusion Software. All behavioral analyses were performed between 9 am and 1 pm.

4.2.11 Blood Collection and Brain Isolation

Mice were euthanized under terminal anesthesia 7 days after TBI to collect blood and brain samples for subsequent biochemical and molecular analyses. Blood samples were collected by cardiac puncture as described elsewhere [116]. Briefly, mice were positioned on their back and anesthetized with inhaled isoflurane (4% induction; 2% maintenance) to minimize discomfort, distress, and pain. Then a V-cut was made through the skin and abdominal wall, and internal organs were moved to the side. The needle was inserted through the diaphragm and into the heart. Blood was collected by applying negative pressure on the syringe plunger. To isolate the brain, we cut at the nape and then extended along the midline from the dorsal cervical area to the tip of the nose. The skin was then pulled away from the skull laterally. The skull was cut and opened by placing the point of the scissors in the foramen magnum and cutting along the midline. After levering away parietal bones from the brain and disrupting the nerve attachments at the

brain stem and the optic chiasm, the brain was removed from the skull, rinsed into sterile, cold PBS, and then frozen in liquid nitrogen and stored at -80 °C [22,116].

4.2.12 Preparation of Protein Extracts and Western Blotting

We harvested the total proteins of mBMEC cells and brain tissues by RIPA lysis buffer based on the manufacturer's instructions. Total proteins were centrifuged at 14000*g for 30 mins. Proteins quantification was assessed using a Pierce BCA protein assay kit. Samples (30 μg for cell lysates and 90 μg for tissue lysates) were then separated by SDS- polyacrylamide gel electrophoresis and transferred to nitrocellulose membranes. Then the membrane was blocked with 5% milk for 2h before incubating overnight at 4 °C with the primary antibodies of interest [67,75]. The membranes were washed thrice with cold TBS containing 0.05% Tween-20 (TBS-T) for 15 min each. It was then re-incubated for 2h at 25 °C with the corresponding secondary antibodies for immunodetection. Immunoblots were detected using West Pico Plus Chemiluminescence Substrate (Thermo Fisher Scientific, #34580) and calculated using Image Studio software. All samples were analyzed in triplicate with normalization to the β- actin.

4.2.13 Thrombomodulin, Inflammatory Cytokines, Superoxide Dismutase, Myeloperoxidase, Matrix Metalloproteinase-9, and Soluble Intercellular Adhesion Molecule 1 Levels Measurement using Enzyme-Linked Immunosorbent assay

mBMEC cell culture supernatant and plasma samples collected from mice were analyzed using Quantikine ELISA kits to evaluate the levels of thrombomodulin, inflammatory cytokines (including IL-6, TNF-α, and IL-10), SOD, MPO, MMP-9, and Soluble ICAM-1 according to the manufacturer’s guidelines.

4.2.14 RNA Extraction and Quantitative Real-Time Polymerase Chain Reaction

Quantitative RT-PCR was performed according to the protocol used in our previous work [113,114]. In brief, the total genomic RNA was extracted from the mBMEC cells and brain tissues using RNeasy plus mini kit described in the manufacturer's guideline (Qiagen Inc, Santa Clarita, CA). Complementary DNA (cDNA) was synthesized using a Hight-Capacity RNA-to-cDNA kit (#4387406) obtained from Thermo Fisher Scientific. Gene expression was determined by quantitative RT-PCR using SYBR Green Master Mix (#A25741)-based fluorescence procedure. The primer pairs (see sequences in Table 4.3) were designed based on PubMed GenBank and synthesized by Integrative DNA Technologies (Coralville, IA, USA). The RNA targets were amplificated using a Bio-Rad CFX96 Touch Real-Time PCR detection system. Relative quantification of mRNA expression was measured using the $2^{-\Delta\Delta CT}$ method. All samples were analyzed in triplicate with normalization to the β- actin.

Table 4.3 Forward and Reverse Primer Sequences (5' -3') for Quantitative RT-PCR.

Target Gene	Forward	Reverse
NRF2	5'- GGC TCA GCA CCT TGT ATC TT -3'	5'- CAC ATT GCC ATC TCT GGT TTG -3'
NQO-1	5'- GAG AAG AGC CCT GAT TGT ACT G -3'	5'- ACC TCC CAT CCT CTC TTC TT -3'
HO-1	5'- CTC CCT GTG TTT CCT TTC TCT C -3'	5'- GCT GCT GGT TTC AAA GTT CAG -3'
NF-kB	5'- AGA CAT CCT TCC GCA AAC TC -3'	5'- TAG GTC CTT CCT GCC CAT AA -3'
Claudin-5	5'- GGT GAA GTA GGC ACC AAA CT -3'	5'- TTT CTC CAG CTG CCC TTT C -3'
Occludin	5'- CAG CAG CAA TGG TAA CCT AGA G -3'	5'- CAC CTG TCG TGT AGT CTG TTT C -3'
VCAM-1	5'- GAG GGA GAC ACC GTC ATT ATC -3'	5'- CGA GCC ATC CAC AGA CTT TA -3'
PECAM-1	5'- CAA CAG AGC CAG CAG TAT GA -3'	5'- TGA CAA CCA CCG CAA TGA -3'
ZO-1	5'- CAT TAC GAC CCT GAA GAG GAT G -3'	5'- AGC AGG AAG ATG TGC AGA AG -3'
B-Actin	5'- GAG GTA TCC TGA CCC TGA AGT A -3'	5'- CAC ACG CAG CTC ATT GTA GA -3'

4.2.15 Cell Viability Assay

The mBMEC cells' viability was measured by the Tetrazolium 3-(4, 5-dimethyl thiazolyl-2)−2, 5- diphenyltetrazolium bromide (MTT) assay [75]. Briefly, 5 mg/ml of MTT was added to each well and incubated at 37 °C for 3h. Metabolically active cells converted the yellow MTT to purple formazan crystals. 1ml of DMSO was added to dissolve the purple formazan compound, and the absorbance at a wavelength of 570 nm was measured on a microplate reader (TECAN - Spark Cyto).

4.2.16 Measurement of Intracellular Reactive Oxygen Species Generation

Intracellular ROS was measured according to the manufacturer's guideline using 2,7-dichlorodihydrofluorescein diacetate (2,7-DCFH-DA). In brief, cultured mBMEC cells on 6-well plates were rinsed with cold PBS and incubated in 25 uM DCFHDA at 37°C for 45 min in the dark. Cells were then rinsed thrice with cold PBS and transferred to a 96-well black plate by scarping the wells' surface. The intensity of dichlorofluorescein (DCF) fluorescence was measured via a microplate reader (TECAN-Spark Cyto) at a wavelength of 485 nm for excitation and 535 nm for emission.

4.2.17 Glutathione Levels Measurement

The mBMEC cell culture supernatant and plasma samples collected from mice were analyzed using the Quantification Kit for Oxidized and Reduced Glutathione (Sigma Aldrich, St. Louis, MO, USA). According to the manufacturer's guidelines, we assessed the levels of oxidized glutathione (GSSG) and reduced glutathione (GSH). Fluorescence intensity was measured via a microplate reader (TECAN-Spark Cyto) at the wavelength of 490 nm for excitation and 520 nm for emission.

4.2.18 Statistical Analysis

All the results were reported as mean ± standard deviation (SD). All statistical analyses were processed using GraphPad Prism 9 Software Inc. (La Jolla, CA, USA) through one-way ANOVA followed by Tukey's or Dunnett's test to evaluate the significance of the data. P values ≤ 0.05 were considered statistically significant.

4.3 Effects of Metformin and Rosiglitazone on Cell Viability *In Vitro*

An MTT cytotoxicity assay was used to assess the effect of MF and RSG on cell viability (Fig. 4.2A). As shown in Fig. 4.2B, MF and RSG reduced the impact of premorbid TS exposure on TBI-induced cells and the effect of TBI itself on the cell cultures' viability compared to drug-untreated cells.

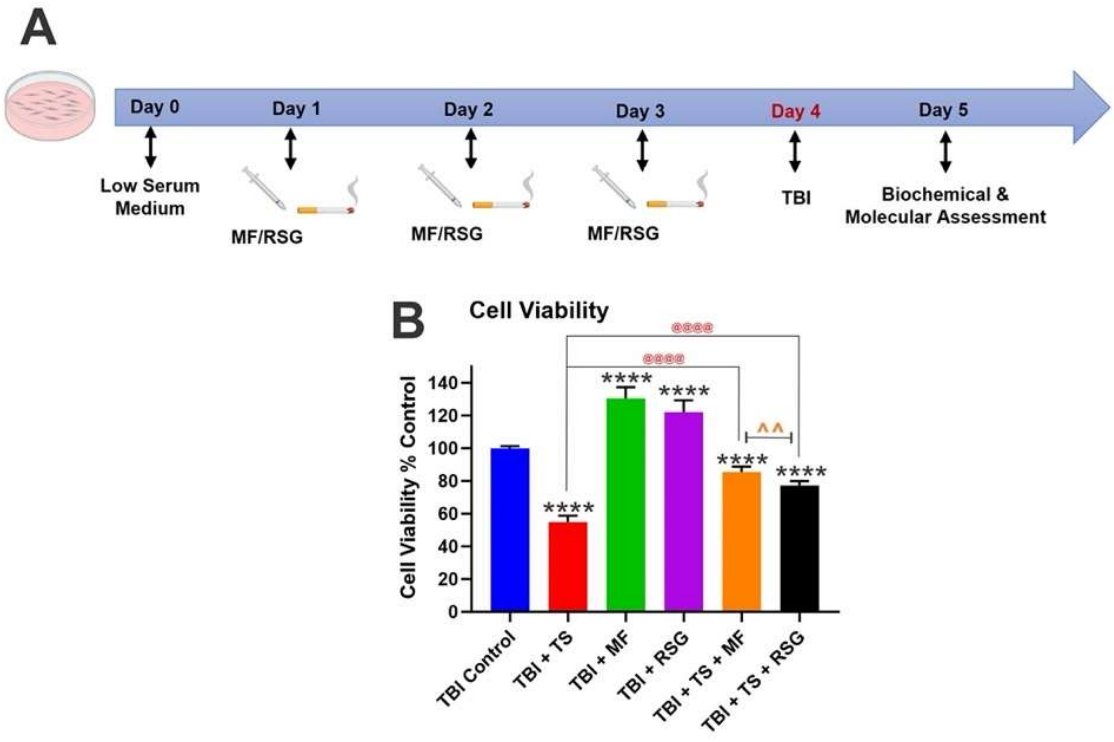

Figure 4.2 Timeline of the *in vitro* study.A) confluent cells culture wells were divided into six groups (6 wells/group), including TBI Control, TBI+TS, TBI+MF, TBI+RSG, TBI+TS+MF and TBI+TS+RSG. Cells were incubated in the low serum media for 24 h. for three consecutive days, treated with MF/RSG, and exposed to TS. All groups underwent TBI on day 4. After 24h, the cells and the corresponding culture supernatant were collected for subsequent biochemical and molecular assessments. (B) MTT cytotoxicity assay for cell viability evaluation. MF and RSG compensated for the decreased viability of TS-exposed and TBI-induced cells. n = 6 biological replicates, ****p < 0.0001 versus control. ^^p < 0.01, MF versus RSG treated group. @@@@p < 0.0001 non-treated versus MF/RSG treated group.

4.4 Metformin and Rosiglitazone Effect on Body Weights and Fasting Blood Glucose Levels of Premorbid Tobacco Smoke-Exposed and Traumatic Brain Injury-induced Mice

C57BL/6J male mice (ranging between 6–8 weeks old and body weight between 20–22 g) undergoing TBI w/wo chronic TS exposure were used to validate the *in vitro* data, as detailed in the method section. Body weights and fasting blood glucose levels were regularly measured to assess whether MF and RSG dosing negatively impacted mice's body weights and glucose levels (Fig. 4.1). As shown in Fig. 4.3, measurements of animals' body weights showed no significant difference within the tested groups at Day 0. However, at the end of the three weeks of TS exposure before TBI, the body weight of animals chronically exposed to cigarette smoke was slightly lower (yet statistically significant) compared to controls, which might be due to the appetite suppressant effect as well as a moderate increase of metabolism promoted by TS [75]. MF and RSG treatment following TBI appeared to renormalize the body weight of all treated animals (Fig. 4.3). Fasting blood glucose levels across the groups were within limits with no remarkable inter-group differences at Day 0 (Fig. 4.4). Still, they became significantly more elevated in TS-exposed animals by the end of the three weeks of premorbid smoke conditioning. This data is consistent with the higher blood glucose levels reported in smokers. Moreover, 3 days and 7 days after TBI, administration of MF and RSG renormalized the blood glucose in all treated animal groups to levels comparable to TBI controls. The longitudinal analysis of body weights and fasting blood glucose levels are also shown in the corresponding Fig. 4.3 and Fig. 4.4, respectively.

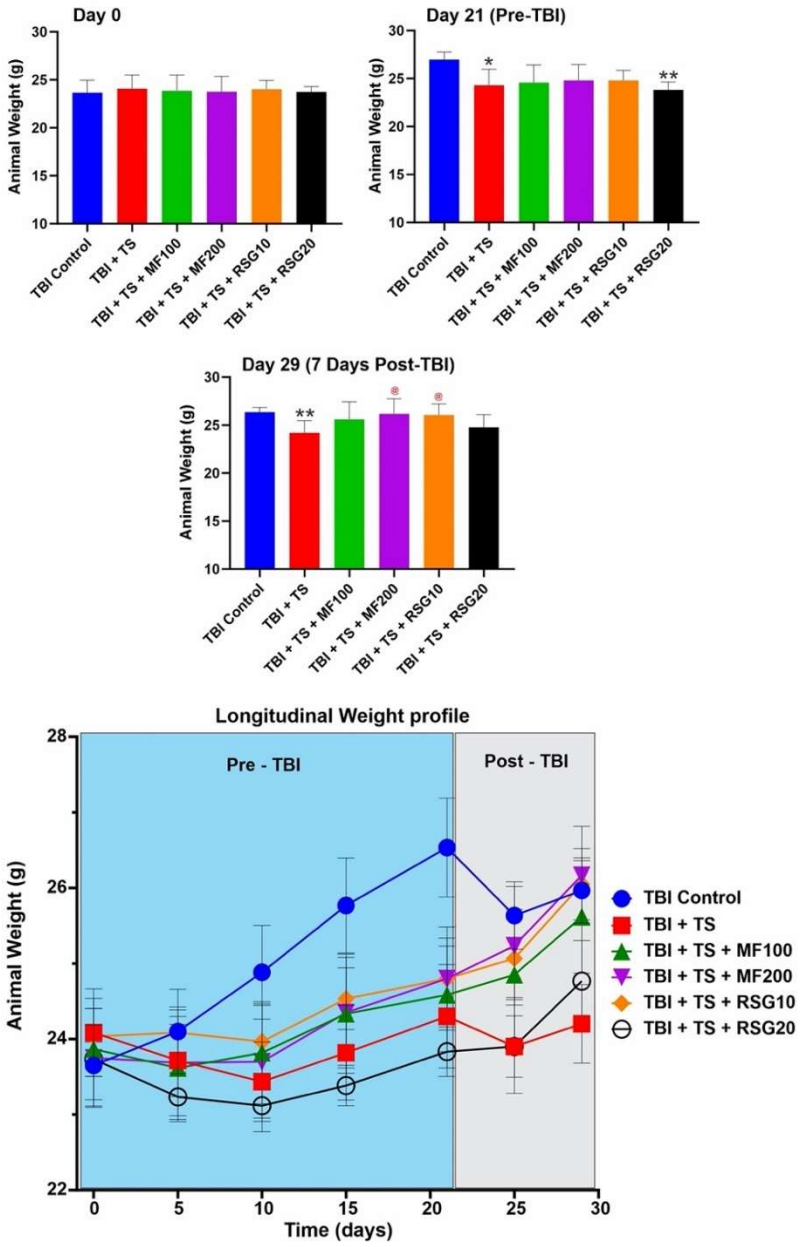

Figure 4.3 Effect of MF and RSG treatments on body weights of TS-exposed and TBI-induced mice.Measurements of animals' body weights did not significantly differ between the tested groups at Day 0. However, at the end of the three weeks of exposure before TBI, animals exposed to TS showed decreased body weights compared to the control. Post-TBI body weights recovered following MF and RSG treatments for TBI. n = 6 biological replicates, *$p < 0.05$, **$p < 0.01$ versus control. @$p < 0.05$, non-treated versus MF/RSG treated group.

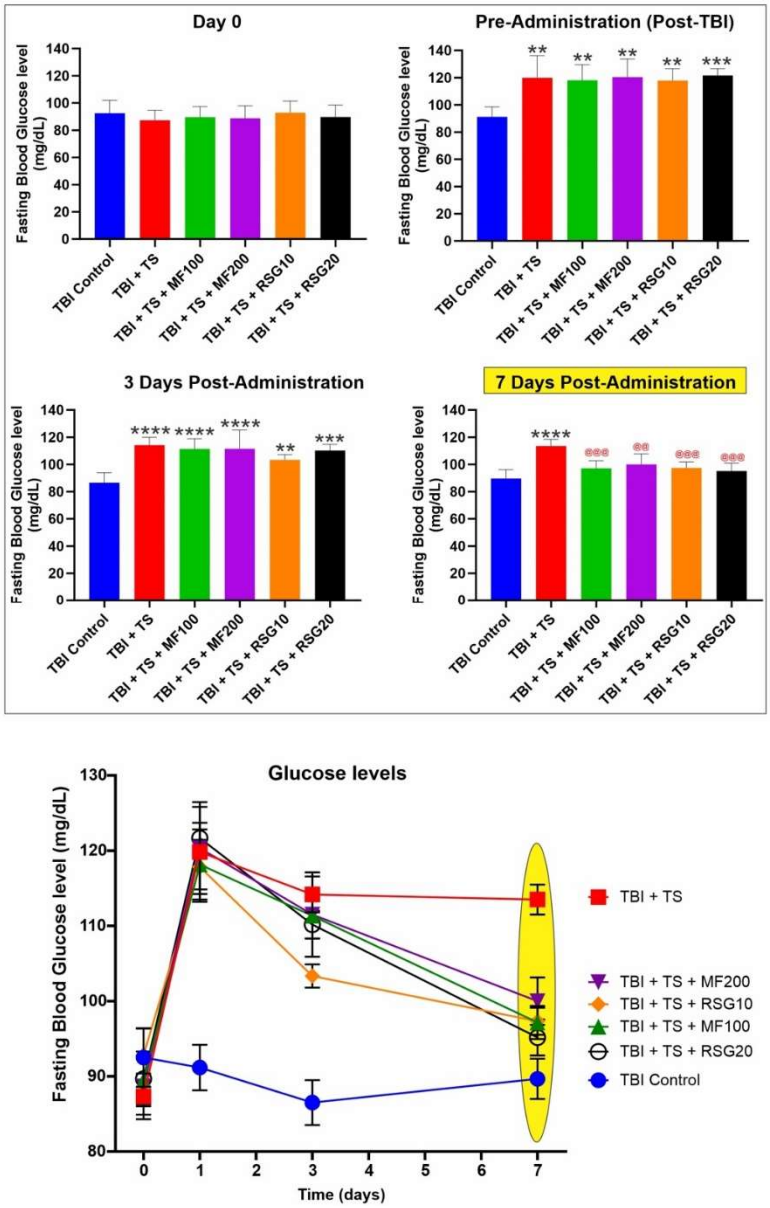

Figure 4.4 Effect of TS-Exposure, MF, and RSG treatments on fasting blood glucose levels of TBI-induced mice.Measurements of animals' fasting blood glucose levels did not significantly differ between the tested groups at Day 0. However, at the end of the three weeks of exposure before TBI, animals exposed to TS showed an increased fasting blood glucose level compared to control. MF and RSG controlled the increasing glucose levels of the mice. n = 6 biological replicates, *p < 0.05, **p < 0.01, ***p < 0.001, ****p < 0.0001 versus control. @@p < 0.01, @@@p < 0.001, non-treated versus MF/RSG treated group.

4.5 Metformin and Rosiglitazone Promote an Antioxidative and Anti-Inflammatory Response by Upregulating NRF2 and its Downstream Effector Molecules

MF and RSG have been reported to exert their antioxidative response via the activation of the nuclear factor erythroid 2-related factor 2 (NRF2), which in turn upregulates the expression of its downstream detoxifying effector molecules Heme oxygenase 1 (HO-1) and NAD(P)H dehydrogenase [quinone] 1 (NQO-1) [22,26,75] and downregulates Nuclear factor kappa B (NF-κB). To check if MF and RSG were acting through the same pathway in the context of TS and TBI, we evaluated the protein expression and respective mRNA levels of NF-kB, NRF2, HO-1, and NQO-1 through WB and quantitative RT-PCR analyses. Consistent with our previous results, chronic TS-exposure significantly upregulated the expression level of NF-kB (an essential modulator and inducer of inflammatory activities, see Fig. 4.5A) and downregulated NRF2 expression (Fig. 4.5B) and its downstream effectors, including HO-1 (Fig. 4.5C) and NQO-1 (Fig. 4.5D).

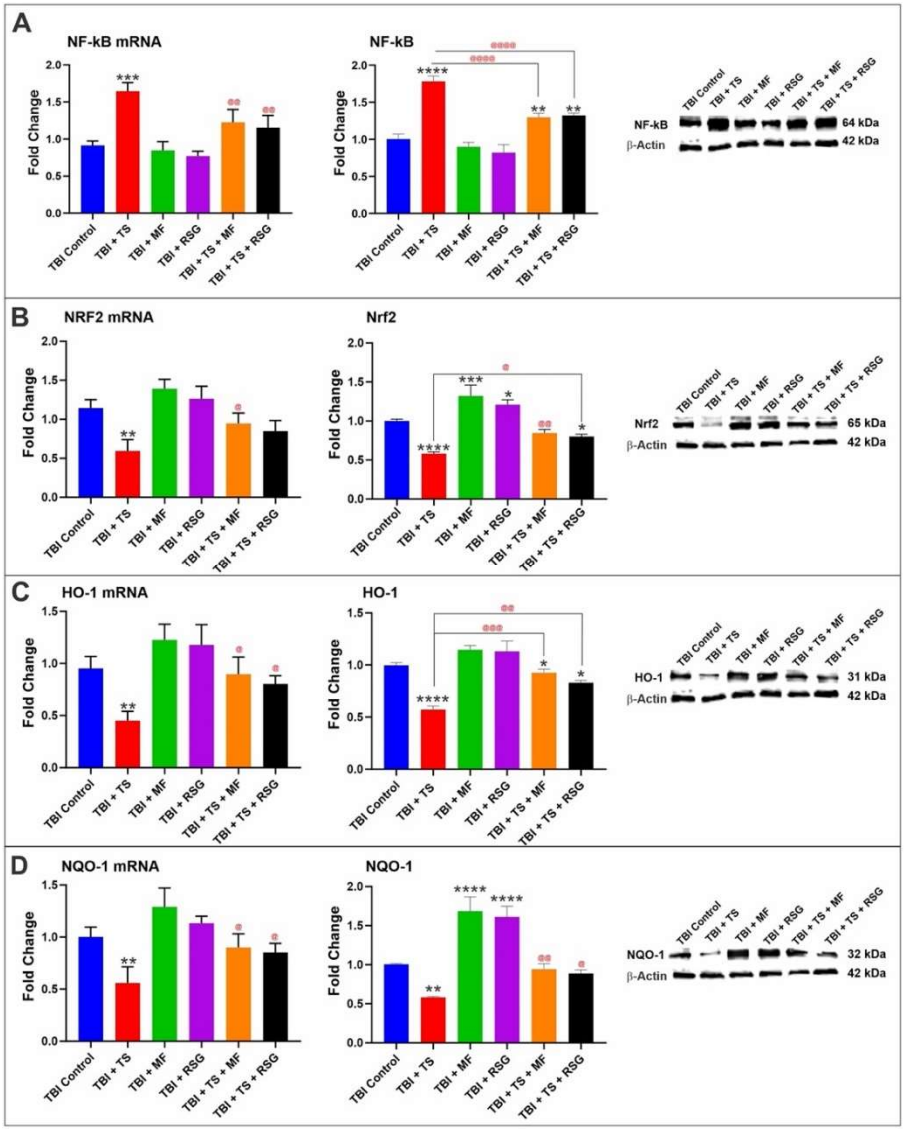

Figure 4.5 MF and RSG downregulate NF-kB and upregulate NRF2 and its downstream detoxifying effector molecules HO-1 and NQO-1 in BBB endothelial cells following premorbid TS-exposure and TBI stimulation.WB and quantitative RT-PCR analyses showed that (A) The enhanced expression levels of NF-kB were independently downregulated by MF and RSG. (B) Data emphasized the protective effects of MF and RSG against chronic TS exposure and TBI in NRF2 expression levels. Alternations of NRF2 expression levels were paralleled by corresponding changes of (C) HO-1 and (D) NQO-1. n = 6 biological replicates, *p < 0.05, **p < 0.01, ***p < 0.001, ****p < 0.0001 versus control. @p < 0.05, @@p < 0.01, @@@p < 0.001, @@@@p < 0.0001 non-treated versus MF/RSG treated group. WB analyses express protein/β-actin ratios.

Parallel *in vivo* experiments were used to confirm the *in vitro* findings. As shown in Fig. 4.6A, TS exposure elicited a similar enhanced pro-inflammatory response leading to a significant increase in the expression of NF-κB and (see Fig. 4.6B) a corresponding decrease of NRF2 (which regulates the cellular defense against toxic and oxidative insults) and the corresponding OS response effectors including NQO-1 (see Fig. 4.6C) and HO-1 (see Fig. 4.6D). Both *in vitro* and *in vivo* data clearly show that MF and RSG effectively reduced the pro-inflammatory impact of TS and promoted a remarkable increase in the protein expression and mRNA levels of the NRF2, HO-1, and NQO-1, compared to the non-treated premorbid TS-exposed and TBI-induced BBB endothelial cells and mice models. Furthermore, our *in vivo* data also show a dose-response effect for both drugs.

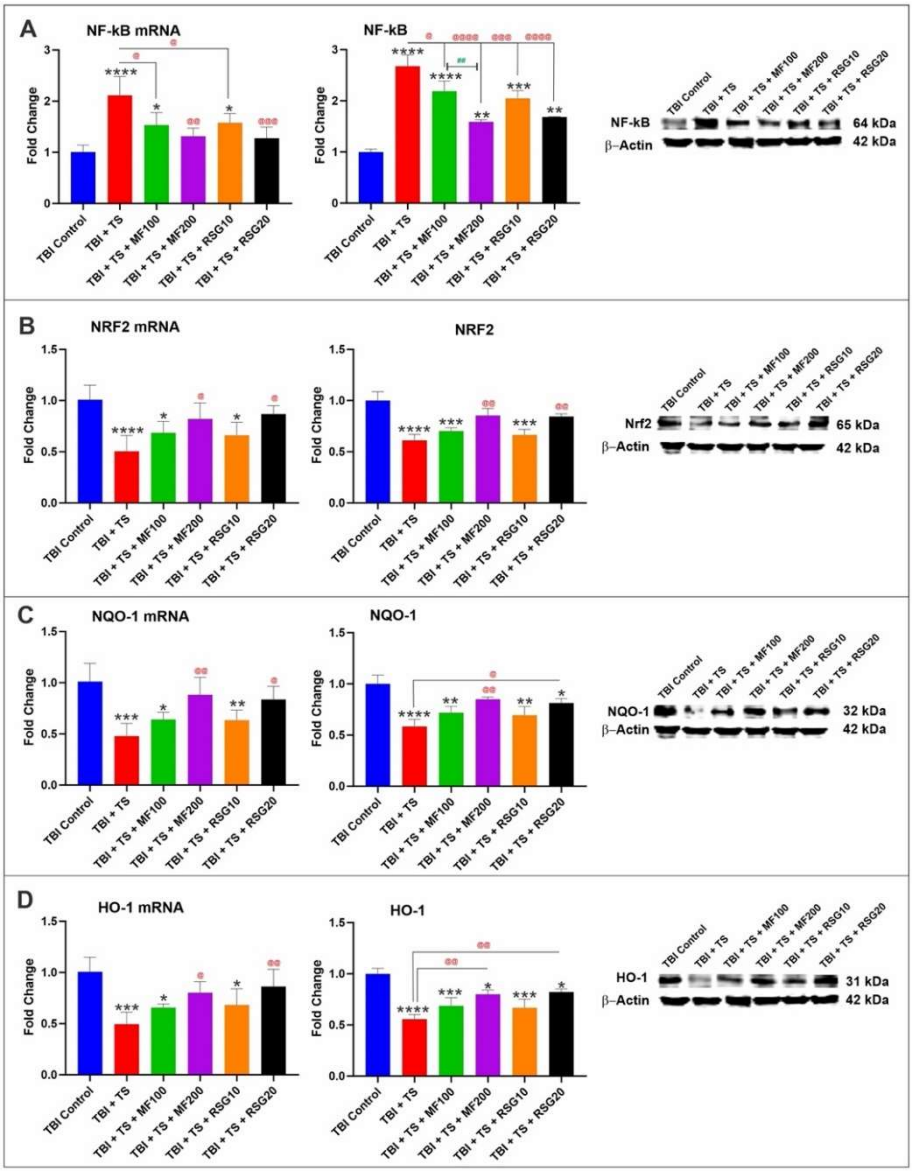

Figure 4.6 Dose-dependent protective effects of MF and RSG on the antioxidative response system *in vivo*.WB and quantitative RT-PCR analyses emphasized the antioxidative effects of MF and RSG on (A) downregulation of NF-kB and (B) activation of NRF2 expression levels in a dose-dependent manner. Changes in NRF2 expression levels were paralleled by corresponding changes in the expression levels of its downstream detoxifying effector molecules (C) NQO-1 and (D) HO-1. n = 6 biological replicates, *p < 0.05, **p < 0.01, ***p < 0.001, ****p < 0.0001 versus control. @p < 0.05, @@p < 0.01, @@@p < 0.001, @@@@p < 0.0001 non-treated versus MF/RSG treated group. ##p < 0.01MF100 versus MF200. WB analyses express protein/β-actin ratios.

4.6 Metformin and Rosiglitazone Affect Oxidative Stress Generated after Premorbid Tobacco Smoke-Exposure and Traumatic Brain Injury

To further investigate the antioxidant activity of MF and RSG in the TS-exposed and TBI-induced samples, we evaluated the intracellular ROS and OS biomarkers (glutathione, SOD, and MPO) levels *in vitro* and *in vivo*. While the total glutathione (oxidated + reduced) in BBB endothelial cells remained unaffected by the tested treatments compared to controls (see Fig. 4.7A), the increase in intracellular ROS elicited by TS exposure (see Fig. 4.7G) was paired with a substantial decrease in reduced glutathione (GSH, Fig. 4.7B) and increased oxidated glutathione (GSSG, Fig. 4.7C). This effect is noticeably in Fig. 4.7D, demonstrating the ratio of GSH/GSSG. Intracellular ROS generation was reduced by MF and RSG treatments (Fig 4.7G). The antioxidative effect was paralleled by a significant increase of GSH (Fig. 4.7B) and a reduction of GSSG (Fig. 4.7C) compared to untreated TS-exposed cultures. As shown in Fig. 4.7E, SOD levels measured in the cell culture supernatant of TS-exposed and TBI-stimulated BBB endothelial cells were significantly lower than controls. The effect was mitigated by MF and RSG (average SOD level in TBI control: 8.47 U/ml). MPO levels also increased in response to TS exposure and TBI stimulation. The effect was significantly dampened by MF and RSG (Fig. 4.7F) (average MPO level in TBI control: 4.82 ng/ml). As shown in Fig. 4.7G, intracellular ROS was substantially higher in premorbid TS-exposed samples. To further validate this *in vitro* data, changes in glutathione (including total, SOD, and MPO levels related to TS exposure and TBI were assessed in the corresponding plasma samples from parallel *in vivo* experiments in C57 mice.

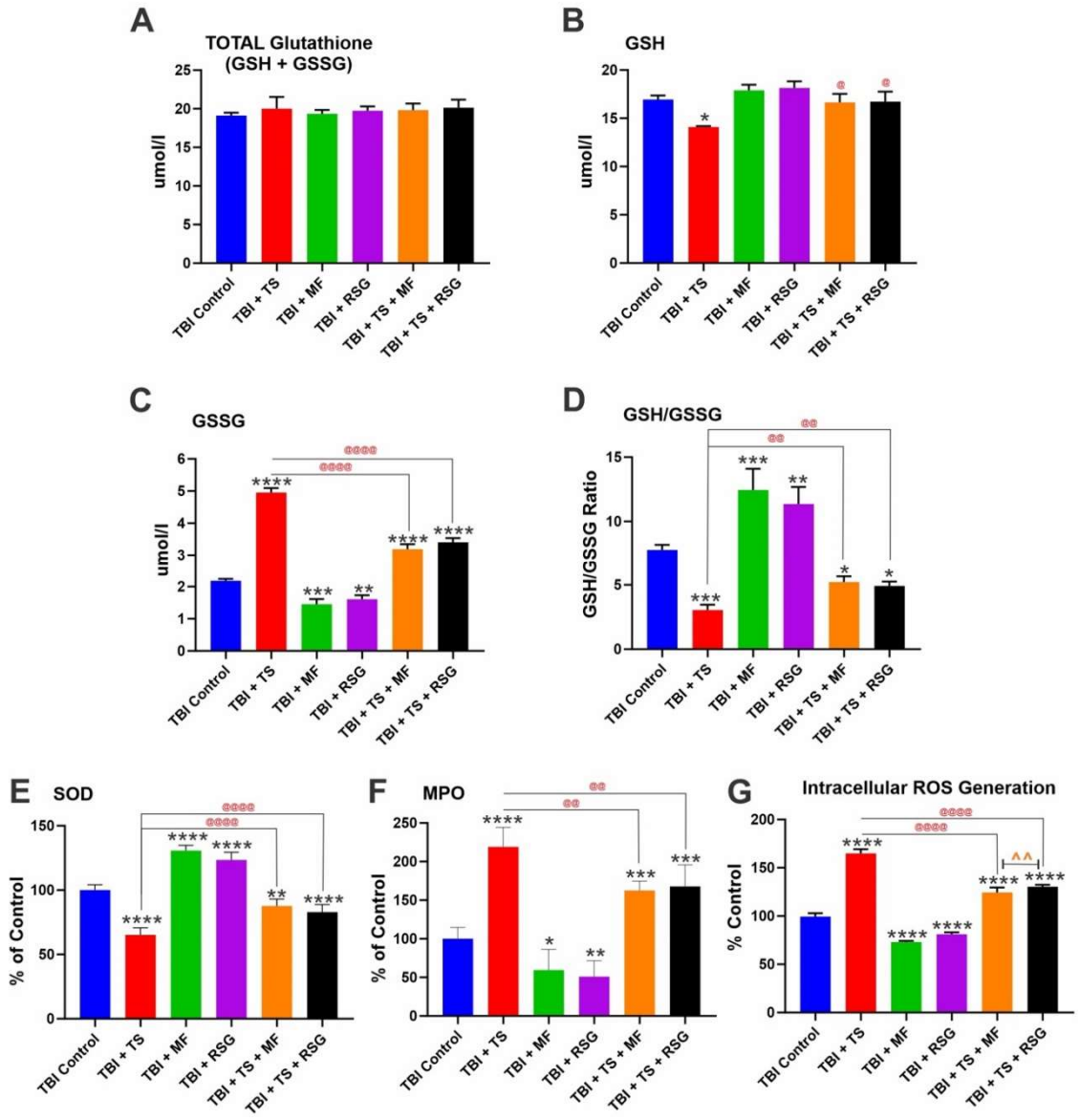

Figure 4.7 Oxidized and reduced glutathione levels represent the protective effect of MF and RSG against generated OS through premorbid TS exposure and TBI in BBB endothelial cells.(A) Total glutathione (GSH+GSSG), (B) Reduced glutathione (GSH), (C) Oxidized glutathione (GSSG), and (D) GSH/GSSG were measured by a microplate reader. MF and RSG also affect intracellular ROS and OS generated through premorbid TS exposure and TBI stimulation. (E) SOD, (F) MPO, (G) Intracellular ROS generation, measured by a microplate reader. n = 6 biological replicates, *p < 0.05, **p < 0.01, ***p < 0.001, ****p < 0.0001 versus control. ^^p < 0.01, MF versus RSG treated group. @p < 0.05, @@p < 0.01, @@@@p < 0.0001 non-treated versus MF/RSG treated group.

As shown in Fig. 4.8, panels A to F, the total glutathione levels (GSH + GSSG; Fig 4.8A) are unaffected by the experimental conditions; however, a specific analysis of the reduced (GSH) and oxidized (GSSG) content of glutathione (Fig 4.8B & C) shows that TS negatively impact the GSH levels which reflects the corresponding increase in GSSG as also evident from the GSH/GSSG ratios (Fig. 4.8D). Noteworthy is the fact that both MS and RSG significantly reduce the impact of TS as denoted by the levels of superoxide dismutase (SOD) and myeloperoxidase (MPO) (average SOD and MPO levels in TBI control: 6.17 U/ml and 16.8 ng/ml, respectively) also assessed in the plasma samples of the same animals (see Figs. 4.8E & 4.8F). *In vivo* data also emphasize the dose-dependent protective effect of MF and RSG.

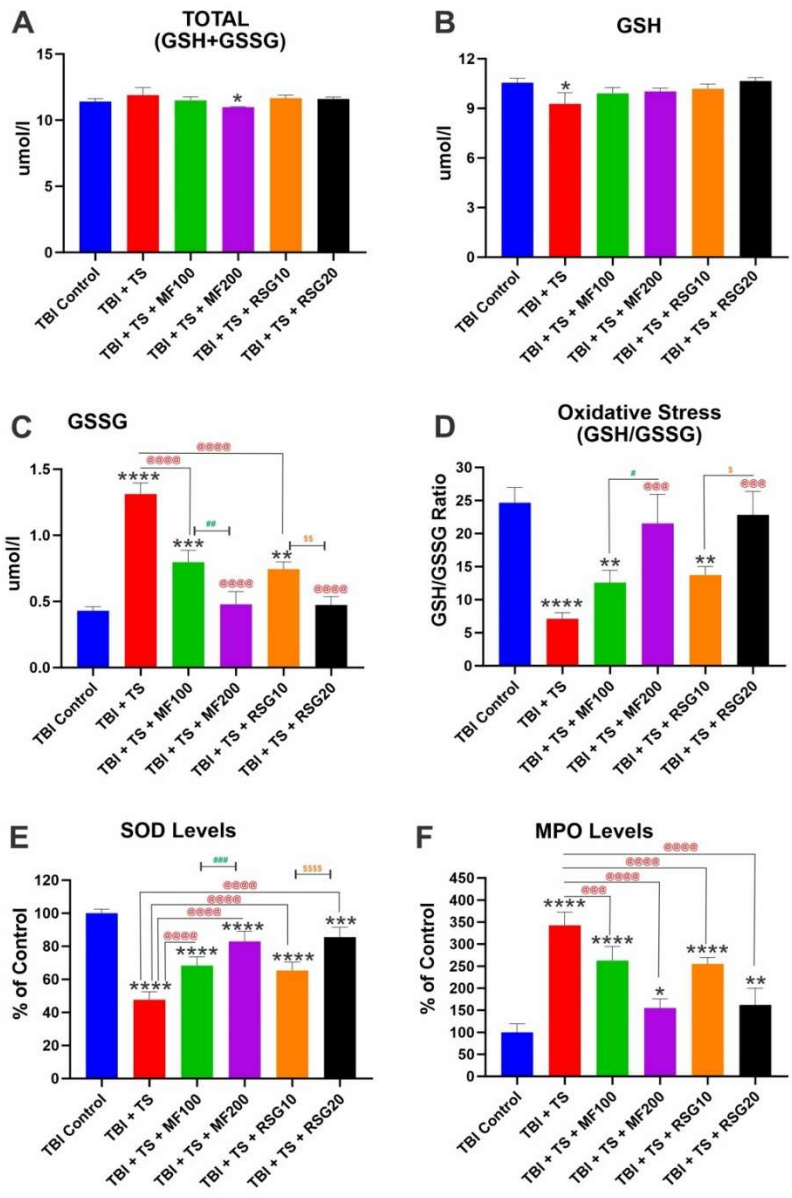

Figure 4.8 MF and RSG affect OS generated after premorbid TS exposure and TBI induction of mice.(A) total glutathione (GSH+ GSSG) (B) reduced glutathione (GSH), (C) oxidized glutathione (GSSG), (D) GSH/GSSG, (E) SOD levels, and (F) MPO levels. n = 6 biological replicates, *p < 0.05, **p < 0.01, ***p < 0.001, ****p < 0.0001 versus control. @@@p < 0.001, @@@@p < 0.0001 non-treated versus MF/RSG treated group. #p < 0.05, ##p < 0.01, ###p < 0.001 MF100 versus MF200. $p < 0.05, $$p < 0.01, $$$$p < 0.0001 RSG10 versus RSG20.

4.7 Metformin and Rosiglitazone Decrease the Inflammatory Responses Induced by Premorbid Tobacco Smoke-Exposure and Traumatic Brain Injury

Inflammatory cytokine expression plays a key role in the inflammatory cascade reactions and neuronal damage after TBI. To determine the influence of MF and RSG on neuroinflammation following TS exposure and TBI, inflammatory cytokines, including TNF-α, IL-6, and IL-10, were evaluated *in vitro* and *in vivo* by ELISA. Elevated expression of inflammatory cytokines, including TNF-α (Fig. 4.9A), IL-6 (Fig. 4.9B), and IL-10 (Fig. 4.9C) in cells culture supernatant of TS-exposed and TBI-induced BBB endothelial cells. MF and RSG reduced the pro-inflammatory impact of TBI and TS + TBI.

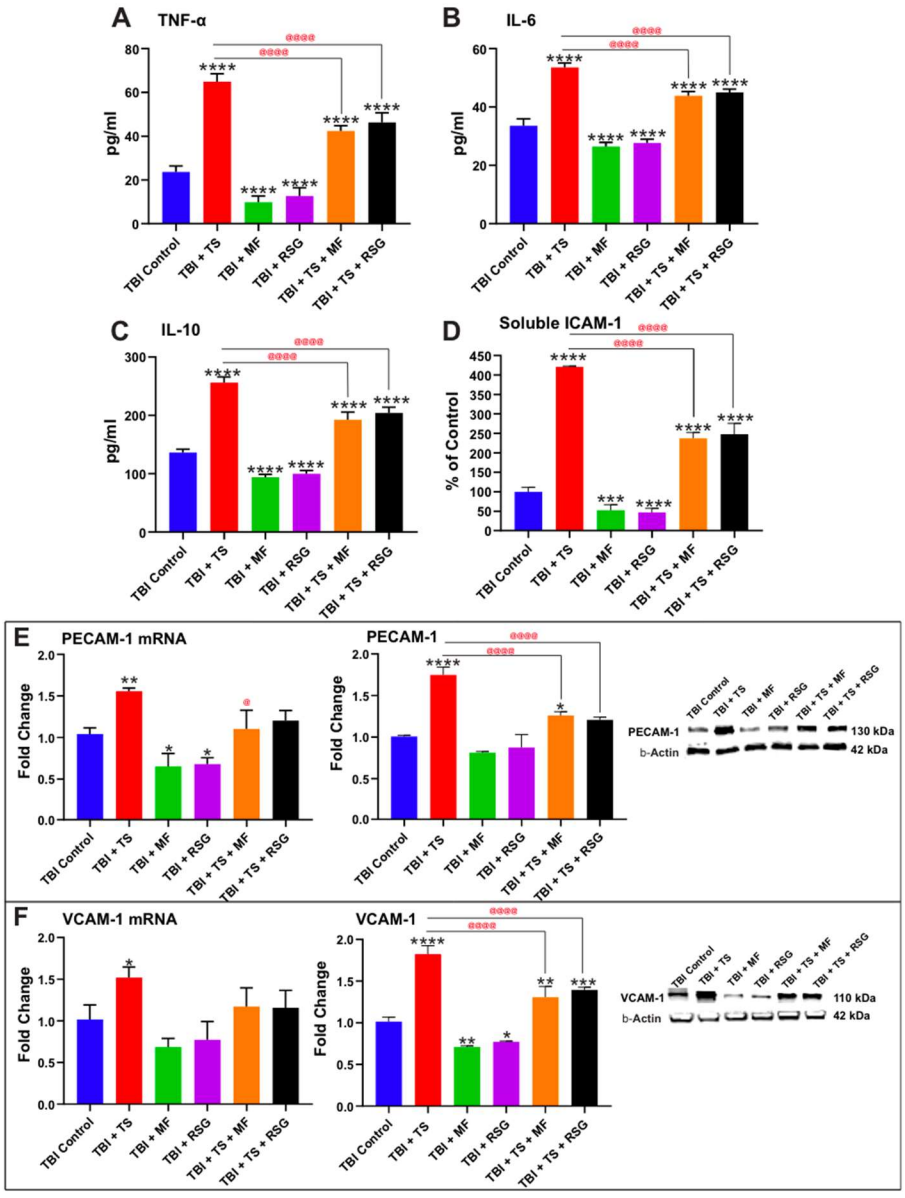

Figure 4.9 MF and RSG protectively affect inflammatory response at the BBB endothelium following premorbid TS exposure and TBI stimulation.Upregulation of the expression levels of inflammatory cytokines A) TNF-α, (B) IL-6, (C) IL-10, and (D) Soluble ICAM-1 (24h after TBI) caused by TS-exposure and TBI was reduced by MF and RSG treatment. A trend similar to inflammatory cytokines was observed for adhesion molecules (E) PECAM-1 and (F) VCAM-1. *$p < 0.05$, **$p < 0.01$, ***$p < 0.001$, ****$p < 0.0001$ versus control. @$p < 0.05$, @@$p < 0.01$, @@@@$p < 0.0001$ non-treated versus MF/RSG treated group. WB analyses express protein/β-actin ratios.

As shown in Figs. 4.10A-C, a similar response to treatment was observed *in vivo*, where the levels of these inflammatory cytokines were measured in mice's plasma samples collected 7 days post-TBI. Soluble ICAM-1 as a biomarker of neuroinflammation *in vitro* (cell culture supernatant of BBB endothelial cells; Fig. 4.9D) and *in vivo* (plasma samples of mice; Fig. 4.10D) was also assessed by ELISA. Data indicate that MF and RSG were effective in reducing soluble ICAM-1 level in TS-exposed and TBI-induced groups, both *in vitro* (average soluble ICAM-1 level in TBI control: 489.81 pg/ml) (Fig. 4.9D) and *in vivo* (average soluble ICAM-1 level in TBI control: 27.98 ng/ml) (Fig. 4.10D). Furthermore, we used a combination of WB and quantitative RT-PCR to measure changes in the expression levels of inflammatory adhesion molecules, including Platelet Endothelial Cell Adhesion Molecule 1 (PECAM-1) and Vascular Cell Adhesion Protein 1 (VCAM-1). We observed a remarkable increase in protein expression and mRNA levels of PECAM-1 (Fig. 4.9E) and VCAM-1 (Fig. 4.9F) in TS-exposed and TBI-stimulated BBB endothelial cells compared to TBI controls, clearly suggesting that TS exposure enhances the vascular inflammatory response to TBI. MF and RSG significantly dampened the inflammatory effect compared to the untreated TBI + TS groups (Fig. 4.9). WB analyses of the corresponding *in vivo* samples confirmed the *in vitro* data. Specifically, the expression level of PECAM-1 (Fig. 4.10E) and VCAM-1 (Fig. 4.10F) in mice exposed to TS and subjected to TBI were significantly higher than in TBI controls, and like *in vitro*, MF and RSG reduced the enhanced inflammatory response elicited by TS on TBI-induced mice. The effect was dose-dependent.

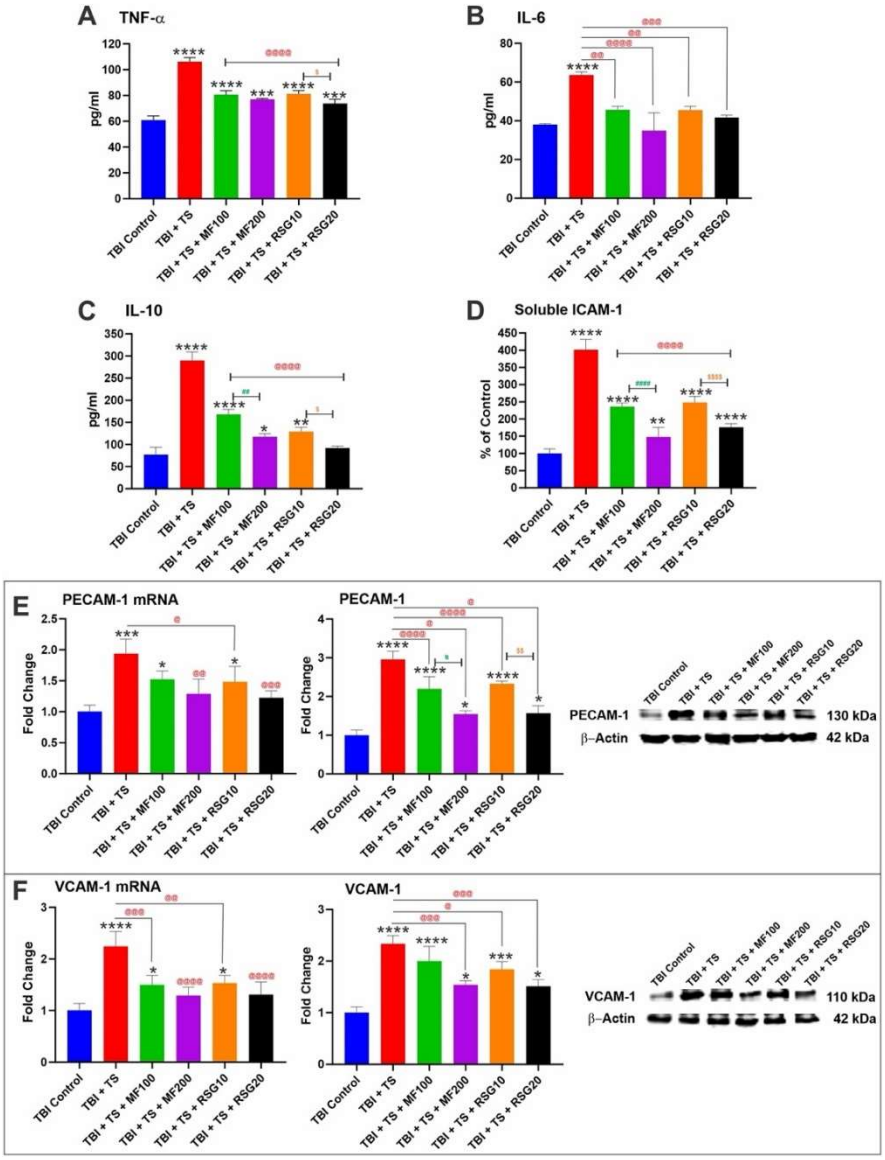

Figure 4.10 MF and RSG decrease inflammatory responses induced by premorbid TS-exposure and TBI induction.ELISA results of pro-inflammatory cytokines (A) TNF-α, (B) IL-6, (C) IL-10, and (D) soluble ICAM-1 7 days after TBI. Protein expression and mRNA levels of the inflammatory adhesion molecules (E) PECAM-1 and (F) VCAM-1 were upregulated by TS exposure and TBI induction. n = 6 biological replicates, *p < 0.05, **p < 0.01, ***p < 0.001, ****p < 0.0001 versus control. @p < 0.05, @@p < 0.01, @@@p < 0.01, @@@@p < 0.0001 non-treated versus MF/RSG treated group. #p < 0.05, ##p < 0.01, ####p < 0.0001 MF100 versus MF200. $p < 0.05, $$p < 0.01, $$$$p < 0.0001 RSG10 versus RSG20. WB analyses express protein/β-actin ratios.

4.8 Metformin and Rosiglitazone Attenuate Blood-Brain Barrier Disruption after Chronic Premorbid TS-Exposure and Traumatic Brain Injury

In our previous works, we revealed that upregulated activity of the NRF2-ARE system by MF and RSG is accompanied by enhanced expression of tight junction (TJ) proteins and reduced BBB permeability [67,79,135]. To verify if MF and RSG were acting through the same pathway in the context of TS and TBI, we explored the expression levels of BBB-related biomarkers of barrier viability by WB, ELISA, and quantitative RT-PCR. Our data showed that TS exposure and TBI induction remarkably decreased the protein expression and the corresponding mRNA levels of ZO-1 and TJ proteins, Claudin-5 and Occludin, in BBB endothelial cell cultures (Fig. 4.11). A similar trend was observed *in vivo* following the analyses of brain tissue homogenate of the corresponding mice groups (Fig. 4.12A to C). In both cases, MF and RSG significantly reduced the loss of TJs' expression, and the effect was dose-dependent. Several studies showed that severe neuroinflammation promotes the expression of MMP-9 and loss of BBB integrity leading to the extravasation of S100B from the brain into the blood circulation [155,156]. Our data showed that TS exposure elicits a significant increase in the levels of MMP-9 and worsens the damage of the BBB, resulting in a significant increase of S100β extravasation. The impact of TS over TBI was significantly dampened by MF and RSG treatments in a dose-dependent fashion. Since MMP-9 is initially released from the cytosol in an inactive form and is subsequently activated by proteolytic cleavage, we quantified the MMP-9 level in cells culture supernatant of BBB endothelial cell (Fig. 4.11D) (average MMP-9 level in TBI control: 1.85 ng/ml).

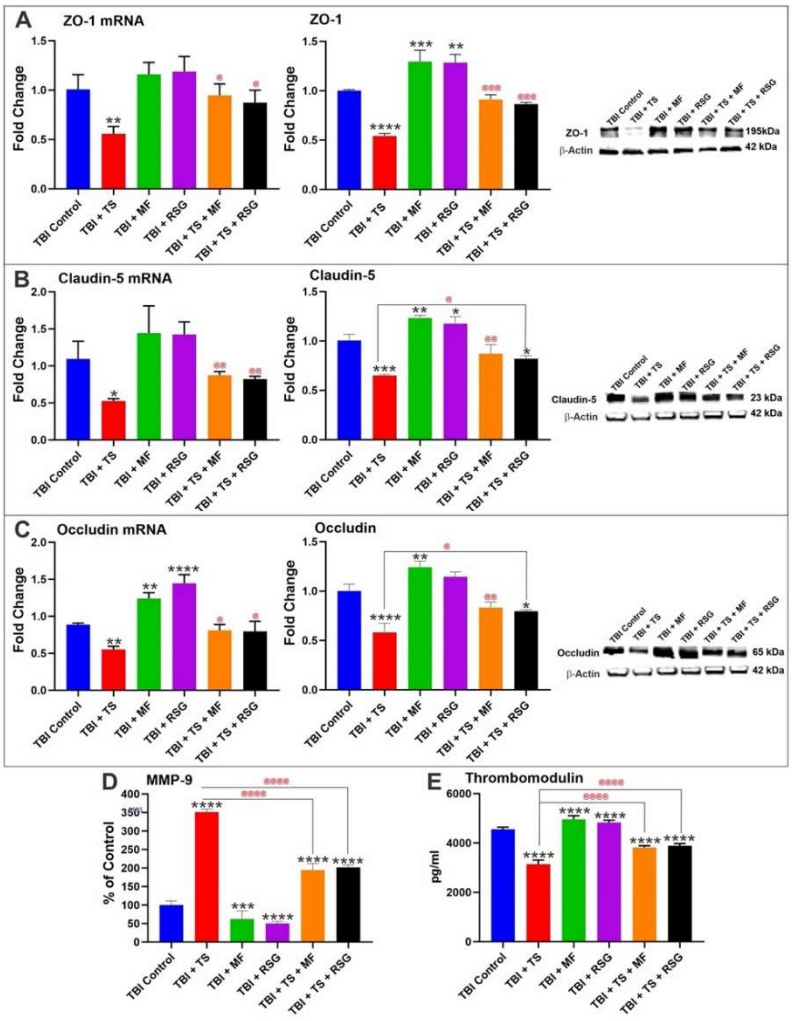

Figure 4.11 MF and RSG effect against loss of barrier integrity caused by premorbid TS-exposure and TBI stimulation in BBB endothelial cells.(A) WB and quantitative RT-PCR analyses demonstrate the upregulation of ZO-1 and its mRNA in cells exposed to TS and/or TBI by MF and RSG treatment. WB and quantitative RT-PCR analyses demonstrated a similar upregulation of (B) Claudin-5 and (C) Occludin in cells treated by MF and RSG. The effect of MF and RSG treatment on the level of (D) MMP-9 and (E) Thrombomodulin in premorbid TS-exposed and TBI-induced BBB endothelial cells was also evaluated. Levels of Thrombomodulin in the supernatants collected at 24h after TBI were measured by ELISA. MF and RSG compensated for the promoted suppression of thrombomodulin caused by TS exposure and TBI and potentially repaired blood hemostasis. n = 6 biological replicates, *p < 0.05, **p < 0.01, ***p < 0.001, ****p < 0.0001 versus control. @p < 0.05, @@p < 0.01, @@@p < 0.001, @@@@p < 0.0001 non-treated versus MF/RSG treated group. WB analyses express protein/β-actin ratios.

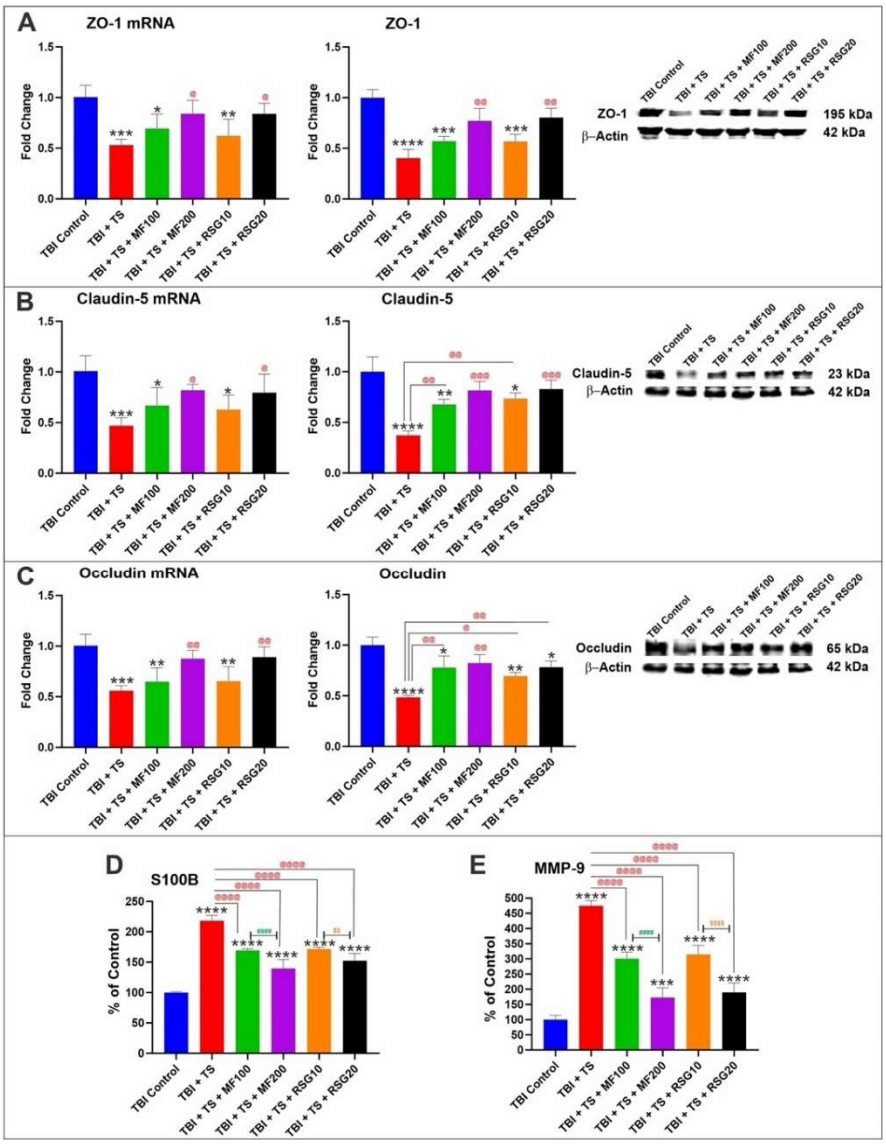

Figure 4.12 Dose-dependent protective effects of MF and RSG against TS and TBI-induced loss of barrier integrity.WB and quantitative RT-PCR analyses demonstrated upregulation of (A) accessory anchoring protein ZO-1 and TJ proteins, (B) Claudin-5, and C) Occludin in MF and RSG-treated mice in a dose-dependent manner. Decreased levels of (D) MMP-9 and (E) S100B as the biomarker of BBB integrity emphasized the dose-dependent protective effect of MF and RSG in mice exposed to TS and induced by TBI. n = 6 biological replicates, *p < 0.05, **p < 0.01, ***p < 0.001, ****p < 0.0001 versus control. @p < 0.05, @@p < 0.01, @@@p < 0.01, @@@@p < 0.0001 non-treated versus MF/RSG treated group. ####p < 0.0001 MF100 versus MF200. $$p < 0.01, $$$$p < 0.0001 RSG10 versus RSG20. WB analyses express protein/β-actin ratios.

In vivo, S100B (Fig. 4.12D) and MMP-9 (Fig. 4.12E) levels were measured in collected plasma samples 7 days after TBI (average MMP-9 and S100B levels in TBI control: 61.14 ng/ml and 1.01 ng/ml, respectively). It is quite remarkable how the increase of S100β in the plasma (Fig. 4.12D), indicating a loss of BBB integrity, closely trends that of MMP9 (Fig. 4.12E) across the various experimental settings

4.9 Metformin and Rosiglitazone Recover the Reduced Level of Thrombomodulin and UCH-L1 After Premorbid Tobacco Smoke-Exposure and Traumatic Brain Injury

As shown *in vitro* in Fig. 4.11E and *in vivo* in Fig. 4.13A, chronic TS exposure reduced the expression level of the anticoagulant factor thrombomodulin. This data suggests that TS can potentially hamper the endothelial response to TBI and enhance the risk of blood coagulation in TBI patients, as previously shown [116,152]. However, TS-dependent downregulation of thrombomodulin was effectively negated by MF and RSG both *in vitro* (Fig. 4.11E) and *in vivo* (Fig. 4.13A). Furthermore, analyses of plasma samples of TS-exposed and TBI-induced mice indicated a reduction in ubiquitin C-terminal hydrolase L1 (UCH-L1) levels. UCH-L1 is thought to play a key role in the maintenance of axonal integrity [157], thus providing neuroprotection. Interestingly, MF and RSG reduced the negative impact of TS on Thrombomodulin and UCH-L1 in a dose-dependent manner (Figs. 4.13A & B) (average UCH-L1 level in TBI control: 16.01 ng/ml).

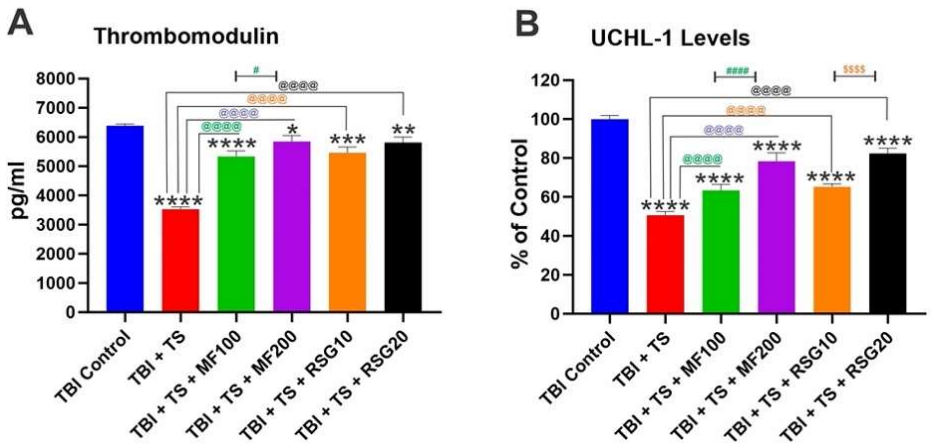

Figure 4.13 MF and RSG recover the reduced plasma level of Thrombomodulin and UCH-L1 in premorbid TS-exposed and TBI-induced mice.ELISA measurement of (A) UCH-L1 and (B) Thrombomodulin levels in the blood samples collected 7 days after TBI. n = 6 biological replicates, *p < 0.05, **p < 0.01, ***p < 0.001, ****p < 0.0001 versus control. @@@@p < 0.0001 non-treated versus MF/RSG treated group. #p < 0.05, ####p < 0.0001 MF100 versus MF200. $$$$p < 0.0001 RSG10 versus RSG20.

4.10 Metformin and Rosiglitazone Recover Reduced Motor Activity after Premorbid Tobacco Smoke-Exposure and Traumatic Brain Injury Induction of Mice

Exploratory behavior and general motor activity of the test mice were regularly recorded to assess the therapeutic effect of MF and RSG administration on TBI outcomes after premorbid TS exposure. As shown in Fig. 4.14, mice chronically exposed to TS demonstrated significantly higher motor activity which is evident from the total distance traveled by the animals after being subjected to chronic TS exposure for three weeks. The data is consistent with the metabolic effect of TS and a craving for TS. Measurements performed at 1, 3, and 7 days post-TBI revealed that TS exposure significantly aggravated TBI-induced neurological impairment as denoted by the remarkable reduction of motor activity compared to TBI controls.

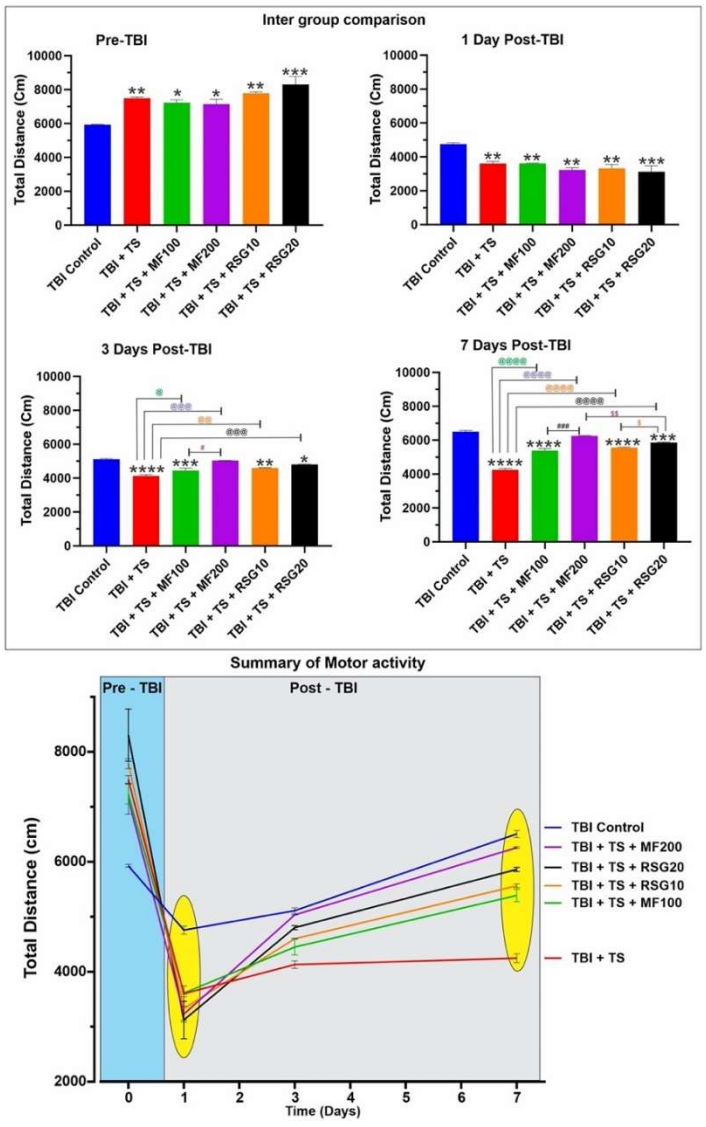

Figure 4.14 Effect of MF and RSG on exploratory behavior and general motor activity after premorbid TS-exposure and TBI induction of mice.Mice undergoing chronic TS exposure demonstrated significantly higher motor activity. Measurements performed at 24h, 3 days, and 7 days post-TBI showed that TS further aggravated TBI injury as denoted by the significant reduction of motor activity compared to the control. However, an assessment of the mice's response to TBI and TS-exposure w/wo MF and RSG showed that treated mice experienced a recovery in motor activity compared to non-treated animals. n = 6 biological replicates, *p < 0.05, **p < 0.01, ***p < 0.001, ****p < 0.0001 versus control. @p < 0.05, @@p < 0.01, @@@p < 0.01, @@@@p < 0.0001 non-treated versus MF/RSG treated group. #p < 0.05, ###p < 0.001 MF100 versus MF200. $p < 0.05, $$p < 0.01 RSG10 versus RSG20.

However, assessment of the mice's response to TBI and TS-exposure w/wo MF and RSG clearly showed that treated mice experienced a recovery of motor activity beginning at day 3 of post-TBI drugs treatment which further improved on day 7 post-TBI following daily administration of the drugs. The positive effect of MF and RSG on the recovery of motor activity was dose-dependent (see also the longitudinal pattern of motor activity). From an exploratory behavioral perspective, rodents typically prefer not to station at the center of the apparatus and tend to walk close to the walls (thigmotaxis) since this is a novel environment for them. As shown in Fig. 4.15A, all animals before TBI exhibited a similar exploratory pattern where mice chronically exposed to TS traveled more distance (see Fig. 4.14) with most movements and very low resting time. However, the walking pattern 24 hr post-TBI showed a significant reduction in traveled distance, movements, and an extended resting time which is remarkably clear in Fig. 4.15B in untreated TS-exposed mice. TS-exposed animals receiving MF and/or RSG showed a more uniform walking pattern across the chamber perimeter with reduced resting time than untreated TS-exposed animals. The walking pattern performed at 3 days and 7 days post-TBI continued to show more traveled distance and movements and less resting time in MF and RSG treated animals compared to TS (see Fig. 4.15C & D), suggesting a faster recovery of motor activity than in non-treated animals.

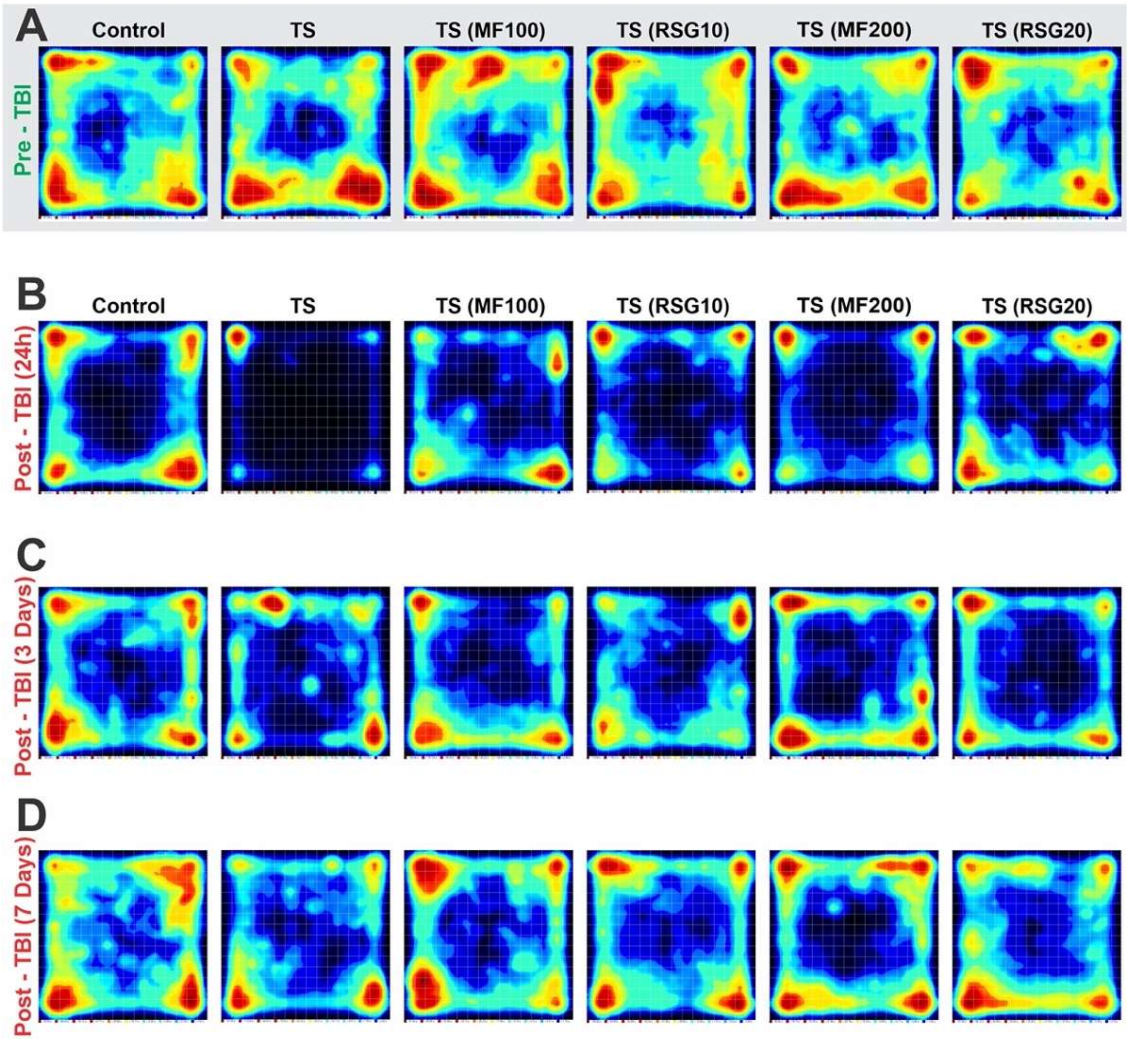

Figure 4.15 Animals' walking patterns and exploratory behavior.(A) Pre-TBI walking patterns of chronically exposed TS mice show the most traveled distance with most movements and very low resting time. However, the walking patterns 24 hr post-TBI clearly show less traveled distance and movements and extended resting time for untreated TS-exposed mice (B). Walking patterns assessed at 3 days (C) and 7 days (D) post-TBI show a similar trend where animals receiving MF or RSG recovered their motor activity and exploratory behavior compared to non-treated animals.

4.11 Discussion

Several pathophysiological mechanisms and prodromal factors involved in the onset of traumatic and post-traumatic brain injuries have been elucidated [158]; however, the complexity of these mechanistic pathways continues to pose a severe drag to the development of more effective therapeutic strategies. It was recently shown that premorbid conditions, such as chronic smoking, negatively impact TBI severity and post-TBI recovery. TS contains over 4700 toxic compounds, including nicotine and ROS, which not only trigger local OS damage and inflammation in the lungs but can initiate OS and inflammation in other tissues remote from the primary exposure site [159], including the cerebrovascular system, thus promoting endothelial dysfunction, particularly at the level of the BBB [160]. Moreover, TS can trigger BBB disruption via oxidative and inflammatory mechanisms [161,162]. It is conceivable that TS synergistically influences TBI by exacerbating BBB disruption and promoting OS and neuroinflammation. Enhanced ROS production and OS have been implicated in the onset and pathogenesis of numerous neurodegenerative and cerebrovascular disorders [163]. In this respect, NRF2 is a transcription factor that regulates the cellular response to OS, increasing cytoprotective enzyme expression. Because of the cross-talk between antioxidant and anti-inflammatory pathways, many of the anti-inflammatory and mitochondrial actions of NRF2 have been considered secondary to its antioxidant impacts. Emerging evidence recently confirmed that the knockout (KO) of NRF2 aggravates TBI pathology, while the treatment of NRF2 activators inhibits neuronal apoptosis and neuroinflammatory responses by alleviating oxidative damage [164]. Unsurprisingly, there is a rising interest

in investigating the association between the impairment of NRF2 signaling and TBI, thus the mounting research interest in identifying new therapeutic potential targeting NRF2 to prevent and/or reduce brain injury. As a first-line biguanide class of oral antidiabetic drugs, MF has been shown to have anti-inflammatory, anti-cancer, cardioprotective, hepatoprotective, and antioxidant effects. Currently, it is being investigated as a drug directly acting on the CNS [109,165-168]. MF can easily cross the BBB, accumulate in the mitochondria, and activate the NRF2 antioxidant pathway, which eventually enhances the expression of antioxidant enzyme genes such as SOD, Glutathione peroxidase 1 (Gpx1), and Catalase (CAT) [169]. With its mild side effects, safe pharmacokinetic profile, and multi-functional properties, MF has become a favorable neurotherapeutic agent for repurposing [151]. Similar to MF, RSG, the PPARγ agonist and a member of the thiazolidinedione family, has been known to have strong anti-inflammatory and antioxidant properties [26,137]. RSG directly affects cellular function by inducing PPARγ, which regulates the transcriptional activity and the expression of downstream target genes. RSG reduces/prevents ROS production and its consequent damaging effect by regulating detoxification enzymes (CAT and SOD) and ROS scavengers [170]. RSG is known to have a lower safety profile than MF, and the FDA has restricted its use following studies that linked the drug to an increased risk of heart attacks. Thus, unlike MF, using RSG cannot be considered a viable long-term preventive strategy. However, RSG possesses significant anti-inflammatory properties on top of its NRF2-enhancing activity, thus providing a feasible post-TBI treatment option over a short period. The major objective of this study was to investigate the effect of MF and RSG to

prevent/reduce the loss of BBB function and integrity and protect the brain from post-TBI exacerbation in response to chronic TS exposure and unravel its putative mechanism of action. The premise for this study builds upon our previous works suggesting that MF and RSG attenuate the cerebrovascular impairments and mortality associated with chronic TS. Through those works, the involvement of common pathogenic modulators of BBB impairment involving angiogenic and inflammatory factors released by BBB endothelial cells in response to hyperglycemia (HG) and exposure to TS was proven [67]. Our previous *in vitro* data demonstrated RSG and MF's effectiveness in preventing and reducing BBB impairment and OS in response to chronic TS exposure, suggesting that RSG and MF could protect the cerebrovascular system from exogenous oxidative stimuli [26,75]. Our previous *in vivo* data also showed the protective effect of RSG (10 or 20 mg/kg) and MF (100 or 200 mg/kg) in a dose-dependent manner against TS-induced cerebrovascular toxicity in a rodent model of chronic TS [22,75]. This study investigated MF and RSG neuroprotection/restoration therapeutic time window as pre-TBI treatment and its role in activating counteractive antioxidative mechanisms to reduce the detrimental effect of TS underlying the exacerbation of TBI in chronically TS-exposed mBMEC cells using a valid *in vitro* TBI model (Fig. 4.2A). We validated the *in vitro* results to confirm the protective effect of MF and RSG as post-TBI treatment over a short period (7 days) to reduce TS toxicity affecting post-traumatic exacerbation of TBI and post-TBI recovery in chronically TS-exposed C57BL/6J male mice and undergoing TBI (using well-established weight-drop TBI model). We screened the MF and RSG neuroprotection /restoration therapeutic time window post-treatment. We evaluated its

impact by assessing a panel of the brain and blood-based biomarkers and behavioral activities (see also Fig. 4.1). We evaluated a panel of biomarkers through these side-by-side *in vitro* and *in vivo* studies, including molecular targets specific to BBB integrity, neuroinflammation, OS, blood hemostasis, and redox metabolism related to the NRF2-ARE signaling pathway. Recently emerging evidence indicated that OS plays an essential role in the development and pathogenesis of TBI [171,172]. Many superoxide radicals are generated immediately in brain microvessels after injury and increase afterward due to the infiltration of neutrophils and macrophages and the overactivation of microglia [164]. On the other hand, scavengers of oxygen radicals, including SOD and catalase, remarkably reduce the level of superoxide radicals and partly reverse the injury of the brain [18]. Therefore, targeting the suppression of OS in the brain is a promising strategy to alleviate the aggravated TBI outcomes of TS exposure and accelerate post-TBI recovery. The findings of our *in vitro* study revealed that the RSG (20 μM) and MF (10 μM) notably inhibited induced intracellular ROS and OS generated through TS-exposure and TBI stimulation confirming the cytoprotective effects of RSG and MF (Fig. 4.7). To investigate the mechanism underlying the antioxidant effect of RSG and MF, we also detected their impact on NRF2 expression and mRNA level, the main regulator of cellular oxidative response, and its downstream signaling molecules, NQO-1, and HO-1. Our *in vitro* and *in vivo* data indicated a remarkable increase in expression and mRNA levels of NRF2, NQO-1, and HO-1 by MF and RSG, which support the notion of the activation of the NRF2-ARE signaling pathway (Fig.4.5 & 4.6). The neurovascular unit physically separates most brain regions from the peripheral circulation to limit the entry

of neurotoxic substances from the periphery into the CNS and maintain structural and functional homeostasis in the brain through BBB [173,174]. BBB is formed by endothelial cells rigidly connected by complex TJ proteins, including Occludins and Claudins. Chronic TS exposure disrupts TJ proteins and triggers an ionic imbalance within the BBB microenvironment. Several studies have reported TS-induced alterations in TJ protein expression and distribution, resulting in an ionic imbalance within the BBB microenvironment and excessive intracellular ROS followed by inflammatory responses [175]. BBB disruption is a major pathophysiological feature of TBI and is accompanied by disrupted TJ proteins and enhanced paracellular permeability [2]. Evidence indicates that excessive neuroinflammation can further compromise BBB integrity [176]. Because of the highly heterogeneous characteristic of the brain, different brain structures are subject to different acceleration rates in response to a direct impact or external forces applied to the head. This results in the generation of considerable tensile, shear, and compressive forces within the brain [21]. Concerning the specific impact on the BBB, our *in vitro* data clearly showed that TS-exposure and TBI reduce TJ Proteins and ZO-1 expression in mBMEC cells, leading to cerebrovascular impairment, which was prevented by RSG and MF (Fig. 4.11). MMP-9, as a biomarker of BBB integrity, regulates vascular remodeling through the degradation of the extracellular matrix [50]. It was proven that inflammatory cytokines are directly linked to increased MMP-9 levels and synergistically impact MMP expression [177]. Thus, the factors affecting MMP release and activation in the BBB-degraded groups are likely responsible for the aberrant BBB function [178]. As TJ proteins expression, impairment of BBB integrity was

reverted by RSG and MF as indicated by promoted MMP-9 level (Fig. 4.11D). Neuroinflammation is involved in the pathogenesis of TBI by contributing to primary brain injury. Solving the inflammatory response can ameliorate brain damage after TBI [144-146]. After TBI, a robust inflammatory response occurs acutely, characterized by the activation of resident cells, the migration and recruitment of peripheral immune cells, and the release of inflammatory mediators [179]. This activation occurs by NF-κB, which triggers the cascade amplification of inflammatory responses, inducing secondary damage after TBI [180]. Therefore, inhibiting NF-κB-mediated TBI activation and modulating the subsequent neuroinflammatory response to an appropriate level have been demonstrated to facilitate recovery after TBI [181]. Interestingly, it was proven that NRF2 and NF-κB signaling pathways could interfere with each other at their corresponding transcription level [16]. NRF2 suppresses the activation of the NF-κB signaling pathway by promoting antioxidant defenses neutralizing ROS, thus reducing ROS-mediated NF-κB activation. By contrast, NF-κB can suppress NRF2 activity, thus preventing ARE gene transcription. Our *in vitro* data revealed that TS exposure and TBI stimulation increased inflammatory biomarkers. Still, both RSG and MF reduced the expression of inflammatory biomarkers, including NF-kB, inflammatory adhesive molecules, and inflammatory cytokines resulting from TS exposure and TBI stimulation compared to untreated cultures (Fig. 4.9). Our *in vivo* data validated the protective effect of RSG (10 or 20 mg/kg) and MF (100 or 200 mg/kg) in a dose-dependent manner against TS-exposure and TBI induction. Data clearly showed a TS-dependent decrease of NRF2 expression leading to BBB impairment (downregulation of ZO-1, Occludin, and

Claudin-5 and upregulation of MMP-9 and S100B) and neuroinflammation (upregulation of NF-kB, inflammatory adhesive molecules, and inflammatory cytokines) which RSG and MF effectively counteracted. It was well evidenced by the renormalization of expression and activity of NRF2 and its downstream effectors (NQO-1 and HO-1) driven by MF and RSG (Fig. 4.6), reduction of OS generated after premorbid TS-exposure and TBI induction (Fig. 4.8), restoration of TJ proteins expression (Fig. 4.12), attenuation of inflammatory responses (Fig. 4.10), and normalization of thrombomodulin levels (Fig. 4.13B) in a dose-dependent manner. MF and RSG normalized aggravated mice's body weight, blood glucose level, and motor activity while recovering from post-traumatic behavior (Figs. 4.3, 4.4, 4.14). Although UCH-L1 is known as the biomarker of TBI severity, it should be considered that all the animal groups in this study were similarly affected by TBI. Based on several studies, increased ROS induce oxidative modification of UCH-L1, leading to pathological alteration of their cellular function. Moreover, UCH-L1 plays a key role in neuroprotection against OS. The inhibition of UCH-L1 leads to a notable increase in ROS level, which is in line with reduced glutathione content (GSH) decline. Our data align with this notion since UCH-L1 was reduced in TS-exposed mice and enhanced in a dose-dependent manner in animal groups treated with MF or RSG (Fig. 4.13A). MF and RSG can negatively affect glycemia. Thus, during *in vivo* study, we frequently checked fasting blood glucose levels and body weights. Note, however, that TS exposure can increase glycemia, in which case MF and RSG treatments will be even more beneficial. Recently published data have also shown that IP injection of MF and RSG did not affect the body weights of treated mice and fasting blood glucose levels

across the experimental groups. Moreover, although IP injection is not a common clinical route, we chose this route because of the practical difficulties of doing repetitive IV injections or repetitive delivery of MF and RSG in drinking water in mice and an understanding that there should not be a big difference in the pharmacokinetic profiles of a small molecule upon IV vs. IP administrations in mice [182,183]. Overall, efficacy and BBB permeability experiments utilizing systemic routes of administration should translate well to future oral administration. Furthermore, we used a male population of C57BL/6J mice chronically exposed to TS. Due to this application's limited scope and time, a more comprehensive investigation involving both genders will be deferred to a later time, pending the results of this study. The use of antidiabetic drugs to prevent/reduce TS-promoted cerebrovascular impairment associated with TBI has been marginally assessed. Thus, this is the first study to evaluate their putative protective effectiveness and therapeutic feasibility while investigating the drugs' mechanisms of action and molecular targets related to BBB integrity and TBI. Our recent data revealed that MF and RSG activate counteractive antioxidative mechanisms, drastically reducing TS toxicity, BBB integrity loss, OS damage, and neuroinflammation [15]. Thus, repurposing or "extending" the use of MF and RSG to counteract BBB damage and/or worsening of TBI by TS exposure is a shift and an extension of practice paradigms and clinical intervention that can enable a rapid response transition to prophylactic and/or therapeutic care.

4.12 Summary

Our results suggest that antidiabetic drugs such as MF and RSG that can positively modulate the NRF2 signaling pathway could be repurposed as potential new treatments for TBI to improve functional recovery. Excessive OS caused by dysregulation of the cellular antioxidant response system is a prominent linking mechanism to worsen TBI severity and delay post-TBI recovery in chronic smokers. Thus, targeting the activation of the NRF2-ARE signaling pathway could be a promising therapeutical strategy for treating TBI in chronic smokers by preventing/reducing BBB damage, diminishing TBI severity, and ameliorating post-TBI recovery. Our data revealed that MF and RSG exhibit potent neuroprotective effects through activating counteractive antioxidative mechanisms, drastically reducing TS toxicity, BBB integrity loss, OS damage, and neuroinflammation. Thus, repurposing the notion of repurposing MF and RSG to counteract the hampering effect of chronic smoking on TBI and BBB damage is a shift and an extension of practice paradigms and clinical intervention tested in this study which can lead to a rapid transition to prophylactic and/or therapeutic care.

CHAPTER FIVE

CONCLUSION AND FUTURE WORK

5.1 Conclusion

The consequences of TBI are a growing concern in the United States. Despite vast studies, the mechanisms and therapeutic strategies to alleviate the impacts of TBI have not been fully understood. Excitotoxicity, OS, cerebral edema formation and neuroinflammation are prominent mechanisms of cell damage and death post-TBI. Several novel promising strategies to treat TBI target the stabilization of BBB integrity. The safekeeping of BBB function could have significant therapeutic relevance to improve TBI outcomes and reduce secondary injury. Indeed, regulating post-traumatic BBB dysfunction would play an active role in reducing morbidity and mortality from TBI. This is even more relevant in patients with premorbid conditions (such as chronic smoking), which negatively affect BBB function and immune responses. TS is highly enriched in ROS constituents and other reactive compounds that have been clearly shown to promote dysfunction of the BBB through activation of oxidative, inflammatory, and immune responses, thus impacting the pathogenesis and progression of cerebrovascular and neurodegenerative disorders, including TBI [22,26,27]. Moreover, vaping EC is now very diffuse among the young population and has been recently shown to negatively affect the cerebrovascular system in similar ways, thus possibly impacting TBI severity and outcome. Despite the epidemiological and translational studies strongly suggesting

activation of pathophysiological pathways by TS/EC that exacerbate TBI outcome and influence recovery, determination and characterization of shared key modulators in BBB impairment due to TS/EC and TBI lies unexplored. Identification and then targeting these putative key modulators could help prevent the initiation of metabolic/cerebrovascular complications due to TBI in smokers and facilitate more targeted and effective interventions to improve post-traumatic outcomes. To this end, I evaluated the putative translational relevance of targeted blood and brain-based biomarkers of BBB integrity, inflammation, OS, redox metabolism, and blood hemostasis concerning the impact of TS/EC exposure on TBI outcome and post-TBI recovery. These studies uncovered possible diagnostic or therapeutic opportunities to treat TBI and provide critical data to assess and compare EC vs TS's potential impact on TBI severity. The NRF2-ARE signaling pathway is significant for cell cytoprotection against OS and maintenance of the proper redox balance in cells and tissues by promoting antioxidative defenses neutralizing ROS and blocking transcription of pro-inflammatory genes. Nowadays, there is a growing research interest in investigating the cerebrovascular and neurodegenerative protective effect of NRF2 pertaining to on the BBB's functional integrity, preventing harmful CNS disorders, and the initiation/progression of neuroinflammation and brain injury [69,82]. Based on current studies, there are effective strategies for restoring NRF2 activity to treat cerebrovascular and neurodegenerative disorders. For example, numerous nutritional dietary phytochemicals and therapeutic agents providing NRF2 enhancing activities which could be used to reduce the burden of major cerebrovascular and neurodegenerative disorders caused by excess ROS generation. For this purpose, I

evaluated the therapeutic feasibility and effectiveness of the administration of MF and RSG to reduce TS/EC-promoted cerebrovascular damage after TBI and/or improve post-TBI recovery. I showed that treatment with MF and RSG (potential cardiovascular side effects have limited its chronic use), attenuates cerebrovascular impairment triggered by TS/EC exposure. My data suggested that MF and RSG's protective mechanism is linked to a counteractive antioxidative response that drastically reduces TS/EC toxicity through the activation of NRF2-ARE signaling pathway while acting as a potent anti-inflammatory drug. These studies provided critical data to identify the cerebrovascular pathophysiological process induced by TS/EC and how they impact TBI outcomes.

5.2 Future Work

This dissertation mainly focused on an innovative approach to investigate the impact of TS/EC on exacerbating the TBI and delaying post-TBI recovery and potential antidiabetic countermeasures. Multiple *in vitro* and *in vivo* studies have been implemented for this work, which were extremely challenging and time-consuming. To reach the ultimate goals of this study, the authors had to narrow down the focus area and leave some of the desired ideas outside the scope of this research. The ideas that I would have liked to test during this research mainly concerns the limitations of the procedure developed in the present work.

The adverse effects of TS/EC observed in the present study may not fully recapitulate those experienced by chronic smokers who have been exposed to TS/EC for many years due to unfeasible comparable long-term experimental conditions in a laboratory setting. Thus, the full extent of the beneficial effects of RSG and MF against

TS/EC-induced cerebrovascular disorders should also be assessed and explored in a clinical setting. Ideally, longer exposure periods could reduce the gap to some extent.

While the impact of TS toxicity on CNS has been widely investigated, in the specific case of EC toxicity, the amount of data currently available is negligible. In this respect, addressing this critical lack of knowledge could positively impact the work of the FDA in its regulatory role and role and to inform the public regarding the potential health impact of these products. We believe that to fully interpret the health risks and consequences associated with TS/EC and TBI we need a multilevel approach that involves using TBI-induced mixed gender population of male and female C57BL/6J and NRF2 KO mice models chronically exposed to TS/EC. Moreover, investigating the most susceptible area to TBI by immunocytochemical staining of brain tissues, assessing cerebral edema by the measurement of brain water content, determining the presence of microglia in the cortex of coronal brain sections-stained slide by CD11b+ surface area quantification and assessing BBB integrity by brain uptake of permeability markers through micro-dialysis of brain tissues are examples of the considered additional analyses for the future.

Moreover, in the specific case of *in vitro* model, a mixed population of neurons/astrocytes/pericytes can be used. In regard to *ex situ* studies, the used of isolated brain microcapillaries could provide more detailed and in-depth analysis of BBB function in response to treatment and possible alteration of the NRF2-ARE signaling pathway since utilizing whole brain tissue and immuno-staining techniques might fail to resolve some of the BBB endothelial alterations with sufficient resolution.

Moreover, since IP administration is not a common clinical procedure, difficulties in doing repetitive IV injections or repetitive delivery of MF and RSG in drinking water in mice make this route of administration more practical without affecting the pharmacokinetic profiles of the drugs. However, efficacy and BBB permeability experiments utilizing systemic routes of administration can translate well to future oral administration.

Besides, dissecting out the specific mechanistic interrelationship between RSG, PPARγ signaling pathway, and NRF2 expression as well as the activity of NRF2 and NF-kB, both *in vitro* and *in vivo* could provide additional mechanistic insights leading to the development of novel and more effective therapeutic targets.

REFERENCES

1. Sharma, R.; Shultz, S.R.; Robinson, M.J.; Belli, A.; Hibbs, M.L.; O'Brien, T.J.; Semple, B.D. Infections after a traumatic brain injury: The complex interplay between the immune and neurological systems. *Brain, Behavior, and Immunity* **2019**.

2. Price, L.; Wilson, C.; Grant, G. Blood–brain barrier pathophysiology following traumatic brain injury. *Translational Research in Traumatic Brain Injury* **2016**.

3. Sivandzade, F.; Cucullo, L. In-vitro blood–brain barrier modeling: A review of modern and fast-advancing technologies. *Journal of Cerebral Blood Flow & Metabolism* **2018**.

4. Hasan, A.; Deeb, G.; Rahal, R.; Atwi, K.; Mondello, S.; Marei, H.E.; Gali, A.; Sleiman, E. Mesenchymal stem cells in the treatment of traumatic brain injury. *Frontiers in Neurology* **2017**.

5. Semple, B.D.; Zamani, A.; Rayner, G.; Shultz, S.R.; Jones, N.C. Affective, neurocognitive and psychosocial disorders associated with traumatic brain injury and post-traumatic epilepsy. *Neurobiology of Disease* **2019**.

6. Zhang, L.; Wang, H.; Fan, Y.; Gao, Y.; Li, X.; Hu, Z.; Ding, K.; Wang, Y.; Wang, X. Fucoxanthin provides neuroprotection in models of traumatic brain injury via the Nrf2-ARE and Nrf2-autophagy pathways. *Scientific Reports* **2017**.

7. Patricia, B.; O'Neil, D.A.; LaPorte, M.J.; Cheng, J.P.; Beitchman, J.A.; Thomas, T.C.; Bondi, C.O.; Kline, A.E. Elucidating opportunities and pitfalls in the treatment of experimental traumatic brain injury to optimize and facilitate clinical translation. *Neuroscience & Biobehavioral Reviews* **2018**.

8. Maas, A.I.; Menon, D.K.; Adelson, P.D.; Andelic, N.; Bell, M.J.; Belli, A.; Bragge, P.; Brazinova, A.; Büki, A.; Chesnut, R.M. Traumatic brain injury: integrated approaches to improve prevention, clinical care, and research. *The Lancet Neurology* **2017**.

9. Durazzo, T.C.; Abadjian, L.; Kincaid, A.; Bilovsky-Muniz, T.; Boreta, L.; Gauger, G.E. The influence of chronic cigarette smoking on neurocognitive recovery after mild traumatic brain injury. *Journal of Neurotrauma* **2013**.

10. Benady, A.; Freidin, D.; Pick, C.G.; Rubovitch, V. GM1 ganglioside prevents axonal regeneration inhibition and cognitive deficits in a mouse model of traumatic brain injury. *Scientific Reports* **2018**.

11. Thal, S.C.; Neuhaus, W. The blood–brain barrier as a target in traumatic brain injury treatment. *Archives of Medical Research* **2014**.

12. Amoo, M.; O'Halloran, P.J.; Leo, A.-M.; O'Loughlin, A.; Mahon, P.; Lim, C. Outcomes of emergency neurosurgical intervention in neuro-critical care patients with traumatic brain injury at Cork University Hospital. *British Journal of Neurosurgery* **2018**.

13. Li, W.; Risacher, S.L.; McAllister, T.W.; Saykin, A.J. Traumatic brain injury and age at onset of cognitive impairment in older adults. *Journal of Neurology* **2016**.

14. Sahyouni, R.; Gutierrez, P.; Gold, E.; Robertson, R.T.; Cummings, B.J. Effects of concussion on the blood–brain barrier in humans and rodents. *Journal of Concussion* **2017**.

15. Sivandzade, F.; Bhalerao, A.; Cucullo, L. Cerebrovascular and neurological disorders: protective role of NRF2. *International Journal of Molecular Sciences* **2019**.

16. Sivandzade, F.; Prasad, S.; Bhalerao, A.; Cucullo, L. NRF2 and NF-κB interplay in cerebrovascular and neurodegenerative disorders: Molecular mechanisms and possible therapeutic approaches. *Redox Biology* **2019**.

17. Dong, W.; Yang, B.; Wang, L.; Li, B.; Guo, X.; Zhang, M.; Jiang, Z.; Fu, J.; Pi, J.; Guan, D. Curcumin plays neuroprotective roles against traumatic brain injury partly via Nrf2 signaling. *Toxicology and Applied Pharmacology* **2018**.

18. Angeloni, C.; Prata, C.; Vieceli Dalla Sega, F.; Piperno, R.; Hrelia, S. Traumatic brain injury and NADPH oxidase: a deep relationship. *Oxidative Medicine and Cellular Longevity* **2015**.

19. Smith, J.A.; Park, S.; Krause, J.S.; Banik, N.L. Oxidative stress, DNA damage, and the telomeric complex as therapeutic targets in acute neurodegeneration. *Neurochemistry International* **2013**.

20. Alves, J.L. Blood–brain barrier and traumatic brain injury. *Journal of Neuroscience Research* **2014**.

21. Sivandzade, F.; Alqahtani, F.; Cucullo, L. Traumatic Brain Injury and Blood–Brain Barrier (BBB): Underlying Pathophysiological Mechanisms and the Influence of Cigarette Smoking as a Premorbid Condition. *International Journal of Molecular Sciences* **2020**.

22. Sivandzade, F.; Cucullo, L. Anti-Diabetic Countermeasures Against Tobacco Smoke-Dependent Cerebrovascular Toxicity: Use and Effect of Rosiglitazone. *International Journal of Molecular Sciences* **2019**.

23. Daneman, R.; Prat, A. The blood–brain barrier. *Cold Spring Harbor Perspectives in Biology* **2015**.

24. Erdő, F.; Denes, L.; de Lange, E. Age-associated physiological and pathological changes at the blood–brain barrier: a review. *Journal of Cerebral Blood Flow & Metabolism* **2017**.

25. Broux, B.; Gowing, E.; Prat, A. Glial regulation of the blood-brain barrier in health and disease. In Proceedings of Seminars in immunopathology; pp. 577-590.

26. Sivandzade, F.; Cucullo, L. Assessing the protective effect of rosiglitazone against electronic cigarette/tobacco smoke-induced blood–brain barrier impairment. *BMC Neuroscience* **2019**.

27. Kaisar, M.A.; Sivandzade, F.; Bhalerao, A.; Cucullo, L. Conventional and electronic cigarettes dysregulate the expression of iron transporters and detoxifying enzymes at the brain vascular endothelium: In vivo evidence of a gender-specific cellular response to chronic cigarette smoke exposure. *Neuroscience Letters* **2018**.

28. Sajja, R.K.; Naik, P.; Cucullo, L. Differential cerebrovascular toxicity of various tobacco products: a regulatory perspective. *Journal of Pharmacovigilance* **2015**.

29. Sajja, R.K.; Rahman, S.; Cucullo, L. Drugs of abuse and blood-brain barrier endothelial dysfunction: A focus on the role of oxidative stress. *Journal of Cerebral Blood Flow & Metabolism* **2016**.

30. Choi, S.; Krishnan, J.; Ruckmani, K.J.B.; Pharmacotherapy. Cigarette smoke and related risk factors in neurological disorders: An update. *Biomedicine and Pharmacotherapy* **2017**

31. Matsuda, T.; Muromoto, R.; Sekine, Y.; Togi, S.; Kitai, Y.; Kon, S.; Oritani, K. Signal transducer and activator of transcription 3 regulation by novel binding partners. *World Journal of Biological Chemistry* **2015**.

32. Villapol, S.; Kryndushkin, D.; Balarezo, M.G.; Campbell, A.M.; Saavedra, J.M.; Shewmaker, F.P.; Symes, A.J. Hepatic expression of serum amyloid A1 is induced by traumatic brain injury and modulated by telmisartan. *The American Journal of Pathology* **2015**.

33. Ladak, A.A.; Enam, S.A.; Ibrahim, M.T. A review of the molecular mechanisms of Traumatic Brain Injury. *World Neurosurgery* **2019**.

34. Quintard, H.; Patet, C.; Suys, T.; Marques-Vidal, P.; Oddo, M. Normobaric hyperoxia is associated with increased cerebral excitotoxicity after severe traumatic brain injury. *Neurocritical Care* **2015**.

35. Abdul-Muneer, P.; Chandra, N.; Haorah, J. Interactions of oxidative stress and neurovascular inflammation in the pathogenesis of traumatic brain injury. *Molecular Neurobiology* **2015**.

36. Tagge, C.A.; Fisher, A.M.; Minaeva, O.V.; Gaudreau-Balderrama, A.; Moncaster, J.A.; Zhang, X.-L.; Wojnarowicz, M.W.; Casey, N.; Lu, H.; Kokiko-Cochran, O.N. Concussion, microvascular injury, and early tauopathy in young athletes after impact head injury and an impact concussion mouse model. *Brain* **2018**.

37. Dulla, C.G.; Coulter, D.A.; Ziburkus, J. From molecular circuit dysfunction to disease: case studies in epilepsy, traumatic brain injury, and Alzheimer's disease. *The Neuroscientist* **2016**.

38. Borutaite, V.; Tolkovsky, A.M.; Fricker, M.; Brown, G.C.; Coleman, M. Neuronal Cell Death. *Physiological Reviews* **2018**.

39. Sun, G.-z.; Gao, F.-f.; Zhao, Z.-m.; Sun, H.; Xu, W.; Wu, L.-w.; He, Y.-c. Endoplasmic reticulum stress-induced apoptosis in the penumbra aggravates secondary damage in rats with traumatic brain injury. *Neural Regeneration Research* **2016**.

40. Liu, G.; Zou, H.; Luo, T.; Long, M.; Bian, J.; Liu, X.; Gu, J.; Yuan, Y.; Song, R.; Wang, Y. Caspase-dependent and caspase-independent pathways are involved in cadmium-induced apoptosis in primary rat proximal tubular cell culture. *PloS One* **2016**.

41. Fujikawa, D.G. The role of excitotoxic programmed necrosis in acute brain injury. *Computational and Structural Biotechnology Journal* **2015**.

42. Zhang, L.; Wang, H.J.F.i.m.n. Autophagy in traumatic brain injury: a new target for therapeutic intervention. *Frontiers in Molecular Neuroscience* **2018**.

43. Chen, X.; Wu, S.; Chen, C.; Xie, B.; Fang, Z.; Hu, W.; Chen, J.; Fu, H.; He, H.J.J.o.n. Omega-3 polyunsaturated fatty acid supplementation attenuates microglial-induced inflammation by inhibiting the HMGB1/TLR4/NF-κB pathway following experimental traumatic brain injury. *Journal of Neuroinflammation* **2017**.

44. Song, Y.; Li, T.; Liu, Z.; Xu, Z.; Zhang, Z.; Chi, L.; Liu, Y.J.C.-b.i. Inhibition of Drp1 after traumatic brain injury provides brain protection and improves behavioral performance in rats. *Neutral Generation Research* **2019**.

45. Lozano, D.; Gonzales-Portillo, G.S.; Acosta, S.; de la Pena, I.; Tajiri, N.; Kaneko, Y.; Borlongan, C.V. Neuroinflammatory responses to traumatic brain injury: etiology, clinical consequences, and therapeutic opportunities. *Neuropsychiatric Disease and Treatment* **2015**.

46. Wang, K.; Cui, D.; Gao, L. Traumatic brain injury: a review of characteristics, molecular basis and management. *Frontiers in Bioscience (Landmark edition)* **2016**.

47. Park, J.-Y.; Amarsanaa, K.; Cui, Y.; Lee, J.-H.; Wu, J.; Yang, Y.-S.; Eun, S.-Y.; Jung, S.-C. Methyl lucidone exhibits neuroprotective effects on glutamate-induced oxidative stress in HT-22 cells via Nrf-2/HO-1 signaling. *Applied Biological Chemistry* **2019**.

48. Xin, H.; Cui, Y.; An, Z.; Yang, Q.; Zou, X.; Yu, N. Attenuated glutamate induced ROS production by antioxidative compounds in neural cell lines. *RSC Advances* **2019**.

49. Nag, S.; Manias, J.; Eubanks, J.H.; Stewart, D.J. Increased Expression of Vascular Endothelial Growth Factor-D Following Brain Injury. *International Journal of Molecular Sciences* **2019**.

50. Suzuki, Y.; Nagai, N.; Umemura, K. A review of the mechanisms of blood-brain barrier permeability by tissue-type plasminogen activator treatment for cerebral ischemia. *Frontiers in Cellular Neuroscience* **2016**.

51. Acosta, S.A.; Tajiri, N.; de la Pena, I.; Bastawrous, M.; Sanberg, P.R.; Kaneko, Y.; Borlongan, C.V. Alpha-synuclein as a pathological link between chronic traumatic brain injury and Parkinson's disease. *Journal of Cellular Physiology* **2015**.

52. Xiong, Y.; Mahmood, A.; Chopp, M. Current understanding of neuroinflammation after traumatic brain injury and cell-based therapeutic opportunities. *Chinese Journal of Traumatology* **2018**.

53. Weston, N.M.; Sun, D. The potential of stem cells in treatment of traumatic brain injury. *Current Neurology and Neuroscience Reports* **2018**.

54. Zhang, Q.; Lenardo, M.J.; Baltimore, D. 30 years of NF-κB: a blossoming of relevance to human pathobiology. *Cell* **2017**.

55. Mettang, M.; Reichel, S.N.; Lattke, M.; Palmer, A.; Abaei, A.; Rasche, V.; Huber-Lang, M.; Baumann, B.; Wirth, T. IKK2/NF-κB signaling protects neurons after traumatic brain injury. *The FASEB Journal* **2018**.

56. Mutinati, M.; Pantaleo, M.; Roncetti, M.; Piccinno, M.; Rizzo, A.; Sciorsci, R. Oxidative stress in neonatology. A review. *Reproduction in Domestic Animals* **2014**.

57. Wang, J.-W.; Wang, H.-D.; Cong, Z.-X.; Zhou, X.-M.; Xu, J.-G.; Jia, Y.; Ding, Y. Puerarin ameliorates oxidative stress in a rodent model of traumatic brain injury. *Journal of Surgical Research* **2014**.

58. Mendes Arent, A.; Souza, L.F.d.; Walz, R.; Dafre, A.L. Perspectives on molecular biomarkers of oxidative stress and antioxidant strategies in traumatic brain injury. *BioMed Research International* **2014**.

59. Rodriguez-Rodriguez, A.; Jose Egea-Guerrero, J.; Murillo-Cabezas, F.; Carrillo-Vico, A. Oxidative stress in traumatic brain injury. *Current Medicinal Chemistry* **2014**.

60. Kumar, A.; Alvarez-Croda, D.-M.; Stoica, B.A.; Faden, A.I.; Loane, D.J. Microglial/macrophage polarization dynamics following traumatic brain injury. *Journal of Neurotrauma* **2016**.

61. He, Y.; Yan, H.; Ni, H.; Liang, W.; Jin, W. Expression of nuclear factor erythroid 2-related factor 2 following traumatic brain injury in the human brain. *NeuroReport* **2019**.

62. Zhou, Y.; Tian, M.; Wang, H.-D.; Gao, C.-C.; Zhu, L.; Lin, Y.-X.; Fang, J.; Ding, K. Activation of the Nrf2-ARE signal pathway after blast induced traumatic brain injury in mice. *International Journal of Neuroscience* **2019**.

63. Lu, X.-Y.; Wang, H.-D.; Xu, J.-G.; Ding, K.; Li, T. Deletion of Nrf2 exacerbates oxidative stress after traumatic brain injury in mice. *Cellular and Molecular Neurobiology* **2015**.

64. Sajja, R.K.; Prasad, S.; Tang, S.; Kaisar, M.A.; Cucullo, L. Blood-brain barrier disruption in diabetic mice is linked to Nrf2 signaling deficits: Role of ABCB10? *Neuroscience Letters* **2017**.

65. Kowluru, R.A.; Mishra, M. Epigenetic regulation of redox signaling in diabetic retinopathy: Role of Nrf2. *Free Radical Biology and Medicine* **2017**.

66. Dinkova-Kostova, A.T.; Abramov, A.Y. The emerging role of Nrf2 in mitochondrial function. *Free Radical Biology and Medicine* **2015**.

67. Prasad, S.; Sajja, R.K.; Park, J.H.; Naik, P.; Kaisar, M.A.; Cucullo, L. Impact of cigarette smoke extract and hyperglycemic conditions on blood–brain barrier endothelial cells. *Fluids and Barriers of the CNS* **201.**

68. Sandberg, M.; Patil, J.; D'angelo, B.; Weber, S.G.; Mallard, C. NRF2-regulation in brain health and disease: implication of cerebral inflammation. *Neuropharmacology* **2014**.

69. Li, T.; Wang, H.; Ding, Y.; Zhou, M.; Zhou, X.; Zhang, X.; Ding, K.; He, J.; Lu, X.; Xu, J., et al. Genetic elimination of Nrf2 aggravates secondary complications except for vasospasm after experimental subarachnoid hemorrhage in mice. *Brain Research* **2014**.

70. Choi, S.; Krishnan, J.; Ruckmani, K. Cigarette smoke and related risk factors in neurological disorders: An update. *Biomedicine & Pharmacotherapy* **2017**.

71. Santín-Márquez, R.; Alarcón-Aguilar, A.; López-Diazguerrero, N.E.; Chondrogianni, N.; Königsberg, M. Sulfoaphane-role in aging and neurodegeneration. *GeroScience* **2019**.

72. Cuadrado, M.P.A.I.R.A. P 087 - NRF2 controls proteostasis through the transcriptional regulation of autophagy. In Proceedings of OCC World Congress and Annual SFRR-E Conference **2017** Metabolic Stress and Redox Regulation, Berlin, Germany.

73. Pajares, M.; Rojo, A.I.; Arias, E.; Diaz-Carretero, A.; Cuervo, A.M.; Cuadrado, A. Transcription factor NFE2L2/NRF2 modulates chaperone-mediated autophagy through the regulation of LAMP2A. *Autophagy* **2018**.

74. Sivandzade, F.; Cucullo, L. In-vitro blood–brain barrier modeling: A review of modern and fast-advancing technologies. *Journal of Cerebral Blood Flow & Metabolism* **2018**.

75. Prasad, S.; Sajja, R.K.; Kaisar, M.A.; Park, J.H.; Villalba, H.; Liles, T.; Abbruscato, T.; Cucullo, L. Role of Nrf2 and protective effects of Metformin against tobacco smoke-induced cerebrovascular toxicity. *Redox Biology* **2017**.

76. Naik, P.; Sajja, R.K.; Prasad, S.; Cucullo, L. Effect of full flavor and denicotinized cigarettes exposure on the brain microvascular endothelium: a microarray-based gene expression study using a human immortalized BBB endothelial cell line. *BMC Neuroscience* **2015**.

77. Sajja, R.K.; Kaisar, M.A.; Vijay, V.; Desai, V.G.; Prasad, S.; Cucullo, L. In Vitro Modulation of Redox and Metabolism Interplay at the Brain Vascular Endothelium: Genomic and Proteomic Profiles of Sulforaphane Activity. *Scientific Report* **2018**.

78. Sivandzade, F.; Prasad, S.; Bhalerao, A.; Cucullo, L. NRF2 and NF-κB interplay in cerebrovascular and neurodegenerative disorders: Molecular mechanisms and possible therapeutic approaches. *Redox Biology* **2018**.

79. Kaisar, M.A.; Villalba, H.; Prasad, S.; Liles, T.; Sifat, A.E.; Sajja, R.K.; Abbruscato, T.J.; Cucullo, L. Offsetting the impact of smoking and e-cigarette vaping on the cerebrovascular system and stroke injury: Is Metformin a viable countermeasure? *Redox Biology* **2017**.

80. Rojo, A.I.; Pajares, M.; Garcia-Yague, A.J.; Buendia, I.; Van Leuven, F.; Yamamoto, M.; Lopez, M.G.; Cuadrado, A. Deficiency in the transcription factor NRF2 worsens inflammatory parameters in a mouse model with combined tauopathy and amyloidopathy. *Redox Biology* **2018**.

81. Buendia, I.; Michalska, P.; Navarro, E.; Gameiro, I.; Egea, J.; León, R. Nrf2–ARE pathway: an emerging target against oxidative stress and neuroinflammation in neurodegenerative diseases. *Pharmacology & therapeutics* **2016**.

82. Wang, X.; Campos, C.R.; Peart, J.C.; Smith, L.K.; Boni, J.L.; Cannon, R.E.; Miller, D.S. Nrf2 upregulates ATP binding cassette transporter expression and activity at the blood–brain and blood–spinal cord barriers. *Journal of Neuroscience* **2014**.

83. Prasad, S.; Sajja, R.K.; Naik, P.; Cucullo, L. Diabetes mellitus and blood-brain barrier dysfunction: an overview. *Journal of Pharmacovigilance* **2014**.

84. Alfieri, A.; Srivastava, S.; Siow, R.C.; Cash, D.; Modo, M.; Duchen, M.R.; Fraser, P.A.; Williams, S.C.; Mann, G.E. Sulforaphane preconditioning of the Nrf2/HO-1 defense pathway protects the cerebral vasculature against blood–brain barrier disruption and neurological deficits in stroke. *Free Radical Biology and Medicine* **2013**.

85. Patel, M. Targeting Oxidative Stress in Central Nervous System Disorders. *Trends in Pharmacological Science* **2016**.

86. Salim, S. Oxidative Stress and the Central Nervous System. *Journal of Pharmacology and Experimental Therapuetics* **2017**.

87. Yaribeygi, H.; Panahi, Y.; Javadi, B.; Sahebkar, A. The Underlying Role of Oxidative Stress in Neurodegeneration: A Mechanistic Review. *CNS Neurol Disord Drug Targets* **2018**.

88. Solleiro-Villavicencio, H.; Rivas-Arancibia, S. Effect of Chronic Oxidative Stress on Neuroinflammatory Response Mediated by CD4(+)T Cells in Neurodegenerative Diseases. *Frontiers in Cellular Neuroscience* **2018**.

89. Prasad, S.; Kaisar, M.A.; Cucullo, L. Unhealthy smokers: scopes for prophylactic intervention and clinical treatment. *BMC Neuroscience* **2017**.

90. Chen, Z.; Mao, X.; Liu, A.; Gao, X.; Chen, X.; Ye, M.; Ye, J.; Liu, P.; Xu, S.; Liu, J. Osthole, a natural coumarin improves cognitive impairments and BBB dysfunction after transient global brain ischemia in C57 BL/6J mice: involvement of Nrf2 pathway. *Neurochemical Research* **2015**.

91. Imai, T.; Takagi, T.; Kitashoji, A.; Yamauchi, K.; Shimazawa, M.; Hara, H. Nrf2 activator ameliorates hemorrhagic transformation in focal cerebral ischemia under warfarin anticoagulation. *Neurobiology of Disease* **2016**.

92. Li, W.; Suwanwela, N.C.; Patumraj, S. Curcumin by down-regulating NF-kB and elevating Nrf2, reduces brain edema and neurological dysfunction after cerebral I/R. *Microvascular Research* **2016**.

93. Mao, L.; Yang, T.; Li, X.; Lei, X.; Sun, Y.; Zhao, Y.; Zhang, W.; Gao, Y.; Sun, B.; Zhang, F. Protective effects of sulforaphane in experimental vascular cognitive impairment: Contribution of the Nrf2 pathway. *Journal of Cerebral Blood Flow & Metabolism* **2018**.

94. Yu, C.; He, Q.; Zheng, J.; Li, L.Y.; Hou, Y.H.; Song, F.Z. Sulforaphane improves outcomes and slows cerebral ischemic/reperfusion injury via inhibition of NLRP3 inflammasome activation in rats. *International Immunopharmacology* **2017**.

95. Holloway, P.M.; Gillespie, S.; Becker, F.; Vital, S.A.; Nguyen, V.; Alexander, J.S.; Evans, P.C.; Gavins, F.N. Sulforaphane induces neurovascular protection against a systemic inflammatory challenge via both Nrf2-dependent and independent pathways. *Vascular Pharmacology* **2016**.

96. Zhao, X.; Wen, L.; Dong, M.; Lu, X. Sulforaphane activates the cerebral vascular Nrf2–ARE pathway and suppresses inflammation to attenuate cerebral vasospasm in rat with subarachnoid hemorrhage. *Brain Research* **2016**.

97. Semple, B.D.; Zamani, A.; Rayner, G.; Shultz, S.R.; Jones, N.C. Affective, neurocognitive and psychosocial disorders associated with traumatic brain injury and post-traumatic epilepsy. *Neurobiology of Disease* **2018**.

98. Zhou, Y.; Tian, M.; Wang, H.D.; Gao, C.C.; Zhu, L.; Lin, Y.X.; Fang, J.; Ding, K. Activation of the Nrf2-ARE signal pathway after blast induced traumatic brain injury in mice. *International Journal of Neuroscience* **2019**.

99. Naik, P.; Cucullo, L. Pathobiology of tobacco smoking and neurovascular disorders: untied strings and alternative products. *Fluids and Barriers of the CNS* **2015**.

100. Kaisar, M.A.; Prasad, S.; Cucullo, L. Protecting the BBB endothelium against cigarette smoke-induced oxidative stress using popular antioxidants: Are they really beneficial? *Brain Research* **2015**.

101. Huang, Y.; Li, W.; Su, Z.-y.; Kong, A.-N.T. The complexity of the Nrf2 pathway: beyond the antioxidant response. *The Journal of Nutritional Biochemistry* **2015**.

102. Ashabi, G.; Khalaj, L.; Khodagholi, F.; Goudarzvand, M.; Sarkaki, A. Pre-treatment with metformin activates Nrf2 antioxidant pathways and inhibits inflammatory responses through induction of AMPK after transient global cerebral ischemia. *Metabolic Brain Disease* **2015**.

103. Liu, Y.; Tang, G.; Li, Y.; Wang, Y.; Chen, X.; Gu, X.; Zhang, Z.; Wang, Y.; Yang, G.Y. Metformin attenuates blood-brain barrier disruption in mice following middle cerebral artery occlusion. *Journal of Neuroinflammation* **2014**.

104. Jin, Q.; Cheng, J.; Liu, Y.; Wu, J.; Wang, X.; Wei, S.; Zhou, X.; Qin, Z.; Jia, J.; Zhen, X. Improvement of functional recovery by chronic metformin treatment is associated with enhanced alternative activation of microglia/macrophages and increased angiogenesis and neurogenesis following experimental stroke. *Brain Behavior, and Immunity* **2014**.

105. Ou, Z.; Kong, X.; Sun, X.; He, X.; Zhang, L.; Gong, Z.; Huang, J.; Xu, B.; Long, D.; Li, J., et al. Metformin treatment prevents amyloid plaque deposition and memory impairment in APP/PS1 mice. *Brain Behavavior, and Immunity* **2018**.

106. Tanokashira, D.; Kurata, E.; Fukuokaya, W.; Kawabe, K.; Kashiwada, M.; Takeuchi, H.; Nakazato, M.; Taguchi, A. Metformin treatment ameliorates diabetes-associated decline in hippocampal neurogenesis and memory via phosphorylation of insulin receptor substrate 1. *FEBS Open Bio* **2018**.

107. Pryor, R.; Cabreiro, F. Repurposing metformin: an old drug with new tricks in its binding pockets. *Biochemical Journal* **2015**.

108. Lee, J.E.; Park, J.H.; Jang, S.J.; Koh, H.C. Rosiglitazone inhibits chlorpyrifos-induced apoptosis via modulation of the oxidative stress and inflammatory response in SH-SY5Y cells. *Toxicology and Applied Pharmacology* **2014**.

109. Markowicz-Piasecka, M.; Sikora, J.; Szydłowska, A.; Skupień, A.; Mikiciuk-Olasik, E.; Huttunen, K.M. Metformin–a future therapy for neurodegenerative diseases. *Pharmaceutical Research* **2017**.

110. Sivandzade, F.; Cucullo, L. Assessing the protective effect of rosiglitazone against electronic cigarette/tobacco smoke-induced blood-brain barrier impairment. *BMC Neuroscience* **2019**.

111. Kadam, L.; Gomez-Lopez, N.; Mial, T.N.; Kohan-Ghadr, H.R.; Drewlo, S. Rosiglitazone Regulates TLR4 and Rescues HO-1 and NRF2 Expression in Myometrial and Decidual Macrophages in Inflammation-Induced Preterm Birth. *Reproductive Sciences* **2017**.

112. Naik, P.; Fofaria, N.; Prasad, S.; Sajja, R.K.; Weksler, B.; Couraud, P.-O.; Romero, I.A.; Cucullo, L. Oxidative and pro-inflammatory impact of regular and denicotinized cigarettes on blood brain barrier endothelial cells: is smoking reduced or nicotine-free products really safe? *BMC Neuroscience* **2014**.

113. Sajja, R.K.; Green, K.N.; Cucullo, L. Altered nrf2 signaling mediates hypoglycemia-induced blood–brain barrier endothelial dysfunction in vitro. *PLoS One* **2015**.

114. Sajja, R.K.; Cucullo, L. Altered glycaemia differentially modulates efflux transporter expression and activity in hCMEC/D3 cell line. *Neuroscience Letters* **2015**.

115. Li, F.; Wang, X.; Zhang, Z.; Zhang, X.; Gao, P. Dexmedetomidine Attenuates Neuroinflammatory–Induced Apoptosis after Traumatic Brain Injury via Nrf2 signaling pathway. *Annals of Clinical and Translational Neurology* **2019**.

116. Sivandzade, F.; Alqahtani, F.; Sifat, A.; Cucullo, L. The cerebrovascular and neurological impact of chronic smoking on post-traumatic brain injury outcome and recovery: an in vivo study. *Journal of Neuroinflammation* **2020**.

117. Lutton, E.M.; Farney, S.K.; Andrews, A.M.; Shuvaev, V.V.; Chuang, G.-Y.; Muzykantov, V.R.; Ramirez, S.H. Endothelial targeted strategies to combat oxidative stress: improving outcomes in traumatic brain injury. *Frontiers in Neurology* **2019**.

118. Lutton, E.M.; Razmpour, R.; Andrews, A.M.; Cannella, L.A.; Son, Y.-J.; Shuvaev, V.V.; Muzykantov, V.R.; Ramirez, S.H. Acute administration of catalase targeted to ICAM-1 attenuates neuropathology in experimental traumatic brain injury. *Scientific Rreports* **2017**.

119. Szarka, N.; Pabbidi, M.R.; Amrein, K.; Czeiter, E.; Berta, G.; Pohoczky, K.; Helyes, Z.; Ungvari, Z.; Koller, A.; Buki, A. Traumatic brain injury impairs myogenic constriction of cerebral arteries: role of mitochondria-derived H2O2 and TRPV4-dependent activation of BKCa channels. *Journal of Neurotrauma* **2018**.

120. Carvalho, C.; Moreira, P.I. Oxidative stress: a major player in cerebrovascular alterations associated to neurodegenerative events. *Frontiers in Physiology* **2018**.

121. Liu, Z.-M.; Chen, Q.-X.; Chen, Z.-B.; Tian, D.-F.; Li, M.-C.; Wang, J.-M.; Wang, L.; Liu, B.-H.; Zhang, S.-Q.; Li, F. RIP3 deficiency protects against traumatic brain injury (TBI) through suppressing oxidative stress, inflammation and apoptosis: Dependent on AMPK pathway. *Biochemical and Biophysical Research Communications* **2018**.

122. Wu, L.; Chung, J.Y.; Saith, S.; Tozzi, L.; Buckley, E.M.; Sanders, B.; Franceschini, M.A.; Lule, S.; Izzy, S.; Lok, J. Repetitive head injury in adolescent mice: A role for vascular inflammation. *Journal of Cerebral Blood Flow & Metabolism* **2019**.

123. Khan, N.M.; Haqqi, T.M. Pleiotropic Roles of Nrf2 as Regulators of Chondrocyte Apoptosis, Oxidative Stress, Inflammatory Response and Catabolic and Anabolic Pathways in Osteoarthritis. *Free Radical Biology and Medicine* **2017**.

124. Ozga, J.E.; Povroznik, J.M.; Engler-Chiurazzi, E.B.; Haar, C.V. Executive (dys) function after traumatic brain injury: special considerations for behavioral pharmacology. *Behavioural Pharmacology* **2018**.

125. Chen, Y.-H.; Kuo, T.-T.; Huang, E.Y.-K.; Hoffer, B.J.; Kao, J.-H.; Chou, Y.-C.; Chiang, Y.-H.; Miller, J. Nicotine-induced conditional place preference is affected by head injury: Correlation with dopamine release in the nucleus accumbens shell. *International Journal of Neuropsychopharmacology* **2018**.

126. Ilie, G.; Adlaf, E.M.; Mann, R.E.; Ialomiteanu, A.; Hamilton, H.; Rehm, J.; Asbridge, M.; Cusimano, M.D. Associations between a history of traumatic brain injuries and current cigarette smoking, substance use, and elevated psychological distress in a population sample of Canadian adults. *Journal of Neurotrauma* **2015**.

127. Caplan, B.; Bogner, J.; Brenner, L.; Ilie, G.; Mann, R.E.; Hamilton, H.; Adlaf, E.M.; Boak, A.; Asbridge, M.; Rehm, J. Substance use and related harms among adolescents with and without traumatic brain injury. *Journal of Head Trauma Rehabilitation* **2015**.

128. Chen, Y.-H.; Kuo, T.-T.; Huang, E.Y.-K.; Chou, Y.-C.; Chiang, Y.-H.; Hoffer, B.J.; Miller, J. Effect of traumatic brain injury on nicotine-induced modulation of dopamine release in the striatum and nucleus accumbens shell. *Oncotarget* **2018**.

129. Sajja, R.K.; Prasad, S.; Tang, S.; Kaisar, M.A.; Cucullo, L. Blood-brain barrier disruption in diabetic mice is linked to Nrf2 signaling deficits: Role of ABCB10? *Neuroscience Letters* **2017**.

130. Wu, L.; Chung, J.Y.; Saith, S.; Tozzi, L.; Buckley, E.M.; Sanders, B.; Franceschini, M.A.; Lule, S.; Izzy, S.; Lok, J. Repetitive head injury in adolescent mice: A role for vascular inflammation. *Journal of Cerebral Blood Flow & Metabolism* **2018**.

131. Bhalerao, A.; Cucullo, L. Impact of tobacco smoke in HIV progression: a major risk factor for the development of NeuroAIDS and associated CNS disorders. *Journal of Public Health* **2019**.

132. Archie, S.R.; Cucullo, L. Cerebrovascular and Neurological Dysfunction under the Threat of COVID-19: Is There a Comorbid Role for Smoking and Vaping? *International Journal of Molecular Sciences* **2020**.

133. Kaisar, M.A.; Villalba, H.; Prasad, S.; Liles, T.; Sifat, A.E.; Sajja, R.K.; Abbruscato, T.J.; Cucullo, L. Offsetting the impact of smoking and e-cigarette vaping on the cerebrovascular system and stroke injury: Is Metformin a viable countermeasure? *Redox Biology* **2017**.

134. Kaisar, M.A.; Sivandzade, F.; Bhalerao, A.; Cucullo, L. Conventional and Electronic cigarettes dysregulate the expression of iron transporters and detoxifying enzymes at the brain vascular endothelium: In Vivo Evidence of a Gender-Specific Cellular Response to Chronic Cigarette Smoke Exposure. *Neuroscience Letters* **2018**.

135. Sajja, R.K.; Green, K.N.; Cucullo, L. Altered nrf2 signaling mediates hypoglycemia-induced blood–brain barrier endothelial dysfunction in vitro. *PLoS One* **2015**.

136. Jimenez, R.; Toral, M.; Gómez-Guzmán, M.; Romero, M.; Sanchez, M.; Mahmoud, A.M.; Duarte, J. The role of Nrf2 signaling in PPARβ/δ-Mediated vascular protection against hyperglycemia-induced oxidative stress. *Oxidative Medicine and Cellular Longevity* **2018**.

137. Kadam, L.; Gomez-Lopez, N.; Mial, T.N.; Kohan-Ghadr, H.-R.; Drewlo, S. Rosiglitazone Regulates TLR4 and Rescues HO-1 and NRF2 Expression in Myometrial and Decidual Macrophages in Inflammation-Induced Preterm Birth. *Reproductive Sciences* **2017**.

138. Sivandzade, F.; Cucullo. Metabolism. In-vitro blood–brain barrier modeling: a review of modern and fast-advancing technologies. *Journal of Cerebral Blood Flow & Metabolism* **2018**.

139. Kaisar, M.A.; Kallem, R.R.; Sajja, R.K.; Sifat, A.E.; Cucullo, L. A convenient UHPLC-MS/MS method for routine monitoring of plasma and brain levels of nicotine and cotinine as a tool to validate newly developed preclinical smoking model in mouse. *BMC Neurosciences* **2017**.

140. Sivandzade, F.; Prasad, S.; Bhalerao, A.; Cucullo. NRF2 and NF-κB interplay in cerebrovascular and neurodegenerative disorders: Molecular mechanisms and possible therapeutic approaches. *Redox Biology* **2018**.

141. Sajja, R.K.; Prasad, S.; Tang, S.; Kaisar, M.A.; Cucullo, L. Blood-brain barrier disruption in diabetic mice is linked to Nrf2 signaling deficits: Role of ABCB10? *Neuroscience Letters* **2017**.

142. Cojocaru, I.M.; Cojocaru, M.; Sapira, V.; Ionescu, A. Evaluation of oxidative stress in patients with acute ischemic stroke. *Romanian Journal of Internal Medicine* **2013**.

143. Moreira, P.I.; Carvalho, C. Oxidative stress: a major player in cerebrovascular alterations associated to neurodegenerative events. *Frontiers in Physiology* **2018**.

144. Bergold, P.J. Treatment of traumatic brain injury with anti-inflammatory drugs. *Experimental Neurology* **2016**.

145. Hellewell, S.; Semple, B.D.; Morganti-Kossmann, M.C. Therapies negating neuroinflammation after brain trauma. *Brain Research* **2016**.

146. Simon, D.W.; McGeachy, M.J.; Bayır, H.; Clark, R.S.; Loane, D.J.; Kochanek, P.M. The far-reaching scope of neuroinflammation after traumatic brain injury. *Nature Reviews Neurology* **2017**.

147. Wang, J.; Jiang, C.; Zhang, K.; Lan, X.; Chen, X.; Zang, W.; Wang, Z.; Guan, F.; Zhu, C.; Yang, X. Melatonin receptor activation provides cerebral protection after traumatic brain injury by mitigating oxidative stress and inflammation via the Nrf2 signaling pathway. *Free Radical Biology and Medicine* **2019.**

148. Fang, J.; Wang, H.; Zhou, J.; Dai, W.; Zhu, Y.; Zhou, Y.; Wang, X.; Zhou, M. Baicalin provides neuroprotection in traumatic brain injury mice model through Akt/Nrf2 pathway. *Drug Design, Development and Therapy* **2018**.

149. Zeng, J.; Chen, Y.; Ding, R.; Feng, L.; Fu, Z.; Yang, S.; Deng, X.; Xie, Z.; Zheng, S. Isoliquiritigenin alleviates early brain injury after experimental intracerebral hemorrhage via suppressing ROS-and/or NF-κB-mediated NLRP3 inflammasome activation by promoting Nrf2 antioxidant pathway. *Journal of Neuroinflammation* **2017**.

150. Wang, M.; Luo, L. An effective NADPH oxidase 2 inhibitor provides neuroprotection and improves functional outcomes in animal model of traumatic brain injury. *Neurochemical Research* **2020**.

151. Sharma, S.; Nozohouri, S.; Vaidya, B.; Abbruscato, T. Repurposing metformin to treat age-related neurodegenerative disorders and ischemic stroke. *Life Sciences* **2021**.

152. Sivandzade, F.; Alqahtani, F.; Cucullo, L. Impact of chronic smoking on traumatic brain microvascular injury: An in vitro study. *Journal of Cellular and Molecular Medicine* **2021**.

153. Kempuraj, D.; Ahmed, M.E.; Selvakumar, G.P.; Thangavel, R.; Raikwar, S.P.; Zaheer, S.A.; Iyer, S.S.; Govindarajan, R.; Nattanmai Chandrasekaran, P.; Burton, C. Acute traumatic brain injury-induced neuroinflammatory response and neurovascular disorders in the brain. *Neurotoxicity Research* **2021**.

154. Kostich, W.; Hamman, B.D.; Li, Y.-W.; Naidu, S.; Dandapani, K.; Feng, J.; Easton, A.; Bourin, C.; Baker, K.; Allen, J., et al. Inhibition of AAK1 kinase as a novel therapeutic approach to treat neuropathic pain. *Journal of Pharmacology and Experimental Therapeutics* **2016**.

155. Fu, X.; Yang, C.; Chen, B.; Zeng, K.; Chen, S.; Fu, Y. Qi-Long-Tian formula extract alleviates symptoms of acute high-altitude diseases via suppressing the inflammation responses in rat. *Respiratory Research* **2021**.

156. Liu, P.; Pan, L.; Cui, L.; Li, T.; Zhao, S.; Hu, Y.; Tao, X.; Deng, H.; Jiang, J.; Zhao, B. Cordycepin ameliorates acute hypobaric hypoxia induced blood-brain barrier disruption, and cognitive impairment partly by suppressing the TLR4/NF-κB/MMP-9 pathway in the adult rats. *European Journal of Pharmacology* **2022**.

157. Reinicke, A.T.; Laban, K.; Sachs, M.; Kraus, V.; Walden, M.; Damme, M.; Sachs, W.; Reichelt, J.; Schweizer, M.; Janiesch, P.C., et al. Ubiquitin C-terminal hydrolase L1 (UCH-L1) loss causes neurodegeneration by altering protein turnover in the first postnatal weeks. *Proceedings of the National Academy of Sciences of the United States of America* **2019**.

158. Qin, D.; Wang, J.; Le, A.; Wang, T.J.; Chen, X.; Wang, J. Traumatic Brain Injury: Ultrastructural Features in Neuronal Ferroptosis, Glial Cell Activation and Polarization, and Blood–Brain Barrier Breakdown. *Cells* **2021**.

159. Bernard, A.; Ku, J.M.; Vlahos, R.; Miller, A.A. Cigarette smoke extract exacerbates hyperpermeability of cerebral endothelial cells after oxygen glucose deprivation and reoxygenation. *Scientific Reports* **2019**.

160. Austin, V.; Crack, P.J.; Bozinovski, S.; Miller, A.A.; Vlahos, R. COPD and stroke: are systemic inflammation and oxidative stress the missing links? *Clinical Science* **2016**.

161. Kim, J.-H.; Cho, M.-H.; Choi, K.-C.; Lee, K.; Kim, K.-S.; Shim, S.-M. Oxidative stress induced by cigarette smoke extracts in human brain cells (T98G) and human brain microvascular endothelial cells (HBMEC) in mono-and co-culture. *Journal of Toxicology and Environmental Health, Part A* **2015**.

162. Naik, P.; Sajja, R.K.; Prasad, S.; Cucullo, L. Effect of full flavor and denicotinized cigarettes exposure on the brain microvascular endothelium: a microarray-based gene expression study using a human immortalized BBB endothelial cell line. *BMC Neuroscience* **2015**.

163. Brandes, M.S.; Gray, N.E. NRF2 as a therapeutic target in neurodegenerative diseases. *Asn Neuro* **2020**.

164. Wu, A.-G.; Yong, Y.-Y.; Pan, Y.-R.; Zhang, L.; Wu, J.-M.; Zhang, Y.; Tang, Y.; Wei, J.; Yu, L.; Law, B.Y.-K. Targeting Nrf2-Mediated Oxidative Stress Response in Traumatic Brain Injury: Therapeutic Perspectives of Phytochemicals. *Oxidative Medicine and Cellular Longevity* **2022**.

165. Scheen, A.; Esser, N.; Paquot, N. Antidiabetic agents: potential anti-inflammatory activity beyond glucose control. *Diabetes & Metabolism* **2015**.

166. Hammad, A.M.; Ibrahim, Y.A.; Khdair, S.I.; Hall, F.S.; Alfaraj, M.; Jarrar, Y.; Abed, A.F. Metformin reduces oxandrolone-induced depression-like behavior in rats via modulating the expression of IL-1β, IL-6, IL-10 and TNF-α. *Behavioural Brain Research* **2021**.

167. Cameron, A.R.; Morrison, V.L.; Levin, D.; Mohan, M.; Forteath, C.; Beall, C.; McNeilly, A.D.; Balfour, D.J.; Savinko, T.; Wong, A.K. Anti-inflammatory effects of metformin irrespective of diabetes status. *Circulation Rresearch* **2016**.

168. Hasanpour Dehkordi, A.; Abbaszadeh, A.; Mir, S.; Hasanvand, A. Metformin and its anti-inflammatory and anti-oxidative effects; new concepts. *Journal of Renal Injury Prevention* **2019**.

169. Tu, W.; Wang, H.; Li, S.; Liu, Q.; Sha, H. The anti-inflammatory and anti-oxidant mechanisms of the Keap1/Nrf2/ARE signaling pathway in chronic diseases. *Aging and Disease* **2019**.

170. Kohan-Ghadr, H.-R.; Kilburn, B.A.; Kadam, L.; Johnson, E.; Kolb, B.L.; Rodriguez-Kovacs, J.; Hertz, M.; Armant, D.R.; Drewlo, S. Rosiglitazone augments antioxidant response in the human trophoblast and prevents apoptosis. *Biology of Reproduction* **2019**.

171. Zhang, H.-M.; Chen, W.; Liu, R.-N.; Zhao, Y. Notch inhibitor can attenuate apparent diffusion coefficient and improve neurological function through downregulating NOX2-ROS in severe traumatic brain injury. *Drug Design, Development and Therapy* **2018**.

172. Jarrahi, A.; Braun, M.; Ahluwalia, M.; Gupta, R.; Wilson, M.; Munie, S. Revisiting traumatic brain injury: from molecular mechanisms to therapeutic interventions. *Biomedicines*. **2020**.

173. Banks, W.A. From blood–brain barrier to blood–brain interface: new opportunities for CNS drug delivery. *Nature Reviews Drug Discovery* **2016**.

174. Chow, B.W.; Gu, C. The molecular constituents of the blood–brain barrier. *Trends in Neurosciences* **2015**.

175. Pimentel, E.; Sivalingam, K.; Doke, M.; Samikkannu, T. Effects of drugs of abuse on the blood-brain barrier: a brief overview. *Frontiers in Neuroscience* **2020**.

176. Hu, J.; Wang, X.; Chen, X.; Fang, Y.; Chen, K.; Peng, W.; Wang, Z.; Guo, K.; Tan, X.; Liang, F. Hydroxychloroquine attenuates neuroinflammation following traumatic brain injury by regulating the TLR4/NF-κB signaling pathway. *Journal of Neuroinflammation* **2022**.

177. Du, G.; Liu, C.; Li, X.; Chen, W.; He, R.; Wang, X.; Feng, P.; Lan, W. Induction of matrix metalloproteinase-1 by tumor necrosis factor-α is mediated by interleukin-6 in cultured fibroblasts of keratoconus. *Experimental Biology and Medicine* **2016**.

178. Lizano, P.; Pong, S.; Santarriaga, S.; Bannai, D.; Karmacharya, R. TNFα and MMP1 in brain microvascular endothelial cells regulate blood-brain barrier dysfunction in psychotic disorders. *Europe PMC* **2022**.

179. Corrigan, F.; Mander, K.A.; Leonard, A.V.; Vink, R. Neurogenic inflammation after traumatic brain injury and its potentiation of classical inflammation. *Journal of Neuroinflammation* **2016**.

180. Chen, X.; Wu, S.; Chen, C.; Xie, B.; Fang, Z.; Hu, W.; Chen, J.; Fu, H.; He, H. Omega-3 polyunsaturated fatty acid supplementation attenuates microglial-induced inflammation by inhibiting the HMGB1/TLR4/NF-κB pathway following experimental traumatic brain injury. *Journal of Neuroinflammation* **2017**.

181. Kumar, A.; Stoica, B.A.; Loane, D.J.; Yang, M.; Abulwerdi, G.; Khan, N.; Kumar, A.; Thom, S.R.; Faden, A.I. Microglial-derived microparticles mediate neuroinflammation after traumatic brain injury. *Journal of Neuroinflammation* **2017**.

182. Ivachtchenko, A.V.; Lavrovsky, Y.; Okun, I. AVN-101: a multi-target drug candidate for the treatment of CNS disorders. *Journal of Alzheimer's Disease* **2016**.

183. Gao, Y.; Shen, J.K.; Choy, E.; Zhang, Z.; Mankin, H.J.; Hornicek, F.J.; Duan, Z. Pharmacokinetics and tolerability of NSC23925b, a novel P-glycoprotein inhibitor: preclinical study in mice and rats. *Scientific Reports* **2016**.